Published for SISSA by Springer

Received: *September 1, 2017*
Revised: *January 25, 2018*
Accepted: *February 23, 2018*
Published: *March 5, 2018*

Searches for heavy ZZ and ZW resonances in the $\ell\ell qq$ and $\nu\nu qq$ final states in pp collisions at $\sqrt{s} = 13$ TeV with the ATLAS detector

The ATLAS collaboration

E-mail: atlas.publications@cern.ch

Abstract: This paper reports searches for heavy resonances decaying into ZZ or ZW using data from proton-proton collisions at a centre-of-mass energy of $\sqrt{s} = 13$ TeV. The data, corresponding to an integrated luminosity of 36.1 fb^{-1}, were recorded with the ATLAS detector in 2015 and 2016 at the Large Hadron Collider. The searches are performed in final states in which one Z boson decays into either a pair of light charged leptons (electrons and muons) or a pair of neutrinos, and the associated W boson or the other Z boson decays hadronically. No evidence of the production of heavy resonances is observed. Upper bounds on the production cross sections of heavy resonances times their decay branching ratios to ZZ or ZW are derived in the mass range 300–5000 GeV within the context of Standard Model extensions with additional Higgs bosons, a heavy vector triplet or warped extra dimensions. Production through gluon-gluon fusion, Drell-Yan or vector-boson fusion are considered, depending on the assumed model.

Keywords: Beyond Standard Model, Hadron-Hadron scattering (experiments)

ArXiv ePrint: 1708.09638

https://doi.org/10.1007/JHEP03(2018)009

JHEP03(2018)009

Contents

1 Introduction

The discovery of a Higgs boson h with a mass of approximately 125 GeV in 2012 [1, 2] represents a major milestone in the understanding of electroweak symmetry breaking. Subsequent studies [3–6] have shown that the properties of the new particle are consistent with those of the Standard Model (SM) Higgs boson. Nevertheless, the possibility that

JHEP03(2018)009

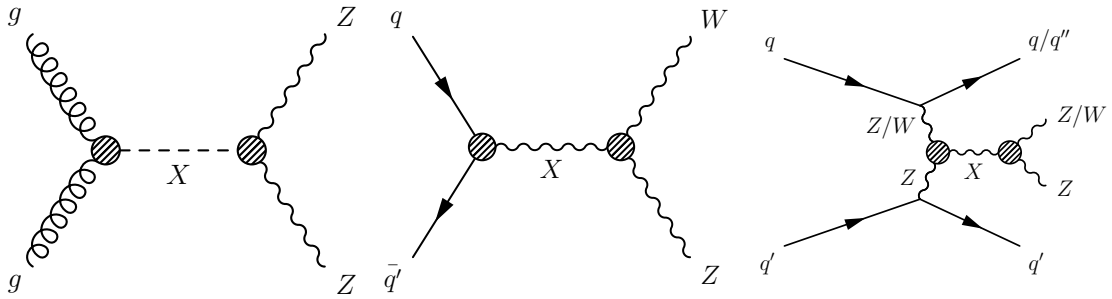

(a) gluon-gluon fusion (b) Drell-Yan (c) vector-boson fusion

Figure 1. Representative Feynman diagrams for the production of heavy resonances X with their decays into a pair of vector bosons.

the particle is part of an extended Higgs sector or other extension of the SM cannot be ruled out. Many of these models, motivated by hierarchy and naturalness arguments [7–9], predict the existence of new heavy resonances decaying into dibosons. In models with an extended Higgs sector, such as the two-Higgs-doublet models (2HDM) [10] and the electroweak-singlet model [11], a heavy spin-0 neutral Higgs boson (H) can decay into a pair of Z bosons. In extended gauge models [12], a heavier version of the SM W boson (W') is predicted to decay into ZW, and in models with warped extra dimensions [13, 14], spin-2 Kaluza-Klein (KK) excitations of the graviton (G_{KK}) are expected to decay into ZZ.

This paper reports searches for heavy resonances X decaying into pairs of vector bosons, ZV ($V = W, Z$). Production through gluon-gluon fusion (ggF), Drell-Yan (DY) and vector-boson fusion (VBF) processes are considered, depending on the assumed model. Representative Feynman diagrams of these processes are shown in figure 1. Two ZV decay modes are explored: one in which there is a Z boson decaying into a pair of light charged leptons (electrons or muons, denoted by ℓ), $Z \to \ell\ell$,[1] and the other in which a Z boson decays into a pair of neutrinos, $Z \to \nu\nu$. In both cases, the vector boson V is required to decay into a pair of quarks, $V \to qq$, leading to $X \to ZV \to \ell\ell qq$ and $X \to ZV \to \nu\nu qq$ decay modes.

Two different reconstruction techniques for the $V \to qq$ decay are considered: resolved and merged. The resolved reconstruction attempts to identify two separate small-radius jets (small-R jet, or j) of hadrons from the $V \to qq$ decay, while the merged reconstruction uses jet substructure techniques to identify the $V \to qq$ decay reconstructed as a large-R jet. When the resonance mass is significantly higher than the V boson mass, the qq pair from the V boson decay can be collimated. In this case, hadrons from the two quarks overlap in the detector and are more efficiently reconstructed as a single large-radius jet (large-R jet, or J). The $X \to ZV \to \ell\ell qq$ searche utilises both reconstruction techniques for the $V \to qq$ decay, whereas the $X \to ZV \to \nu\nu qq$ search uses only the merged reconstruction.

[1]To simplify the notation, antiparticles are not explicitly labelled in this paper.

JHEP03(2018)009

Heavy resonances would manifest themselves as resonant structures above the SM background in the invariant-mass distributions of the $\ell\ell qq$ final state and as broad enhancements in the transverse-mass distributions of the $\nu\nu qq$ final state. Thus for the $ZV \to \ell\ell qq$ decay mode, the invariant masses of the $\ell\ell J$ system ($m_{\ell\ell J}$) from the merged reconstruction and of the $\ell\ell jj$ system ($m_{\ell\ell jj}$) from the resolved reconstruction are used as the final discriminants for signal-background separation. For the $ZV \to \nu\nu qq$ decay mode, the final discriminant used is the transverse mass (m_{T}) of the large-R jet and the missing transverse momentum ($E_{\mathrm{T}}^{\mathrm{miss}}$).

Both the ATLAS and CMS collaborations have reported searches for heavy resonances in ZV decays in proton-proton (pp) collisions at $\sqrt{s} = 8\,\mathrm{TeV}$ and $13\,\mathrm{TeV}$ [15–19]. In addition to $\ell\ell qq$ and $\nu\nu qq$, these searches include fully hadronic ($qqqq$), semileptonic ($qq\ell\nu$), and fully leptonic ($\ell\ell\ell\ell$, $\ell\ell\ell\nu$, $\ell\ell\nu\nu$) final states. This paper extends previous ATLAS searches for ZV resonances in the $\ell\ell qq$ and $\nu\nu qq$ final states at $\sqrt{s} = 13\,\mathrm{TeV}$ reported in ref. [18] and uses a dataset more than ten times larger.

2 ATLAS detector

The ATLAS detector [20] at the Large Hadron Collider (LHC) [21] covers nearly the entire solid angle[2] around the collision point, and consists of an inner tracking detector surrounded by a thin superconducting solenoidal magnet producing a 2 T magnetic field, electromagnetic and hadronic calorimeters, and a muon spectrometer incorporating three large toroid-magnet assemblies. The inner detector (ID) consists of a high-granularity silicon pixel detector, including an insertable B-layer [22, 23], and a silicon microstrip tracker, together providing precision tracking in the pseudorapidity range $|\eta| < 2.5$, complemented by a transition radiation tracker, providing tracking and electron identification information for $|\eta| < 2.0$. A lead/liquid-argon (LAr) electromagnetic calorimeter covers the region $|\eta| < 3.2$, and hadronic calorimetry is provided by steel/scintillator-tile calorimeters for $|\eta| < 1.7$ and by copper/LAr hadronic calorimeters for $1.7 < |\eta| < 3.2$. The forward region is covered by additional LAr calorimeters with copper and tungsten absorbers. The muon spectrometer (MS) consists of precision tracking chambers covering the region $|\eta| < 2.7$, and separate trigger chambers covering $|\eta| < 2.4$. A two-level trigger system [24] reduces the event rate to approximately 1 kHz for offline investigations.

3 Data, signal models and simulation

3.1 Data

The data used in the searches were collected with the ATLAS detector in 2015 and 2016 pp collisions at a centre-of-mass energy of 13 TeV, corresponding to a total integrated luminosity of $36.1\,\mathrm{fb}^{-1}$.

[2] ATLAS uses a right-handed coordinate system with its origin at the nominal interaction point (IP) in the centre of the detector and the z-axis along the beam pipe. The x-axis points from the IP to the centre of the LHC ring, and the y-axis points upward. Cylindrical coordinates (r, ϕ) are used in the transverse plane, ϕ being the azimuthal angle around the z-axis. The pseudorapidity is defined in terms of the polar angle θ as $\eta = -\ln\tan(\theta/2)$.

JHEP03(2018)009

Events used in the $X \to ZV \to \ell\ell qq$ search were recorded with a combination of multiple single-electron or single-muon triggers with varying transverse energy E_{T} (electron) and transverse momentum p_{T} (muon), quality, and isolation requirements. The lowest E_{T} or p_{T} requirement without trigger prescaling was 26 GeV for both the electrons and muons. Events for the $X \to ZV \to \nu\nu qq$ search were recorded with an $E_{\mathrm{T}}^{\mathrm{miss}}$ trigger of varying threshold. The lowest threshold without prescaling is 100 GeV. This trigger is fully efficient for events passing the selection described below.

Events are retained for analysis if they were recorded with all detector systems operating normally and pass data-quality requirements [25]. Collision vertices are formed from tracks with $p_{\mathrm{T}} > 400$ MeV. If an event contains more than one vertex candidate, the one with the highest $\sum p_{\mathrm{T}}^2$ of its associated tracks is selected as the primary vertex. All events are required to contain a primary vertex with at least two associated tracks.

3.2 Signal models and simulation

Three classes of models of physics beyond the Standard Model are used as benchmarks for the interpretation of the results. Different resonances are predicted by each of these: a neutral heavy spin-0 Higgs boson H using the narrow-width approximation [26], a spin-1 W' boson of the heavy vector triplet (HVT) model [27, 28], and a spin-2 KK graviton G_{KK} from the bulk Randall-Sundrum model [13, 29, 30]. The new HVT bosons couple to the SM Higgs boson and gauge bosons with coupling strength $c_H g_V$ and to the SM fermions with coupling strength $(g^2/g_V)c_F$, where g is the SM $\mathrm{SU(2)_L}$ coupling constant. The parameter g_V characterises the interaction strength of the new vector bosons, while the dimensionless coefficients c_H and c_F parameterise departures of this typical strength from interactions with the SM Higgs and gauge bosons and with fermions, respectively, and are expected to be of order unity in most models. In *Model A* with $g_V = 1$, the branching ratios of the new heavy vector boson to known fermions and gauge bosons are comparable, while in *Model B* with $g_V = 3$, fermionic couplings to the new heavy vector boson are suppressed, giving rise to larger branching ratios for decays into ZW final states than in *Model A*. In a third model, *VBF Model*, the couplings to gauge bosons are similar to those in *Model A*, but the couplings to fermions are set to 0. In the bulk RS graviton model, the G_{KK} couplings to light fermions are suppressed and decays into final states involving heavy fermions, gauge bosons or Higgs bosons are favoured. The strength of the coupling depends on $k/\overline{M}_{\mathrm{Pl}}$, where k corresponds to the curvature of the warped extra dimension and $\overline{M}_{\mathrm{Pl}}$ is the effective four-dimensional Planck scale $\overline{M}_{\mathrm{Pl}} = 2.4 \times 10^{18}$ GeV. The cross section and intrinsic width scale as the square of $k/\overline{M}_{\mathrm{Pl}}$.

Monte Carlo (MC) samples of $H \to ZZ$ were generated by Powheg-Box v1 [31–34] with the CT10 [35] parton distribution functions (PDF) assuming a Higgs boson with width far smaller than the experimental resolution. Both the ggF and VBF production processes are considered. Benchmark samples of HVT $W' \to ZW$ and RS graviton $G_{\mathrm{KK}} \to ZZ$ were generated with MadGraph5_aMC@NLO 2.2.2 [36], using the NNPDF23LO [37] PDF set. For the HVT model, two production modes of the charged vector triplet W', DY and VBF, are considered. The W' resonance from DY production of *Model A* has a width approximately 2.6% of its mass, while for VBF production the width is much narrower,

JHEP03(2018)009

since its couplings to fermions are set to 0 in the VBF signal. For HVT *Model B*, the resonance widths and experimental signatures are similar to those obtained for *Model A*. Thus results derived from *Model A* can be directly applied to benchmark *Model B* by rescaling the relevant branching ratios. The G_{KK} has a mass-dependent width, 3.7% at 500 GeV and 6.4% at 5000 GeV relative to its mass, for $k/\overline{M}_{\mathrm{Pl}} = 1$. An RS graviton with $k/\overline{M}_{\mathrm{Pl}} = 0.5$ is also considered and the samples were obtained by reweighting the generated samples for $k/\overline{M}_{\mathrm{Pl}} = 1$ to account for the resonance width and cross-section differences. The parton showering and hadronisation were modelled with Pythia 8.186 [38] using the A14 set of the tuned parameters (tune) for the underlying event [39] for the W' and G_{KK} samples and the AZNLO tune [40] for the H samples. Potential signal and background interference effects were ignored in the signal modelling.

MC simulated events are also used to model background processes. The main background sources are Z and W bosons produced in association with jets (Z+jets and W+jets), with significant contributions from top quark production (both $t\bar{t}$ pair and single-top) and non-resonant vector-boson pair production (ZZ, WZ and WW). The Z+jets and W+jets events were simulated using the Sherpa 2.2.1 [41] event generator. Matrix elements were calculated for up to two partons at NLO and up to four partons at LO using the Comix [42] and OpenLoops [43] programs. Diboson processes with one of the bosons decaying hadronically and the other leptonically were simulated using Sherpa 2.1.0. They were simulated for up to one (ZZ) or zero (WZ, WW) additional partons at NLO and up to three additional partons at LO using the Comix and OpenLoops programs. For both Z+jets and diboson simulation, the matrix-element calculations were merged with the Sherpa parton shower using the ME+PS@NLO prescription [44]. The CT10 PDF set was used in conjunction with a dedicated parton shower tuning developed by the Sherpa authors. The $Z \to \tau\tau$ and $W \to \tau\nu$ events were included in the Z+jets and W+jets samples. For the generation of top quark pairs, the Powheg-Box v2 [45] event generator with the CT10 PDF set in the matrix element calculations was used. Electroweak t-channel, s-channel and Wt-channel single-top quark events were generated using the Powheg-Box v1 event generator [46–48]. This event generator uses the four-flavour scheme for the NLO matrix-element calculations together with the fixed four-flavour PDF set CT10f4 [35]. For all top quark processes, top quark spin correlations were preserved (for t-channel, top quarks were decayed using MadSpin). The parton shower, fragmentation, and underlying event were simulated using Pythia 6.428 [49] with the CTEQ6L1 [50] PDF set and the corresponding Perugia 2012 tune (P2012) [51]. The top quark mass was set to 172.5 GeV. The EvtGen v1.2.0 program [52] was used to decay bottom and charm hadrons for the Powheg-Box samples.

Cross sections were calculated with up to next-to-next-to-leading order (NNLO) QCD corrections for Z+jets and W+jets production [53]. Cross sections for diboson production were calculated at NLO including LO contributions with two additional partons [41, 54]. The $t\bar{t}$ production cross section is calculated at NNLO in QCD, including resummation of next-to-next-to-leading logarithmic (NNLL) soft-gluon terms [55, 56]. The single-top production cross sections were calculated to NLO in QCD [57], including the soft-gluon resummation at NNLL [58] for the Wt process.

JHEP03(2018)009

In the simulation of the Z+jets events for the $ZV \to \ell\ell qq$ search, jets are labelled according to the true flavours of the hadrons with $p_{\mathrm{T}} > 5\,\mathrm{GeV}$ found within a cone of size $\Delta R = \sqrt{(\Delta\eta)^2 + (\Delta\phi)^2} = 0.3$ around the reconstructed jet axes. If a b-hadron is found, the jet is labelled as a b-jet; if one is not found and a charmed hadron is found, the jet is labelled as a c-jet; if neither is found, the jet is labelled as a light (i.e., u-, d-, or s-quark, or gluon) jet. A simulated Z+jets event is labelled as Z+heavy-flavour if a b- or c-jet is found in the event, and otherwise as Z+light-flavour. The classification allows for flavour-dependent corrections for differences between data and MC.

MC events were processed with a detailed detector simulation [59] based on GEANT4 [60]. Additional inelastic simulated pp collisions generated with Pythia 8.186 were overlaid to model both the in- and out-of-time effects from additional pp collisions in the same and neighbouring bunch crossings (pile-up). MC samples were reweighted to match the pile-up conditions in the data. All simulated events were processed using the same reconstruction algorithms as the data.

4 Event reconstruction

Electrons are identified as isolated energy clusters in the electromagnetic calorimeter matched to ID tracks, with requirements that the transverse energy $E_{\mathrm{T}} > 7\,\mathrm{GeV}$ and pseudorapidity $|\eta| < 2.47$. A likelihood-based requirement [61] is imposed to reduce the background from misidentified or non-prompt electrons. Electrons are classified as either 'loose', 'medium' or 'tight' according to the likelihood-based identification criteria described in ref. [61].

Muons are reconstructed by a combined fit to the ID and MS tracks, and are required to have $p_{\mathrm{T}} > 7\,\mathrm{GeV}$ and $|\eta| < 2.5$. Muons must pass identification requirements, based on the numbers of hits in the ID and MS subsystems, and the significance of the difference $|q/p_{\mathrm{MS}} - q/p_{\mathrm{ID}}|$ [62], where q is the charge and p_{MS} (p_{ID}) is the momentum of the muon measured in the MS (ID). Similar to electrons, muons are classified as either 'loose', 'medium' or 'tight', following the criteria in ref. [62].

All electrons and muons are required to be isolated using selections on the sum of track p_{T} (excluding the track associated with the lepton) in a p_{T}-dependent cone around their directions. The isolation selection criteria are designed to maintain a constant efficiency of 99% in the p_{T}–η plane for the reconstructed leptons from $Z \to \ell\ell$ decays, and to minimise efficiency loss for highly boosted Z bosons in the relevant kinematic range. Furthermore, leptons are required to have associated tracks satisfying $|d_0/\sigma_{d_0}| < 5$ (3) and $|z_0 \times \sin\theta| < 0.5$ mm for electrons (muons), where d_0 is the transverse impact parameter with respect to the beam line, σ_{d_0} is its uncertainty, and z_0 is the distance between the longitudinal position of the track along the beam line at the point where d_0 is measured and the longitudinal position of the primary vertex.

Small-R jets are reconstructed using the anti-k_t algorithm [63, 64] with a radius parameter of $R = 0.4$. Energy- and η-dependent correction factors derived from MC simulations are applied to correct jets back to the particle level [65]. Jets are required to have $p_{\mathrm{T}} > 20\,\mathrm{GeV}$ for $|\eta| < 2.5$ and $p_{\mathrm{T}} > 30\,\mathrm{GeV}$ for $2.5 < |\eta| < 4.5$. Jets with $p_{\mathrm{T}} > 30\,\mathrm{GeV}$

JHEP03(2018)009

and $|\eta| < 2.5$ are called 'signal' jets. To suppress jets from pile-up interactions, a jet vertex tagger [66] is applied to jets with $p_{\mathrm{T}} < 60\,\mathrm{GeV}$ and $|\eta| < 2.4$, based on information about tracks associated with the primary vertex and pile-up vertices.

The 'signal' jets containing b-hadrons are identified using a multivariate algorithm (b-tagging) [67] which is based on information such as track impact-parameter significances and positions of explicitly reconstructed secondary decay vertices. The b-tagging is used for identifying $Z \to b\bar{b}$ decays. The chosen b-tagging algorithm has an efficiency of 70% for b-quark jets in simulated $t\bar{t}$ events, with a light-flavour jet rejection factor of about 380 and a c-jet rejection of about 12 [68]. Correction factors are applied to the simulated event samples to compensate for differences between data and simulation in the b-tagging efficiency for b-, c- and light-jets. The correction for b-jets is derived from $t\bar{t}$ events with final states containing two leptons, and the corrections are consistent with unity with uncertainties at the level of a few percent over most of the jet p_{T} range.

Large-R jets are reconstructed with the anti-k_t algorithm, but with the radius parameter increased to $R = 1.0$. To mitigate the effects of pile-up and soft radiation, the large-R jets are trimmed [69]. Trimming takes the original constituents of the jet and reclusters them using the k_t algorithm [70] with a smaller radius parameter, R_{subjet}, to produce a collection of subjets. These subjets are discarded if they carry less than a specific fraction (f_{cut}) of the original jet p_{T}. The trimming parameters optimised for this search are $R_{\mathrm{subjet}} = 0.2$ and $f_{\mathrm{cut}} = 5\%$. The large-R jet four-momenta are recomputed from the selected subjets, and the jet energies are calibrated to particle-level using correction factors derived from MC simulations [71]. The mass of a large-R jet (m_J) is computed using a combination of calorimeter and tracking information [72]. The large-R jets are required to have $p_{\mathrm{T}} > 200\,\mathrm{GeV}$ and $|\eta| < 2.0$.

A default ATLAS-wide overlap-removal procedure is applied to the selected leptons and jets to prevent double-counting. For nearby electrons and small-R jets, the jet is removed if the separation between the electron and jet is within $\Delta R < 0.2$; the electron is removed if the separation is within $0.2 < \Delta R < 0.4$. For nearby muons and small-R jets, the jet is removed if the separation between the muon and jet is within $\Delta R < 0.2$ and if the jet has less than three tracks or the energy and momentum differences between the muon and the jet are small; otherwise the muon is removed if the separation satisfies $\Delta R < 0.4$. To prevent double-counting of energy from an electron inside the large-R jet, the large-R jet is removed if the separation between the electron and the large-R jet is within $\Delta R < 1.0$.

Boson tagging [73, 74] is applied to the large-R jets to select those from the $V \to qq$ decays. A p_{T}-dependent requirement is applied to the jet substructure variable D_2, which is defined as a ratio of two- and three-point energy correlation functions [75, 76] that are based on the energies and pairwise angular distances of particles within a jet. This variable is optimised to distinguish between jets originating from a single parton and those coming from the two-body decay of a heavy particle. A detailed description of the optimisation can be found in refs. [73, 74]. The V boson jets are then selected by requiring the large-R jet mass m_J to be in a p_{T}-dependent window centred around the expected value of the boson mass from simulations. The boson tagging is designed

JHEP03(2018)009

to provide a constant efficiency (working point) independent of the large-R jet p_{T} for the signals studied. Two such working points, 50% efficiency and 80% efficiency, are used, with corresponding misidentification rates for jets from multijet production of $\sim 2\%$ and $\sim 10\%$, respectively. For the 50% working point, the width of the $W\,(Z)$ mass window varies from 23 (28) GeV at $p_{\mathrm{T}} = 500\,\mathrm{GeV}$ to 33 (37) GeV at $p_{\mathrm{T}} = 2000\,\mathrm{GeV}$; the maximum D_2 value for the $W\,(Z)$ tagger varies from 1.25 (1.22) at $p_{\mathrm{T}} = 500\,\mathrm{GeV}$ to 1.97 (1.85) at $p_{\mathrm{T}} \geq 2000\,\mathrm{GeV}$. For the 80% working point, the width of the $W\,(Z)$ mass window varies from 33 (42) GeV at $p_{\mathrm{T}} = 500\,\mathrm{GeV}$ to 54 (57) GeV at $p_{\mathrm{T}} = 2000\,\mathrm{GeV}$; the maximum D_2 value for the $W\,(Z)$ tagger varies from 1.92 (1.90) at $p_{\mathrm{T}} = 500\,\mathrm{GeV}$ to 2.76 (2.62) at $p_{\mathrm{T}} \geq 2000\,\mathrm{GeV}$.

The missing transverse momentum ($\vec{E}_{\mathrm{T}}^{\mathrm{miss}}$) is calculated as the negative vectorial sum of the transverse momenta of calibrated electrons, muons, and small-R jets. Large-R jets are not included in the $\vec{E}_{\mathrm{T}}^{\mathrm{miss}}$ calculation to avoid double-counting of energy between the small-R jets and large-R jets. Energy depositions due to the underlying event and other soft radiation are taken into account by constructing a 'soft term' from ID tracks associated with the primary vertex but not with any reconstructed object [77–79]. The track-based missing transverse momentum, $\vec{p}_{\mathrm{T}}^{\mathrm{miss}}$, is the negative vectorial sum of the transverse momenta of all good-quality inner detector tracks that are associated with the primary vertex.

5 $X \to ZV \to \ell\ell\,qq$ search

The $X \to ZV \to \ell\ell qq$ search explores the VBF and ggF production of a heavy Higgs boson H, the VBF and DY production of an HVT W' boson, and the ggF production of a bulk RS graviton G_{KK}. It also utilises both the merged and resolved reconstruction for the $V \to qq$ decay. The search begins with the identification of the $Z \to \ell\ell$ decay, followed by classifying events into the VBF or ggF/DY categories and finally the selection of either the $ZV \to \ell\ell J$ or $ZV \to \ell\ell jj$ final states. Multiple signal regions (SRs) are defined to enhance the sensitivity of the search. Figure 2 shows a schematic view of the selection. The event selection, the expected signal performance and background estimations are described below.

5.1 Selection of $Z \to \ell\ell$

The $Z \to \ell\ell$ candidates are identified by requiring two isolated same-flavour leptons (electrons or muons) satisfying the 'loose' criteria. The leading electron (muon) must satisfy E_{T} (p_{T}) $> 28\,\mathrm{GeV}$. Opposite charges are required for the muon pairs but not for the electron pairs. Electrons are more susceptible to charge misidentification due to the conversions of photons from bremsstrahlung, especially at high E_{T}. The dilepton invariant mass $m_{\ell\ell}$ is required to be consistent with the Z boson mass. For electrons, a fixed $m_{\ell\ell}$ window $[83, 99]\,\mathrm{GeV}$ is applied. To account for the effect of dimuon mass-resolution degradation at high transverse momentum ($p_{\mathrm{T}}^{\ell\ell}$), a $p_{\mathrm{T}}^{\ell\ell}$-dependent mass window $[85.6\,\mathrm{GeV} - 0.0117 p_{\mathrm{T}}^{\ell\ell},\ 94.0\,\mathrm{GeV} + 0.0185 p_{\mathrm{T}}^{\ell\ell}]$ is used for muons. For both electrons and muons, the mass windows are chosen to ensure that the $Z \to \ell\ell$ selection efficiency is approximately 95% and independent of the heavy resonance mass. Events with additional leptons passing the 'loose' criteria are vetoed.

JHEP03(2018)009

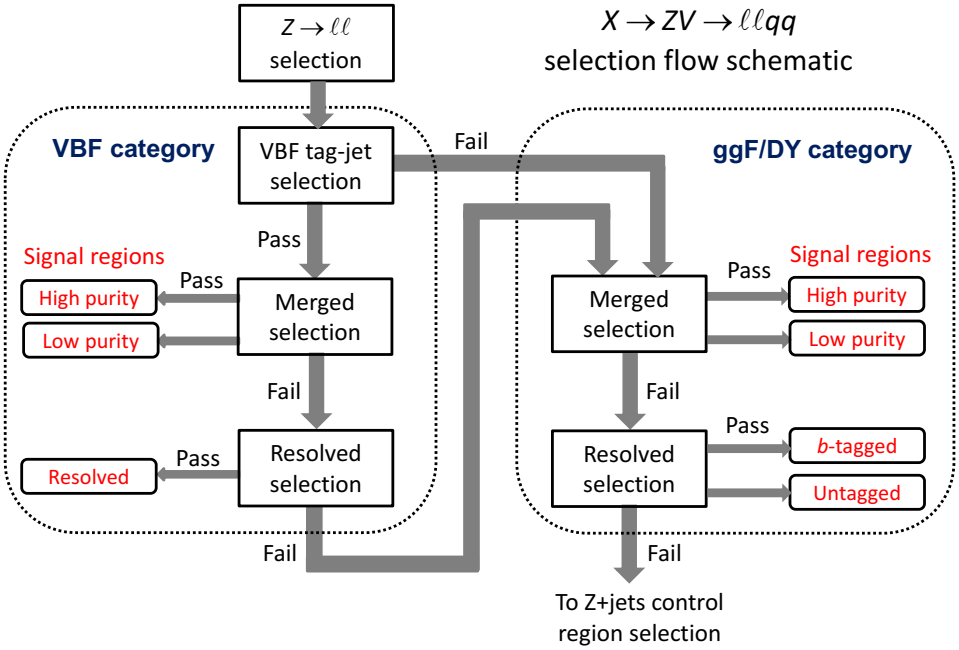

Figure 2. Illustration of the selection flow and seven signal regions of the $X \to ZV \to \ell\ell qq$ search. The VBF category is targeted for VBF production whereas the ggF/DY category is for the rest, including events failing the selection for the VBF category. The selected VBF tag-jets are removed from the subsequent selection for the VBF category. However, if an event fails to be selected for the VBF category, these jets are kept for the ggF/DY category selection. The $H \to ZZ$ search utilises all seven signal regions and the $W' \to ZW$ search uses six signal regions by combining the b-tagged and untagged regions of the ggF/DY category. The $G_{\mathrm{KK}} \to ZZ$ search bypasses the VBF selection, so it has only four signal regions.

5.2 VBF and ggF/DY categories

Signal events from VBF production possess unique kinematic signatures. In addition to the presence of a pair of vector bosons from the resonance decay, VBF events have two additional jets (referred to as tag-jets). These jets typically have a large separation in pseudorapidity and a large dijet invariant mass. They offer a powerful means for background rejection. Hence for the $H \to ZZ$ and $W' \to ZW$ searches, for which the VBF production is considered, two categories are introduced. Events are subject to the selection designed for VBF production first (VBF category), and if they fail, to the selection designed for ggF or DY production (ggF/DY category). For the $G_{\mathrm{KK}} \to ZZ$ search, the VBF selection is bypassed as VBF production is not considered.

For the VBF category, events are required to have two tag-jets identified from the small-R jets that fail the b-tagging described in section 4. The two jets must be in opposite pseudorapidity hemispheres, i.e., $\eta_1 \cdot \eta_2 < 0$, with a pseudorapidity separation $|\Delta\eta_{jj}^{\mathrm{tag}}| > 4.7$, and have an invariant mass $m_{jj}^{\mathrm{tag}} > 770\,\mathrm{GeV}$. Those values are chosen to optimise the search sensitivity to VBF signals for all masses considered. If there is more than one pair of jets satisfying these requirements, the one with the highest m_{jj}^{tag} value is chosen. These jets

JHEP03(2018)009

are not considered in the $ZV \to \ell\ell qq$ selection, and large-R jets lying $\Delta R < 1.5$ of either of these two small-R jets are not considered either.

For the ggF/DY category, no tag-jets requirement is applied. Events in the VBF and ggF/DY categories are subject to an identical $ZV \to \ell\ell qq$ selection. All events not selected for the VBF category are passed to the ggF/DY selection. This includes events that contain jets satisfying the VBF requirements but which fail the $ZV \to \ell\ell qq$ selection, cf. figure 2. In this case, jets excluded from consideration for the $ZV \to \ell\ell qq$ candidate in the VBF category are considered for the ggF/DY category.

5.3 Selection of $ZV \to \ell\ell qq$

Identification of $ZV \to \ell\ell qq$ decays proceeds by applying the merged $ZV \to \ell\ell J$ selection followed by the resolved $ZV \to \ell\ell jj$ selection. The order is motivated by a smaller background expectation in the $ZV \to \ell\ell J$ final states. These selection criteria are summarised in table 1 and are explained below.

5.3.1 Merged $ZV \to \ell\ell J$ selection

The $ZV \to \ell\ell J$ candidates are selected from the $Z \to \ell\ell$ events containing at least one large-R jet, among which the one with the highest p_{T} is assumed to be from the $V \to qq$ decay. Events are further required to have $\min(p_{\mathrm{T}}^{\ell\ell}, p_{\mathrm{T}}^{J})/m_{\ell\ell J} > 0.3$ for the $H \to ZZ$ search and > 0.35 for the $W' \to ZW$ and $G_{\mathrm{KK}} \to ZZ$ searches. The criteria are optimised to reduce backgrounds while retaining high efficiencies for signals. The looser requirement for the $H \to ZZ$ search is motivated by the expected softer $p_{\mathrm{T}}^{\ell\ell}$ and p_{T}^{J} spectra resulting from a spin-0 resonance. This requirement suppresses background significantly at large $m_{\ell\ell J}$ while maintaining high efficiencies for signal events.

Figure 3(a) shows the distribution of the large-R jet mass m_J of the $H \to ZZ$ search, comparing data with the expected backgrounds. Next the boson tagging discussed in section 4 is applied to select the $V \to qq$ decays. Two signal regions are defined, one for events passing the 50% working point of the boson tagging requirement and the other for events failing the 50% but passing the 80% working point requirement. The former is called the high-purity (HP) SR, and the latter the low-purity (LP) SR. Background contributions are mostly from the Z+jets, top quark and diboson production (section 5.5).

5.3.2 Resolved $ZV \to \ell\ell jj$ selection

The $ZV \to \ell\ell jj$ candidates are selected from the $Z \to \ell\ell$ events that have failed the $ZV \to \ell\ell J$ selection, by requiring at least two small-R 'signal' jets. The leading jet p_{T} is required to be greater than 60 GeV.

Similarly to the merged $ZV \to \ell\ell J$ selection, the kinematic quantity $\sqrt{\left(p_{\mathrm{T}}^{\ell\ell}\right)^2 + \left(p_{\mathrm{T}}^{jj}\right)^2} \Big/ m_{\ell\ell jj}$ is required to be greater than 0.4 for $H \to ZZ$ and 0.5 for $W' \to ZW$ and $G_{\mathrm{KK}} \to ZZ$. Here p_{T}^{jj} is the transverse momentum of the dijet system. Signal events are expected to have a dijet invariant mass, m_{jj}, consistent with a $V \to qq$ decay. Figure 3(b) shows the m_{jj} distributions of the $H \to ZZ$ search. The dijet invariant mass must be in the window [70, 105] GeV for $Z \to qq$ and in the window [62, 97] GeV for $W \to qq$. The choice of

JHEP03(2018)009

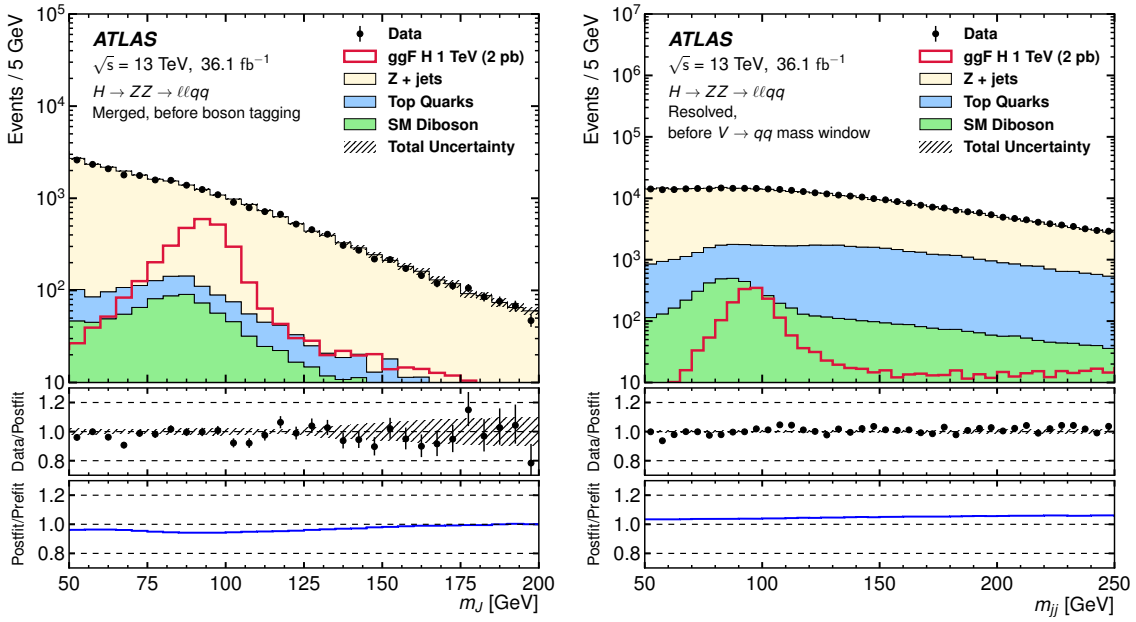

(a) (b)

Figure 3. Observed and expected distributions of (a) the large-R jet mass m_J of the $ZV \to \ell\ell J$ candidate and (b) the dijet mass m_{jj} of the $ZV \to \ell\ell jj$ candidate. These distributions are for the $H \to ZZ$ search before the identification of the $V \to qq$ decay, combining VBF and ggF/DY categories. Background contributions are obtained from the combined likelihood fit to the data, as explained in section 8. For illustration, expected distributions from the ggF production of a 1 TeV Higgs boson with $\sigma \times \mathcal{B}(H \to ZZ) = 2$ pb are also shown. The middle panes show the ratios of the observed data to the background predictions. The uncertainty in the total background prediction, shown as bands, combines statistical and systematic contributions. The bottom panes are the ratios of the post-fit and pre-fit background predictions.

asymmetric windows around m_V is motivated by the asymmetry of the m_{jj} distribution expected from $V \to qq$.

About 21% of the $Z \to qq$ decays have two b-quark jets, whereas the dominant background, Z+jets, has a smaller heavy-quark content. To exploit this, the $ZV \to \ell\ell jj$ candidates are divided into two signal regions: events with two b-tagged jets (b-tagged SR) and events with fewer than two b-tagged jets (untagged SR). Events with more than two b-tagged jets are rejected. No enhancement of b-tagged jets is expected from the $W \to qq$ decay, thus the two signal regions are combined for the $W' \to ZW$ search. Due to the small number of events, the two regions are also combined for the VBF category.

5.4 Signal regions, selection efficiencies and mass resolutions

Signal regions used in the search depend on the signal model under study. There are seven, six and four signal regions, respectively, for the searches for $H \to ZZ$, $W' \to ZW$ and $G_{\mathrm{KK}} \to ZZ$.

JHEP03(2018)009

Selection	$ZV \to \ell\ell J$	$ZV \to \ell\ell jj$
$Z \to \ell\ell$	Two opposite-flavour leptons with $p_{\mathrm{T}}(E_{\mathrm{T}}) > 7\,\mathrm{GeV}$	
	leading lepton with $p_{\mathrm{T}}(E_{\mathrm{T}}) > 28\,\mathrm{GeV}$	
	$83 < m_{ee} < 99\,\mathrm{GeV}$	
	$85.6\,\mathrm{GeV} - 0.0117 \times p_{\mathrm{T}}^{\ell\ell} < m_{\mu\mu} < 94.0\,\mathrm{GeV} + 0.0185 \times p_{\mathrm{T}}^{\ell\ell}$	
Tag-jet selection for VBF category	Two non-b-tagged small-R jets with $\eta_1 \cdot \eta_2 < 0$, $\left\lvert\Delta\eta_{jj}^{\mathrm{tag}}\right\rvert > 4.7$ and $m_{jj}^{\mathrm{tag}} > 770\,\mathrm{GeV}$	
Jet requirements	≥ 1 large-R jet with $p_{\mathrm{T}} > 200\,\mathrm{GeV}$	≥ 2 'signal' jets with $p_{\mathrm{T}} > 30\,\mathrm{GeV}$ $p_{\mathrm{T}} > 60\,\mathrm{GeV}$ for the leading jet no events with > 2 b-tagged jets
Kinematic criteria	$\min(p_{\mathrm{T}}^{\ell\ell}, p_{\mathrm{T}}^{J}) / m_{\ell\ell J}$	$\sqrt{\left(p_{\mathrm{T}}^{\ell\ell}\right)^2 + \left(p_{\mathrm{T}}^{jj}\right)^2} / m_{\ell\ell jj}$
H	> 0.3	> 0.4
W' or G_{KK}	> 0.35	> 0.5
V boson tagging	p_{T}-dependent criteria in D_2 and m_J	$70 < m_{jj} < 105\,\mathrm{GeV}$ $(V = Z)$ $62 < m_{jj} < 97\,\mathrm{GeV}$ $(V = W)$

Table 1. Summary of the $X \to ZV \to \ell\ell qq$ selection criteria.

Signal selection efficiencies are dependent on the signal model, the production process and the mass of the heavy resonance. As an example, figure 4 shows the acceptance times efficiency ($A \times \epsilon$) of the $H \to ZZ \to \ell\ell qq$ search as a function of the Higgs boson mass for both ggF and VBF production. The $ZV \to \ell\ell J$ selection is more efficient for masses over approximately 500 GeV, while the $ZV \to \ell\ell jj$ selection contributes more at lower masses. This reflects the expected large Lorentz boost of the Z bosons from heavy Higgs boson decays and the higher priority given to the $ZV \to \ell\ell J$ selection. The $A \times \epsilon$ values of the $W' \to ZW$ and $G_{\mathrm{KK}} \to ZZ$ searches are similar with the exception of noticeable decreases, by about 40% from 2 TeV to 4 TeV, due to the merging of the electrons from the $Z \to ee$ decays for resonance masses above approximately 3 TeV.

Distributions of the invariant masses $m_{\ell\ell J}$ and $m_{\ell\ell jj}$ are used to search for potential signals. To mitigate the impact of muon momentum-resolution degradation at high p_{T}, a scale factor of $m_Z/m_{\mu\mu}$ is applied to the four-momentum of the dimuon system in $Z \to \mu\mu$ events, effectively fixing its mass to $m_Z = 91.187\,\mathrm{GeV}$ [80]. The scaling improves the $m_{\ell\ell J}$ resolution of the dimuon final state by approximately 13% (40%) for a heavy Higgs boson at 1 (3) TeV. For the $ZV \to \ell\ell jj$ final states, a scale factor of m_V/m_{jj} is also applied to the dijet four-momentum to fix the dijet mass to m_V, 91.187 GeV for the Z boson and 80.385 GeV for the W boson [80]. The m_{jj} scaling improves the $m_{\ell\ell jj}$ resolution by approximately 14% for a 600 GeV Higgs boson. No m_V/m_J scale factor is applied to the $ZV \to \ell\ell J$ final states as the expected improvement in the $m_{\ell\ell J}$ resolution is negligible.

JHEP03(2018)009

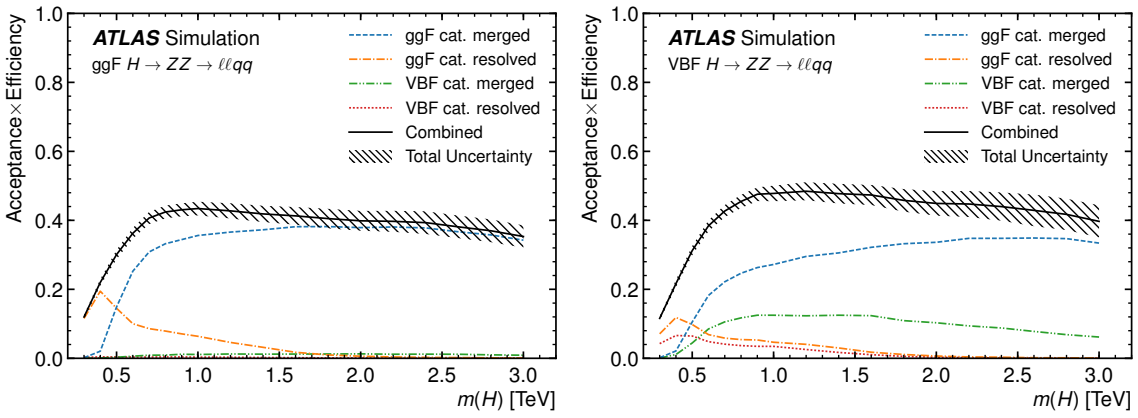

(a) (b)

Figure 4. Selection acceptance times efficiency for the $H \to ZZ \to \ell\ell qq$ events from MC simulations as a function of the Higgs boson mass for (a) ggF and (b) VBF production, combining the HP and LP signal regions of the $ZV \to \ell\ell J$ selection and the b-tagged and untagged regions of the $ZV \to \ell\ell jj$ selection. The hatched band represents the total statistical and systematic uncertainties.

The reconstructed $m_{\ell\ell J}$ and $m_{\ell\ell jj}$ distributions have widths of 2–3% of the resonance mass for the Higgs boson and HVT W' boson of VBF production for the entire mass range studied. Given the negligible intrinsic widths of these resonances, the widths largely reflect the detector resolution. For DY-produced HVT W' signal, the widths of the $m_{\ell\ell J}$ and $m_{\ell\ell jj}$ distributions are slightly larger at 3–4% since the W' boson in this production mode has an intrinsic width of approximately 2.6% of its mass. The widths of the $m_{\ell\ell J}$ and $m_{\ell\ell jj}$ distributions are 4% at 500 GeV for the bulk RS graviton signal with $k/\overline{M}_{\mathrm{Pl}} = 1$ and rise to 8% at 5000 GeV. The increase can be attributed to the increase in the intrinsic width of the signal. For a given resonance mass, the $m_{\ell\ell J}$ distributions are narrower than those of $m_{\ell\ell jj}$.

5.5 Data control regions and background estimation

The dominant backgrounds to the $X \to ZV \to \ell\ell qq$ search are the Z+jets, top quark and diboson processes. Their contributions are estimated from a combination of MC and data-driven techniques. In all cases, the shapes of kinematic variables, including those of the final discriminants $m_{\ell\ell J}$ and $m_{\ell\ell jj}$, are taken from MC simulations. The multijet background is estimated to be negligible.

The Z+jets events are expected to have smooth distributions of m_J and m_{jj}, while the signal events should exhibit resonance structures at the mass of the vector-boson V. Thus, a Z+jets control region (CR) is defined for every signal region by reversing the m_J or m_{jj} requirement. Events in the control regions are selected in exactly the same way as those in their corresponding signal regions except for the requirement on m_J or m_{jj}. For the $ZV \to \ell\ell J$ selection, the leading large-R jet mass is required to be outside the large-R jet mass window of the 80% working point of the boson tagging. For the $ZV \to \ell\ell jj$ selection,

JHEP03(2018)009

$V \to qq$ recon.	Signal regions	H (1 TeV) ggF	H (1 TeV) VBF	Background estimates Z+jets	Background estimates Diboson	Background estimates Top quarks	Background estimates Total	Data
VBF category								
Merged	HP	0.42 (±) 0.08	5.1 (±) 1.0	29.0 (±) 2.6	3.8 (±) 0.6	1.1 (±) 0.4	33.9 (±) 2.7	32
	LP	0.33 (±) 0.08	3.4 (±) 0.4	113 (±) 7	8.4 (±) 1.2	1.8 (±) 0.6	123 (±) 7	109
Resolved		0.23 (±) 0.05	2.3 (±) 0.4	1307 (±) 34	60 (±) 9	66 (±) 7	1433 (±) 34	1434
ggF/DY category								
Merged	HP	14.2 (±) 1.6	11.0 (±) 2.1	1728 (±) 34	177 (±) 21	20.6 (±) 2.2	1926 (±) 32	1906
	LP	10.0 (±) 0.9	7.5 (±) 0.8	6060 (±) 60	285 (±) 31	69 (±) 6	6420 (±) 60	6375
Resolved	b-tagged	1.02 (±) 0.12	0.62 (±) 0.08	1740 (±) 40	167 (±) 22	908 (±) 24	2810 (±) 40	2843
	Untagged	3.31 (±) 0.34	2.5 (±) 0.5	82200 (±) 400	2280 (±) 250	1500 (±) 130	86030 (±) 280	85928

Table 2. Numbers of events observed in the data and predicted for background processes from background-only fits to the signal and control regions (section 8) in the seven signal regions of the $H \to ZZ \to \ell\ell qq$ search. The numbers of signal events expected from the ggF and VBF production of a heavy Higgs boson with mass of 1 TeV are also shown. The signal yields are calculated using $\sigma \times \mathcal{B}(H \to ZZ) = 20\,\text{fb}$ for both processes. The uncertainties combine statistical and systematic contributions. The fit constrains the background estimate towards the observed data, which reduces the total background uncertainty by correlating those from the individual backgrounds.

a requirement of $50 < m_{jj} < 62\,\text{GeV}$ or $105 < m_{jj} < 150\,\text{GeV}$ is applied. These CRs are dominated by the Z+jets contribution, with a purity higher than 96% in all regions, except for the b-tagged CR where the top quark and Z+jets contributions are comparable. They are therefore used to constrain its contribution in signal regions through simultaneous fits as discussed in section 8.

Top quark production is a significant background source in the b-tagged signal region of the resolved $ZV \to \ell\ell jj$ selection. Its contribution is constrained using a top-quark-enhanced control region. Events in this control region must have two different-flavour leptons, $e\mu$, with their invariant mass within $[76, 106]\,\text{GeV}$, and two b-tagged jets with their invariant mass in the range $[50, 150]\,\text{GeV}$. The leading b-tagged jet is required to have $p_{\text{T}} > 60\,\text{GeV}$. This selection yields a sample of top quark events with a purity higher than 99%. This top quark control region is used to constrain top quark contributions for all signal regions.

Diboson production, mainly from the SM ZZ and ZW processes, is also a significant background source. The contribution from those processes is estimated completely from MC simulation.

As an example, table 2 shows the numbers of events observed in the data and estimated from background processes in the seven signal regions of the $H \to ZZ \to \ell\ell qq$ search. The numbers of background events are extracted through a background-only fit of the signal and control regions discussed in section 8.

JHEP03(2018)009

6 $X \to ZV \to \nu\nu\, qq$ search

Events containing a $X \to ZV \to \nu\nu qq$ signal are characterised by a hadronically decaying V boson recoiling against a large missing transverse momentum. Only the merged reconstruction of the $V \to qq$ decay is considered. The selection closely follows that of the $X \to ZV \to \ell\ell qq$ search as illustrated in figure 2 with additional requirements to remove multijet backgrounds but without the resolved selection.

6.1 Selection of $ZV \to \nu\nu qq$

An initial selection is made by requiring $E_{\mathrm{T}}^{\mathrm{miss}} > 250$ GeV, and vetoing events with electrons or muons passing the 'loose' quality requirements. The multijet background, originating primarily from the presence of mismeasured jets, and non-collision backgrounds are suppressed by using a track-based missing transverse momentum, $\vec{p}_{\mathrm{T}}^{\,\mathrm{miss}}$, as defined in section 4. The requirements are $p_{\mathrm{T}}^{\mathrm{miss}} > 50\,\mathrm{GeV}$ and the azimuthal separation between $\vec{E}_{\mathrm{T}}^{\mathrm{miss}}$ and $\vec{p}_{\mathrm{T}}^{\,\mathrm{miss}}$ directions satisfies $\Delta\phi(\vec{E}_{\mathrm{T}}^{\mathrm{miss}}, \vec{p}_{\mathrm{T}}^{\,\mathrm{miss}}) < 1$. An additional requirement is imposed on the azimuthal separation between the directions of $\vec{E}_{\mathrm{T}}^{\mathrm{miss}}$ and the nearest small-R jet with $\min[\Delta\phi(\vec{E}_{\mathrm{T}}^{\mathrm{miss}}, \text{small}-R \text{ jet})] > 0.4$. The multijet background is found to be negligible after these selections.

As in the $\ell\ell qq$ search, both the VBF and ggF categories are considered in the signal event selection for the $H \to ZZ$ and $W' \to ZW$ searches; the VBF selection is not motivated by the $G_{\mathrm{KK}} \to ZZ$ search. The VBF tag-jets are selected in the same manner as in the $\ell\ell qq$ search, but they are required to satisfy $m_{jj}^{\mathrm{tag}} > 630\,\mathrm{GeV}$ and $|\Delta\eta_{jj}^{\mathrm{tag}}| > 4.7$. Those values are chosen to optimise the search sensitivity for signals from VBF production, considering all signal masses. Events failing the VBF tag-jets selection are kept in the ggF category. For both the VBF and ggF categories, events are then subject to the selections described below.

Unlike the $\ell\ell qq$ search, this search utilises only the merged selection of the $V \to qq$ decay, i.e., considering only the $ZV \to \nu\nu J$ final state, since the resolved selection has little acceptance for the given high $E_{\mathrm{T}}^{\mathrm{miss}}$ trigger threshold. The selection of the large-R jets and the boson tagging are identical to those of the $\ell\ell qq$ search and are described in section 4. Similarly, candidate events are split into HP and LP signal regions. The $H \to ZZ$ search and the $W' \to ZW$ search use all the four signal regions, while the $G_{\mathrm{KK}} \to ZZ$ search bypasses the VBF selection, so has only two signal regions. The distributions of the mass and D_2 of the leading large-R jet before the boson tagging are shown in figure 5. There is a small overprediction of the background at high mass region, but those events are not selected in any signal regions and sidebands. The selection criteria for the $\nu\nu qq$ search are summarised in table 3.

It is not possible to fully reconstruct the invariant mass of the $\nu\nu J$ system due to the presence of neutrinos in the final state, so the transverse mass is used as the final discriminant:

$$m_{\mathrm{T}} = \sqrt{\left(E_{\mathrm{T},J} + E_{\mathrm{T}}^{\mathrm{miss}}\right)^2 - \left(\vec{p}_{\mathrm{T},J} + \vec{E}_{\mathrm{T}}^{\mathrm{miss}}\right)^2},$$

JHEP03(2018)009

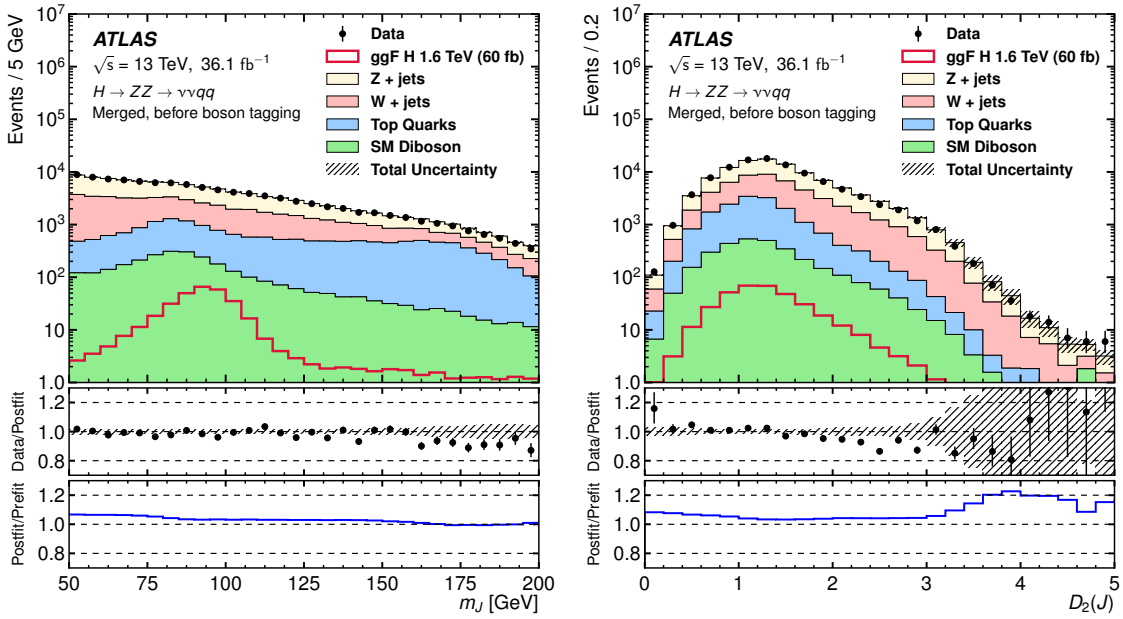

(a) (b)

Figure 5. Observed and expected distributions of (a) mass of the large-R jet and (b) D_2 of the large-R jet in $ZV \to \nu\nu J$ candidates in the ggF category. All selections other than the requirements on the mass and D_2 are applied. Background contributions in these distributions are after applying the combined likelihood fit to the data, as explained in section 8. For illustration, expected distributions from the ggF production of a 1.6 TeV Higgs boson with $\sigma \times \mathcal{B}(H \to ZZ) = 60\,\text{fb}$ are also shown. The middle panes show the ratios of the observed data to the background predictions. The uncertainty in the total background prediction, shown as bands, combines statistical and systematic contributions. The bottom panes are the ratios of the post-fit and pre-fit background predictions.

$Z \to \nu\nu$	$E_{\text{T}}^{\text{miss}} > 250\,\text{GeV}$
Multijet removal	$p_{\text{T}}^{\text{miss}} > 50\,\text{GeV}$ $\Delta\phi(\vec{E}_{\text{T}}^{\text{miss}}, \vec{p}_{\text{T}}^{\text{miss}}) < 1$ $\min[\Delta\phi(\vec{E}_{\text{T}}^{\text{miss}}, \text{small}-R\text{ jet})] > 0.4$
Tag-jet selection for VBF category	Two non-b-tagged small-R jets with $\eta_1 \cdot \eta_2 < 0$, $\left\lvert\Delta\eta_{jj}^{\text{tag}}\right\rvert > 4.7$ and $m_{jj}^{\text{tag}} > 630\,\text{GeV}$
Jet requirements	≥ 1 large-R jet with $p_{\text{T}} > 200\,\text{GeV}$
V boson tagging	p_{T}-dependent criteria on D_2 and m_J

Table 3. Summary of the $X \to ZV \to \nu\nu qq$ selection criteria.

where $E_{\text{T},J} = \sqrt{m_J^2 + p_{\text{T},J}^2}$. The resolution of the transverse mass is about 10% of the signal mass and the ratio of the resolution to the signal mass has little dependence on the signal model or the resonance mass.

JHEP03(2018)009

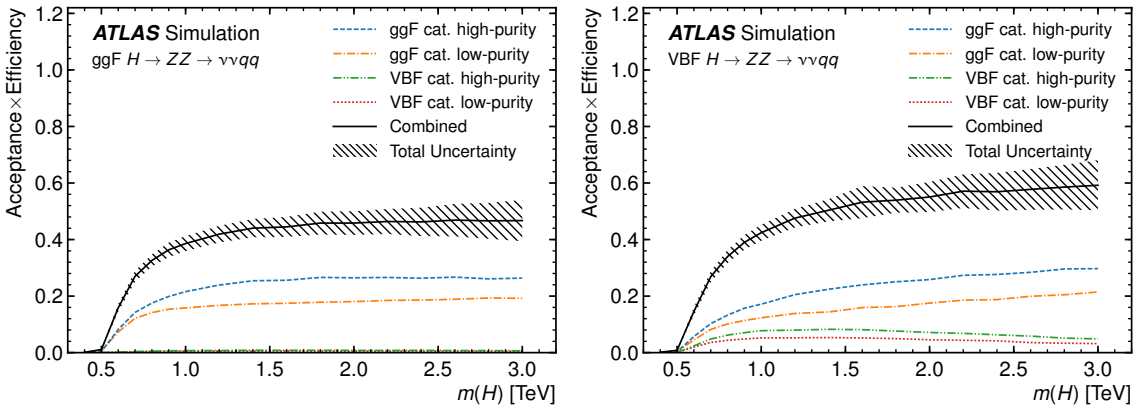

(a) (b)

Figure 6. Selection acceptance times efficiency for the $H \to ZZ \to \nu\nu qq$ events from MC simulations as a function of the Higgs boson mass for (a) ggF and (b) VBF production, combining the HP and LP signal regions. The hatched band represents the total statistical and systematic uncertainties.

The signal selection efficiency strongly depends on the signal model and the mass of the resonance. As an example, figure 6 shows the selection acceptance times efficiency as a function of $m(H)$ for $H \to ZV \to \nu\nu qq$. Similar results are obtained for the $W' \to ZW$ and $G_{\mathrm{KK}} \to ZZ$ searches.

6.2 Background estimation

The main backgrounds for this search arise from Z+jets, W+jets and $t\bar{t}$ production. Data control regions are defined to check the modelling of each contribution. As in the $\ell\ell qq$ search, the shapes of kinematic variables, including the final discriminant m_{T}, are taken from MC simulations.

The normalisation of the Z+jets background is determined using the Z+jets control region from the $\ell\ell qq$ search (section 5.5). Control regions specific to the $\nu\nu qq$ search are also defined to constrain the W+jets and top quark backgrounds. Events in these control regions are selected in the same way as those in the signal regions except that they must have exactly one muon passing the 'tight' quality requirement. These events are then split into the top quark and W+jets control regions according to the number of b-tagged jets that do not overlap with the large-R jet. Events in the top quark control region must have at least one b-tagged jet and events in the W+jets control region must not have any b-tagged jets. For the W+jets control region, the jet mass requirement used in the signal region selection is inverted, to ensure that there is no resonant diboson signal contamination via $X \to WV \to \ell\nu qq$ decay, while for the top quark control region, the leading large-R jet is required to be consistent with the mass of the W boson.

For the W+jets and top quark CRs, the muon is treated as a missing particle to make the boson p_{T} acceptance more similar to the signal region, and because the trigger does not include muons in the $E_{\mathrm{T}}^{\mathrm{miss}}$ calculation. Specifically, $E_{\mathrm{T,no}\ \mu}^{\mathrm{miss}}$ ($p_{\mathrm{T,no}\ \mu}^{\mathrm{miss}}$) is computed by

JHEP03(2018)009

Signal regions	H (1.6 TeV)		Background estimates					Data
	ggF	VBF	Z+jets	W+jets	Diboson	Top quarks	Total	
VBF category								
HP	0.49 (±) 0.15	4.9 (±) 1.1	35.0 (±) 3.3	25 (±) 4	6.7 (±) 1.1	37 (±) 4	104 (±) 6	105
LP	0.36 (±) 0.09	3.2 (±) 0.5	137 (±) 10	94 (±) 13	12.7 (±) 2.0	70 (±) 8	315 (±) 13	335
ggF category								
HP	15.5 (±) 3.3	14.5 (±) 3.2	2880 (±) 80	1990 (±) 100	490 (±) 60	1500 (±) 90	6870 (±) 70	6888
LP	10.6 (±) 1.5	9.7 (±) 1.4	11160 (±) 210	7200 (±) 300	830 (±) 90	2710 (±) 180	21910 (±) 140	21936

Table 4. Numbers of events predicted from background processes and observed in the data in the signal regions of the $H \to ZZ \to \nu\nu qq$ search from the background-only fit of both the signal and control regions (section 8). The numbers of signal events expected from a Higgs boson with mass of 1.6 TeV are also shown. The signal yields are calculated assuming $\sigma \times \mathcal{B}(H \to ZZ) = 6$ fb for both ggF and VBF at 1.6 TeV. The uncertainties combine statistical and systematic contributions.

removing the muon p_{T} contribution from the $E_{\mathrm{T}}^{\mathrm{miss}}$ ($p_{\mathrm{T}}^{\mathrm{miss}}$) calculation. The requirements on $E_{\mathrm{T}}^{\mathrm{miss}}$ and $p_{\mathrm{T}}^{\mathrm{miss}}$ in the signal regions are used for $E_{\mathrm{T,no}\ \mu}^{\mathrm{miss}}$ and $p_{\mathrm{T,no}\ \mu}^{\mathrm{miss}}$ respectively for the control regions.

Table 4 summarises the numbers of events observed in the data and estimated from background processes in the signal regions from the background-only fit of both the signal and control regions discussed in section 8. The expected numbers of events from both ggF and VBF production of a 1.6 TeV heavy Higgs boson, assuming $\sigma \times \mathcal{B}(H \to ZZ) = 6$ fb, are also included for comparison.

7 Systematic uncertainties

Systematic uncertainty sources impacting the search can be divided into three categories: experimental uncertainties related to the detector or to the reconstruction algorithms, uncertainties in the estimations of background contributions, and uncertainties in modelling the signal. Unless explicitly stated, the uncertainties quoted below are the uncertainties in the quantities themselves, not the impact on the search sensitivity.

The uncertainty in the integrated luminosity of the dataset is determined to be 3.2%. It is derived, following a methodology similar to the one detailed in ref. [81], from a preliminary calibration of the luminosity scale using a pair of x–y beam-separation scans performed in August 2015 and May 2016. This uncertainty is applied to the normalisation of the signal and also to background contributions whose normalisations are derived from MC simulations. A variation in the pile-up reweighting of MC events is included to cover the uncertainty in the ratio of the predicted and measured inelastic cross section in ref. [82].

The efficiencies of the lepton triggers for events with selected leptons are high, nearly 100% in the electron channel and approximately 96% in the muon channel. The corresponding uncertainties are negligible. For the selection used in the $\nu\nu qq$ search, the efficiency of the $E_{\mathrm{T}}^{\mathrm{miss}}$ trigger is also close to 100% with negligible associated uncertainty. The modelling of the electron and muon reconstruction, identification and isolation efficiencies is studied with a tag-and-probe method using $Z \to \ell\ell$ events in data and simulation

JHEP03(2018)009

at $\sqrt{s} = 13$ [83, 84]. Small corrections are applied to the simulation to better model the performance seen in data. These corrections have associated uncertainties of the order of 1%. For the $\nu\nu qq$ search, the uncertainty is instead in the efficiency of the lepton veto, and is at the sub-percent level. Uncertainties in the lepton energy (or momentum) scale and resolution are also taken into account.

Uncertainties in the jet energy scale and resolution for small-radius jets are estimated using MC simulation and *in situ* techniques [65]. For central jets ($|\eta| < 2.0$), the total uncertainty in the jet energy scale ranges from about 6% for jets with $p_{\mathrm{T}} = 25$ GeV to about 2% for $p_{\mathrm{T}} = 1$ TeV. There is also an uncertainty in the jet energy resolution [85], which ranges from 10% to 20% for jets with a p_{T} of 20 GeV to less than 5% for jets with $p_{\mathrm{T}} > 200$ GeV. Uncertainties in the lepton and jet energy scales and resolutions are propagated into the uncertainty in $E_{\mathrm{T}}^{\mathrm{miss}}$. Uncertainties in the energy scale and resolution of the track soft term are also propagated into the uncertainty in $E_{\mathrm{T}}^{\mathrm{miss}}$ [79], which is about 2% for the $\nu\nu qq$ search. Uncertainties in the efficiency for tagging b-jets and in the rejection factor for light jets are determined from $t\bar{t}$ samples [86, 87].

The uncertainties in the scale of the large-R jet p_{T}, mass and D_2 are of the order of 2–5%. They are estimated using comparisons of data and simulation in ref. [73]. An absolute uncertainty of 2% is assigned to the large-R jet energy resolution, and relative uncertainties of 20% and 15% are assigned to the resolution of the large-R jet mass and D_2, respectively.

For the $\ell\ell qq$ search the uncertainty in the spectrum of the final discriminant, $m_{\ell\ell J}$ or $m_{\ell\ell jj}$, for Z+jets, is assessed by comparing the shape difference between data and MC simulations in the control regions. The uncerainty is found to be approximately 20% for $m_{\ell\ell jj}$ and varies from 3% at low mass to 20% at high mass for $m_{\ell\ell J}$. For the $\nu\nu qq$ search the uncertainty in the modelling of the m_{T} distribution for Z+jets and W+jets production is assessed by comparing the nominal Sherpa MC sample with alternative samples generated by doubling or halving the renormalisation, resummation and factorisation scales independently and varying the matrix-element matching. The uncertainties are of the order of 5–30%. The approach is different from that used in the $\ell\ell qq$ search, since it is difficult to obtain a pure control region for Z+jets or W+jets in the $\nu\nu qq$ search.

An uncertainty in the shape of the $m_{\ell\ell J}$ or m_{T} distribution for the $t\bar{t}$ background is derived by comparing the Powheg-Box sample with the distribution obtained using MadGraph5_aMC@NLO 2.2.2. This uncertainty is found to be approximately 15%. Additional systematic uncertainties are estimated by comparing the nominal sample showered with Pythia 6.428 using the P2012 tune to one showered with Herwig++ 2.7.1 [88] and using the UEEE5 underlying-event tune. The uncertainty varies between 10–40%. Samples of $t\bar{t}$ events with the factorisation and renormalisation scales doubled or halved are compared to the nominal, and the differences observed are taken as an additional uncertainty. These uncertainties are small, typically less than 3%.

The uncertainties in the diboson cross sections are estimated to be 10% [41, 89], and the shape uncertainty is obtained by comparing MC samples generated by Sherpa and Powheg-Box.

JHEP03(2018)009

The signals acceptance uncertainty due to PDF uncertainties is estimated by taking the uncertainty from the PDF error sets, CT10 for the heavy Higgs boson signal and NNPDF23LO for the HVT and bulk RS signals, and adding it in quadrature to the acceptance difference obtained with the use of alternative PDF sets: MMHT2014LO [90] and NNPDF30NLO [91] for the Higgs boson, and CT10 and MMHT2014LO for the HVT and bulk RS graviton. For the HVT signal, the uncertainty ranges from 1% (2%) to 6% (12%) for the $\ell\ell qq$ ($\nu\nu qq$) search depending on the mass being tested. Similar results are obtained for the heavy Higgs boson signal, while for the bulk RS signal, the uncertainty is generally less than 1%. The signal acceptance uncertainty due to initial- and final-state radiation (ISR/FSR) is estimated by varying relevant parameters in the A14-NNPDF tune [39] for the HVT and bulk RS signals. This uncertainty ranges from less than 1% to 4% (6%) for the $\ell\ell qq$ ($\nu\nu qq$) search depending on the mass being tested. The effect of the QCD scale uncertainty on the heavy Higgs boson signal acceptance is estimated by varying the factorisation and renormalisation scales. It ranges from 1% (2%) to 4% (8%) for the $\ell\ell qq$ ($\nu\nu qq$) search depending on the mass being tested.

8 Results

8.1 Statistical and fit procedures

The statistical analysis is based on the framework described in refs. [92–94]. A binned likelihood function $\mathcal{L}(\mu, \theta)$ is constructed as a product of Poisson probability terms over all bins of the fit templates considered in the search. This function depends on the signal-strength parameter μ, a multiplicative factor applied to the theoretical signal production cross section, and θ, a set of nuisance parameters that encode the effects of systematic uncertainties in the signal and expected backgrounds, described in section 7. The binning is chosen based on the expected mass resolution and numbers of events. The nuisance parameters are either free to float, or constrained using Gaussian terms defined by external studies. The likelihood function for the combination of the $\ell\ell qq$ and $\nu\nu qq$ channels is the product of the Poisson likelihoods of these individual channels. However, only one constraint term per common nuisance parameter is included in the product.

For each signal process considered, a simultaneous maximum-likelihood fit is performed to the observed distributions of the final discriminants in the signal regions, $m_{\ell\ell J}$ or $m_{\ell\ell jj}$ for the $X \to ZV \to \ell\ell qq$ search and m_{T} for the $X \to ZV \to \nu\nu qq$ search, to extract the signal rate information. The shapes of the signal distributions are interpolated using the moment-morphing method [95] for intermediate mass points where simulated signal samples are not available. The product of acceptance and efficiency for each interpolated signal mass point is obtained from an interpolation with cubic splines between the simulated mass points. The Z+jets, W+jets and top quark control regions are included in the fit's likelihood calculation with one bin per region, i.e., using only their event-count information. Background contributions, including their shapes in the signal regions, are taken from MC simulations. However, they are allowed to vary independently within their uncertainties in each bin. Moreover, normalisation scale factors (SFs) are applied to the MC estimates of the Z+jets, W+jets and top quark contributions. These scale factors are free parameters in

JHEP03(2018)009

the fit and are therefore constrained by the data in both the signal and control regions. The diboson contribution is constrained to the theoretical estimate within the corresponding uncertainties.

In general, one SF is introduced per control region for its intended background component with the following exceptions to take into account different MC modellings in the different phase spaces of the same background component. One common Z+jets SF is used for HP and LP regions of the merged selection of both the $ZV \to \ell\ell qq$ and $ZV \to \nu\nu qq$ searches. However, independent SFs are used for the VBF and ggF categories. For the resolved $ZV \to \ell\ell qq$ selection, two independent Z+jets SFs are used for the b-tagged and untagged regions: one for the Z+heavy-flavour component and the other for the Z+light-jet component (section 3). The $ZV \to \ell\ell qq$ search defines a top quark control region and consequently applies one top quark SF to all regions. The $ZV \to \nu\nu qq$ search shares the Z+jets control regions with $ZV \to \ell\ell qq$ and hence applies the same SFs to its Z+jets background contributions. The $ZV \to \nu\nu qq$ search has its own W+jets and top quark control regions. Similar to Z+jets, one common W+jets SF is used for HP and LP regions, but independent SFs are used for the VBF and ggF categories. All the top quark control regions in the $ZV \to \nu\nu qq$ search share one common SF and it is distinguished from the top quark SF in the $ZV \to \ell\ell qq$ search.

The test statistic q_μ is defined as the profile likelihood ratio [96], $q_\mu = -2\ln(\mathcal{L}(\mu, \hat{\hat{\theta}}_\mu)/\mathcal{L}(\hat{\mu}, \hat{\theta}))$, where $\hat{\mu}$ and $\hat{\theta}$ are the values of the parameters that maximise the likelihood function (with the constraint $0 \leq \hat{\mu} \leq \mu$), and $\hat{\hat{\theta}}_\mu$ are the values of the nuisance parameters that maximise the likelihood function for a given value of μ. The test statistic q_μ is used to measure the compatibility of the observed data with the background-only hypothesis. In the absence of a signal, constraints on the production of a heavy resonance decaying into ZV pairs are derived. The exclusion limits are calculated with a modified frequentist method [97], also known as $\mathrm{CL_s}$, in the asymptotic approximation [98] for resonance masses below 2 TeV. Above 2 TeV, the small number of events makes the asymptotic approximation unreliable and the limits are calculated using pseudo-experiments. All limits are set at the 95% confidence level (CL).

8.2 Limits on the production of heavy resonances

The observed distributions of $m_{\ell\ell J}$ or $m_{\ell\ell jj}$ from the $H \to ZZ \to \ell\ell qq$ search are compared with the background estimates in figure 7 for the three signal regions of the VBF category and in figure 8 for the four signal regions of the ggF category. Similarly, figures 9 and 10 show the m_{T} distributions from the $H \to ZZ \to \nu\nu qq$ search in the signal regions of the VBF and ggF categories, respectively. There are no events in the data beyond the ranges of the distributions shown. Background contributions shown are obtained from background-only fits described previously. The numbers of events observed and estimated in control regions are summarised in figure 11.

The data distributions are reasonably well reproduced by the estimated background contributions in all these distributions. Similar levels of agreement are observed for the $W' \to ZW$ and $G_{\mathrm{KK}} \to ZZ$ searches. The largest difference between the observed data

JHEP03(2018)009

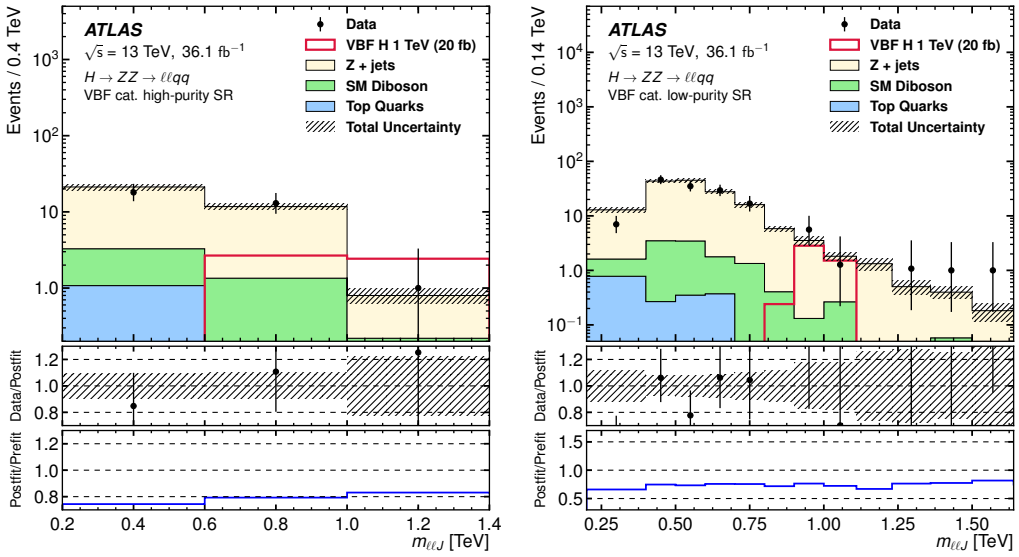

(a) (b)

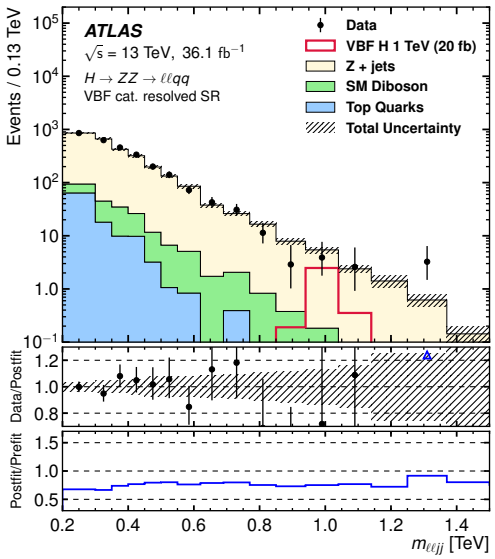

(c)

Figure 7. Comparisons of the observed data and expected background distributions of the final discriminants of the VBF category for the $H \to ZZ \to \ell\ell qq$ search: $m_{\ell\ell J}$ of (a) high-purity and (b) low-purity signal regions; (c) $m_{\ell\ell jj}$ of the resolved signal region. For illustration, expected distributions from the VBF production of a 1 TeV Higgs boson with $\sigma \times \mathcal{B}(H \to ZZ) = 20\,\text{fb}$ are also shown. The middle panes show the ratios of the observed data to the background predictions. The uncertainty in the total background prediction, shown as bands, combines statistical and systematic contributions. The blue triangles in the middle panes indicate bins where the ratio is nonzero and outside the vertical range of the plot. The bottom panes show the ratios of the post-fit and pre-fit background predictions.

JHEP03(2018)009

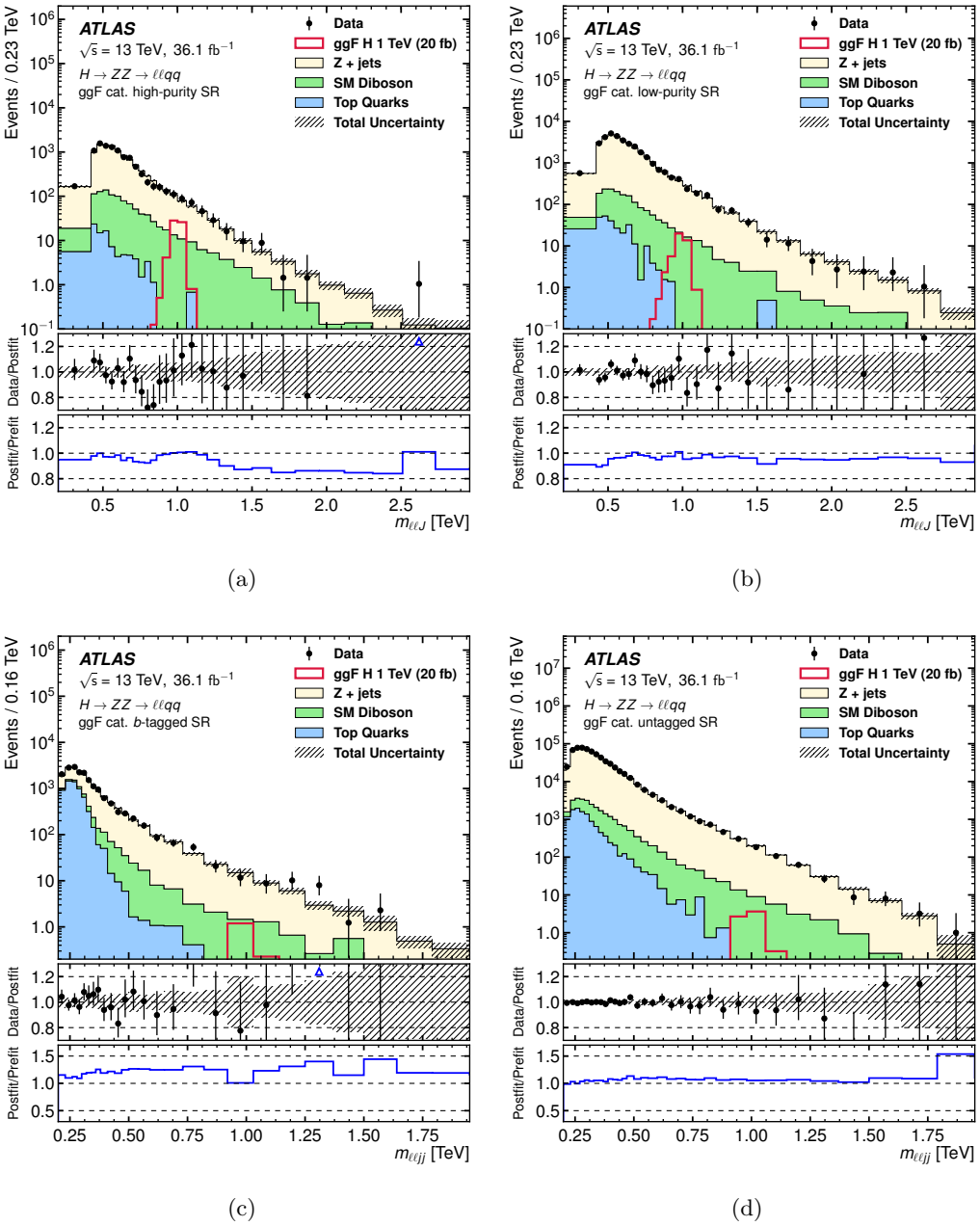

Figure 8. Comparisons of the observed data and expected background distributions of the final discriminants of the ggF category for the $H \to ZZ \to \ell\ell qq$ search: $m_{\ell\ell J}$ of (a) high-purity and (b) low-purity signal regions; $m_{\ell\ell jj}$ of (c) b-tagged and (d) untagged signal regions. For illustration, expected distributions from the ggF production of a 1 TeV Higgs boson with $\sigma \times \mathcal{B}(H \to ZZ) = 20\,\text{fb}$ are also shown. The middle panes show the ratios of the observed data to the background predictions. The uncertainty in the total background prediction, shown as bands, combines statistical and systematic contributions. The blue triangles in the middle panes indicate bins where the ratio is nonzero and outside the vertical range of the plot. The bottom panes show the ratios of the post-fit and pre-fit background predictions.

JHEP03(2018)009

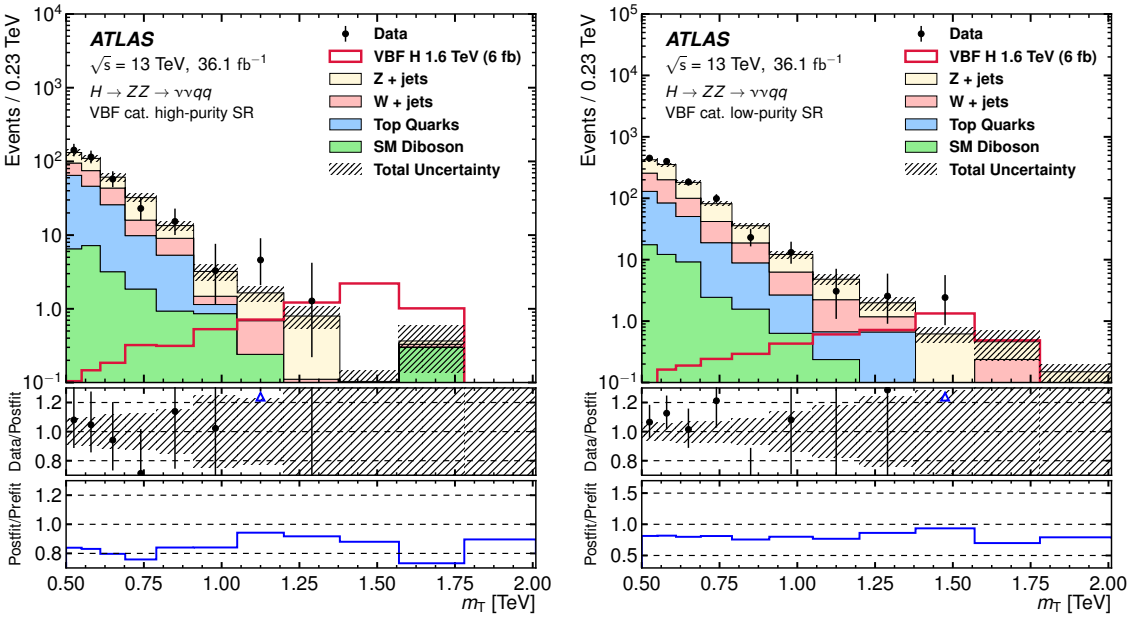

(a) (b)

Figure 9. Comparisons of the observed data and expected background distributions of m_{T} in the VBF category of the $H \to ZZ \to \nu\nu qq$ search: (a) high-purity and (b) low-purity signal regions. For illustration, expected distributions from the VBF production of a 1.6 TeV Higgs boson with $\sigma \times \mathcal{B}(H \to ZZ) = 6\,\mathrm{fb}$ are also shown. The middle panes show the ratios of the observed data to the background predictions. The uncertainty in the total background prediction, shown as bands, combines statistical and systematic contributions. The blue triangles in the middle panes indicate bins where the ratio is nonzero and outside the vertical range of the plot. The bottom panes show the ratios of the post-fit and pre-fit background predictions.

and the SM background prediction is in the $H \to ZZ \to \ell\ell qq$ search, high-purity signal region, as shown in figure 8(a). A deficit in data is seen around $m_{\ell\ell J}$ of 800 GeV, with a local significance of 3.0σ, and by taking into account the look-elsewhere effect [99] in the full $m_{\ell\ell J}$ spectrum, a global significance of 1.9σ. Upper limits are set on the product of the production cross section of new resonances and their decay branching ratio to ZV, $\sigma \times \mathcal{B}(X \to ZV)$.

Limits are presented for both the ggF and VBF productions of $H \to ZZ$ in figure 12 in the resonance mass range between 300 GeV and 3 TeV. The observed limit on $\sigma \times \mathcal{B}(H \to ZZ)$ varies from 1.7 (0.42) pb at 300 GeV to 1.4 (1.1) fb at 3 TeV for ggF (VBF) $H \to ZZ$ production.

Figure 13 shows the limits on $\sigma \times \mathcal{B}(W' \to ZW)$ for DY and VBF production of a W' boson in the HVT model. The observed limit ranges from 5.7 pb at 300 GeV to 1.3 fb at 5 TeV for DY production and from 0.98 pb at 300 GeV to 2.8 fb at 4 TeV for VBF production. The theoretical predictions of the HVT *Model A*, *Model B* and *VBF Model* are overlaid for comparison. The observed limits exclude an HVT W' boson produced in the DY process lighter than 2.9 TeV for *Model A* and 3.2 TeV for *Model B*, while none of

JHEP03(2018)009

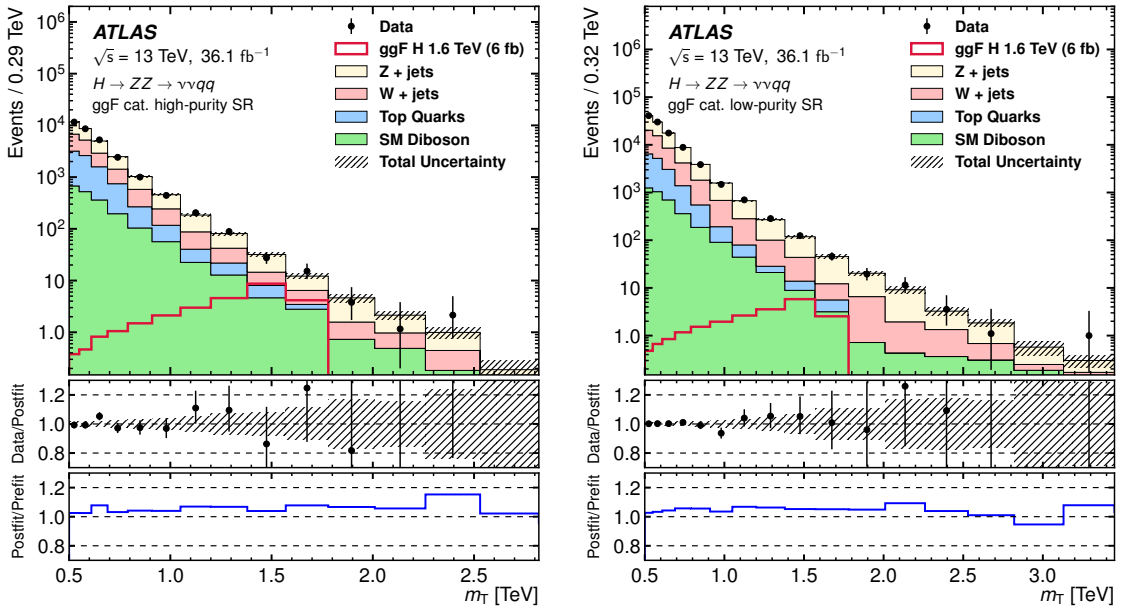

(a) (b)

Figure 10. Comparisons of the observed data and expected background distributions of m_{T} in the ggF category of the $H \to ZZ \to \nu\nu qq$ search: (a) high-purity and (b) low-purity signal regions. For illustration, expected distributions from the ggF production of a 1.6 TeV Higgs boson with $\sigma \times \mathcal{B}(H \to ZZ) = 6$ fb are also shown. The middle panes show the ratios of the observed data to the background predictions. The uncertainty in the total background prediction, shown as bands, combines statistical and systematic contributions. The blue triangles in the middle panes indicate bins where the ratio is nonzero and outside the vertical range of the plot. The bottom panes show the ratios of the post-fit and pre-fit background predictions.

the HVT model space can be excluded for the VBF process with the current sensitivity of the analysis. HVT models generally predict a near-by neutral vector boson (Z') that decays into a Z boson and a SM Higgs boson h. The Z' production could contaminate both the signal and control regions of the HVT W' search. Assuming the $Z' \to Zh$ production having the same cross section as the observed upper limit on $\sigma \times \mathcal{B}(W' \to ZW)$, the impacts of the potential contamination to the $W' \to ZW$ search are found to be negligible.

For $G_{\mathrm{KK}} \to ZZ$, limits are presented for two different couplings: $k/\overline{M}_{\mathrm{Pl}} = 1$ and $k/\overline{M}_{\mathrm{Pl}} = 0.5$, for masses between 300 GeV and 5 TeV, as shown in figure 14. The observed limits on $\sigma \times \mathcal{B}(G_{\mathrm{KK}} \to ZZ)$ vary from 3.3 pb at 300 GeV to 0.74 fb at 5 TeV for the bulk RS model with $k/\overline{M}_{\mathrm{Pl}} = 1$. The exclusion limit on the mass in this model is 1.3 (1.6) TeV for the observed (expected) limit. Similar results are obtained for bulk RS model with $k/\overline{M}_{\mathrm{Pl}} = 0.5$, with a mass exclusion upper limit of 1.0 TeV for both observed and expected limits.

These results are comparable or extend beyond previously published results [17, 18].

JHEP03(2018)009

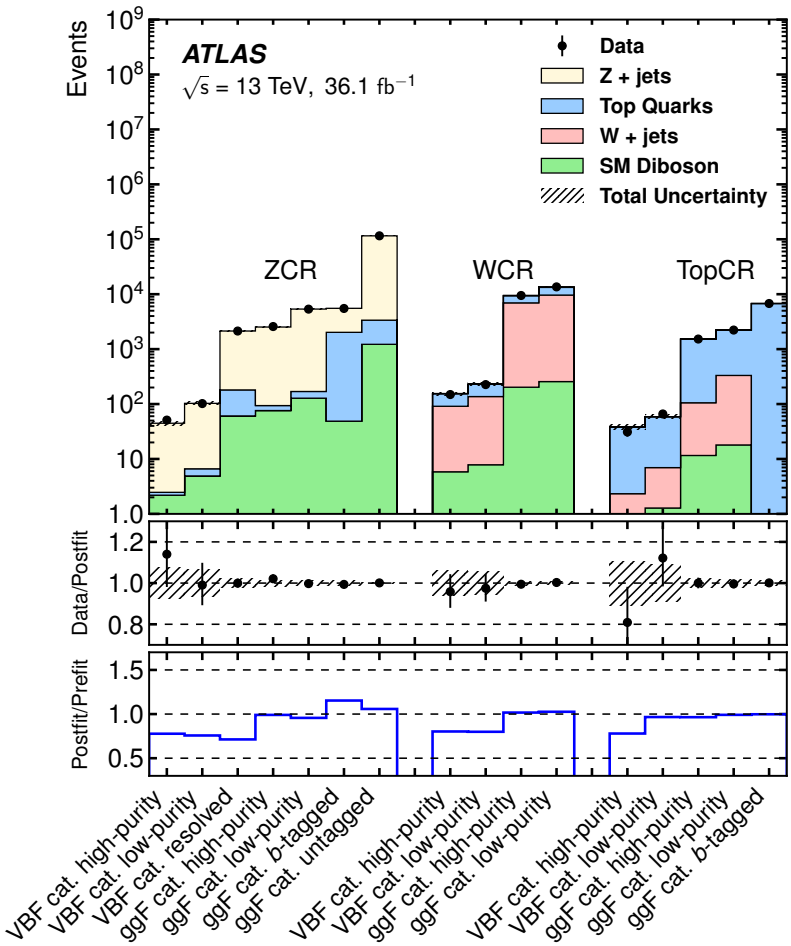

Figure 11. Comparisons of the observed data and expected background event yields in each control region. The middle pane shows the ratios of the observed data to the post-fit background predictions. The uncertainty in the total background prediction, shown as bands, combines statistical and systematic contributions. The bottom pane shows the ratios of the post-fit and pre-fit background predictions.

8.3 Effects of systematic uncertainties

The effects of systematic uncertainties are studied for hypothesised signals using the signal-strength parameter μ. The relative uncertainties in the best-fit μ value from the leading sources of systematic uncertainty are shown in table 5 for ggF $H \to ZZ$ production with $m(H) = 600\,\text{GeV}$ and $1.2\,\text{TeV}$. Apart from the statistical uncertainties in the data, the uncertainties with the largest impact on the sensitivity of the searches are from the size of the MC samples, measurements of small-R and large-R jets, $E_{\text{T}}^{\text{miss}}$ measurement, background modelling and luminosity. For signals with higher mass, the data statistical uncertainty becomes dominant. The effects of systematic uncertainties for the other searches are similar to those shown for the ggF $H \to ZZ$ search.

JHEP03(2018)009

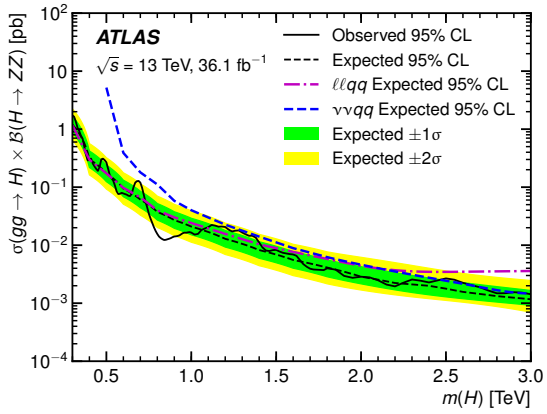

(a) ggF $H \to ZZ$

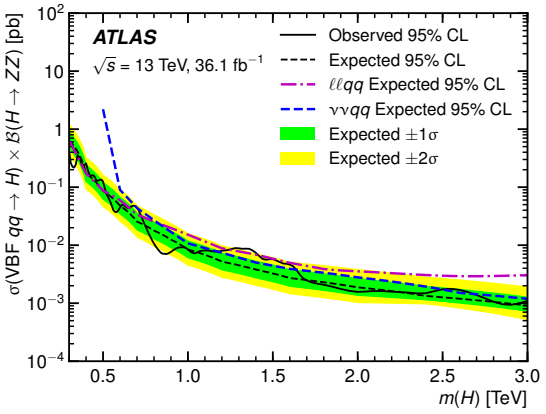

(b) VBF $H \to ZZ$

Figure 12. Observed (black solid curve) and expected (black dashed curve) 95% CL upper limits on $\sigma \times \mathcal{B}(H \to ZZ)$ at $\sqrt{s} = 13\,\text{TeV}$ for the (a) ggF and (b) VBF production of a heavy Higgs boson as a function of its mass, combining $\ell\ell qq$ and $\nu\nu qq$ searches. Limits expected from individual searches (dashed curves in blue and magenta) are also shown for comparison. Limits are calculated in the asymptotic approximation below 2 TeV and are obtained from pseudo-experiments above that. The green (inner) and yellow (outer) bands represent the $\pm 1\sigma$ and $\pm 2\sigma$ uncertainty in the expected limits.

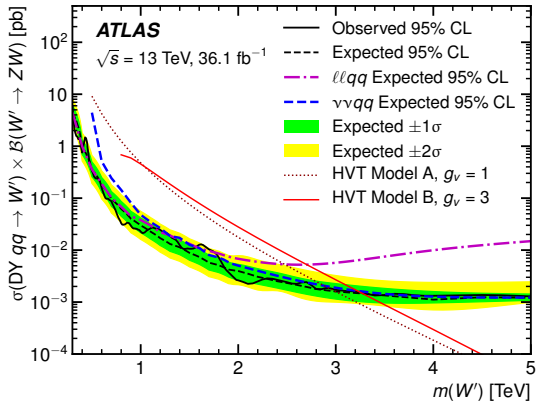

(a) DY $W' \to ZW$

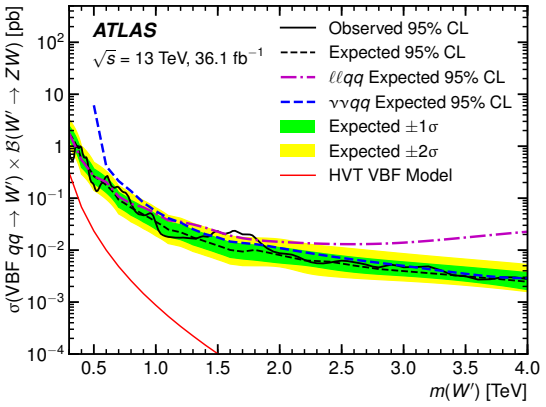

(b) VBF $W' \to ZW$

Figure 13. Observed (black solid curve) and expected (black dashed curve) 95% CL upper limits on $\sigma \times \mathcal{B}(W' \to ZW)$ at $\sqrt{s} = 13\,\text{TeV}$ for the (a) DY and (b) VBF production of a W' boson in the HVT model as a function of its mass, combining $\ell\ell qq$ and $\nu\nu qq$ searches. Limits expected from individual searches (dashed curves in blue and magenta) are also shown for comparison. Limits are calculated in the asymptotic approximation below 2 TeV and are obtained from pseudo-experiments above that. Theoretical predictions are overlaid in (a) for HVT *Model A* and *Model B* and in (b) for HVT *VBF Model*. The green (inner) and yellow (outer) bands represent the $\pm 1\sigma$ and $\pm 2\sigma$ uncertainty in the expected limits.

JHEP03(2018)009

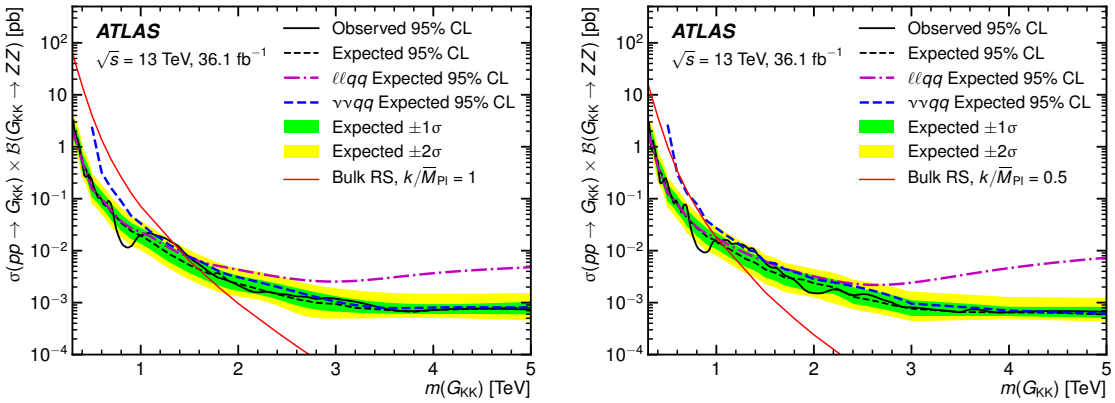

(a) Bulk RS $G_{\mathrm{KK}} \to ZZ$, with $k/\overline{M}_{\mathrm{Pl}} = 1$

(b) Bulk RS $G_{\mathrm{KK}} \to ZZ$, with $k/\overline{M}_{\mathrm{Pl}} = 0.5$

Figure 14. Observed (black solid curve) and expected (black dashed curve) 95% CL upper limits on $\sigma \times \mathcal{B}(G_{\mathrm{KK}} \to ZZ)$ at $\sqrt{s} = 13\,\mathrm{TeV}$ for the production of a G_{KK} in the bulk RS model with couplings of (a) $k/\overline{M}_{\mathrm{Pl}} = 1$ and (b) $k/\overline{M}_{\mathrm{Pl}} = 0.5$ as a function of the graviton mass, combining $\ell\ell qq$ and $\nu\nu qq$ searches. Limits expected from individual searches (dashed curves in blue and magenta) are also shown for comparison. Limits are calculated in the asymptotic approximation below 2 TeV and are obtained from pseudo-experiments above that. The theoretical predictions for $\sigma \times \mathcal{B}(G_{\mathrm{KK}} \to ZZ)$ as a function of resonance mass for a bulk RS graviton are also shown. The green (inner) and yellow (outer) bands represent the $\pm 1\sigma$ and $\pm 2\sigma$ uncertainty in the expected limits.

$m(H) = 600\,\mathrm{GeV}$		$m(H) = 1.2\,\mathrm{TeV}$	
Uncertainty source	$\Delta\mu/\mu$ [%]	Uncertainty source	$\Delta\mu/\mu$ [%]
Pseudo-data statistics	36	Pseudo-data statistics	41
Total systematics	33	Total systematics	29
MC statistics	20	Large-R jet	20
Large-R jet	16	Background modelling	13
$E_{\mathrm{T}}^{\mathrm{miss}}$ uncertainties	13	MC statistics	13
Small-R jet	11	Luminosity	6.5
Background modelling	9.6	Small-R jet	5.9
Luminosity	9.1	Leptons	3.9

Table 5. The relative uncertainties from the leading uncertainty sources in the best-fit signal-strength parameter μ of hypothesised signal production of ggF $H \to ZZ$ with $m(H) = 600\,\mathrm{GeV}$ and $m(H) = 1.2\,\mathrm{TeV}$. For this study, the $H \to ZZ$ production cross section is assumed to be 95 fb at 600 GeV and 13 fb at 1.2 TeV, corresponding to approximately the expected median upper limits at these two mass values.

JHEP03(2018)009

9 Conclusion

Searches for heavy resonances decaying into ZZ or ZW are performed using proton-proton collision data produced at $\sqrt{s} = 13\,\text{TeV}$ and recorded by the ATLAS detector at the LHC in 2015 and 2016. The data correspond to a combined integrated luminosity of $36.1\,\text{fb}^{-1}$. The searches explore the final states with one Z boson decaying either into a pair of charged leptons or into a pair of neutrinos, and the other Z boson or the W boson decaying into a pair of quarks, identified either as two separate jets or as one large-radius jet. Moreover, the searches are performed in two event categories, targeting VBF and non-VBF production of the resonances.

The data are found to be consistent with the SM background predictions and no evidence of heavy resonance production is observed. Upper limits on the production cross section times branching ratio, $\sigma \times \mathcal{B}(X \to ZV)$, as a function of the resonance mass are derived at 95% CL. In the case of a heavy Higgs boson, upper limits on $\sigma \times \mathcal{B}(H \to ZZ)$ range from 1.7 (0.42) pb at $m(H) = 300\,\text{GeV}$ to 1.4 (1.1) fb at $m(H) = 3\,\text{TeV}$ for the ggF (VBF) production process. For the phenomenological heavy-vector-triplet benchmark *Model A* (*Model B*) with coupling constant $g_V = 1$ ($g_V = 3$), a spin-1 vector triplet produced via the Drell-Yan process is excluded for $m(W') < 2.9$ (3.2) TeV. Upper limits on $\sigma \times \mathcal{B}(W' \to ZW)$ are also set for an HVT *VBF Model* with values of 0.98 pb at $m(W') = 300\,\text{GeV}$ and 2.8 fb at $m(W') = 4\,\text{TeV}$. For the bulk Randall-Sundrum model with $k/\overline{M}_{\text{Pl}} = 1$ ($k/\overline{M}_{\text{Pl}} = 0.5$), a spin-2 Kaluza-Klein graviton is excluded for $m(G_{\text{KK}}) <$ 1.3 (1.0) TeV.

These results extend previously published results [18] obtained from the combinations of $\nu\nu qq$, $\ell\nu qq$, $\ell\ell qq$ and $qqqq$ final states based on a data sample of $3.2\,\text{fb}^{-1}$ at $\sqrt{s} = 13\,\text{TeV}$ recorded in 2015.

Acknowledgments

We thank CERN for the very successful operation of the LHC, as well as the support staff from our institutions without whom ATLAS could not be operated efficiently.

We acknowledge the support of ANPCyT, Argentina; YerPhI, Armenia; ARC, Australia; BMWFW and FWF, Austria; ANAS, Azerbaijan; SSTC, Belarus; CNPq and FAPESP, Brazil; NSERC, NRC and CFI, Canada; CERN; CONICYT, Chile; CAS, MOST and NSFC, China; COLCIENCIAS, Colombia; MSMT CR, MPO CR and VSC CR, Czech Republic; DNRF and DNSRC, Denmark; IN2P3-CNRS, CEA-DRF/IRFU, France; SRNSF, Georgia; BMBF, HGF, and MPG, Germany; GSRT, Greece; RGC, Hong Kong SAR, China; ISF, I-CORE and Benoziyo Center, Israel; INFN, Italy; MEXT and JSPS, Japan; CNRST, Morocco; NWO, Netherlands; RCN, Norway; MNiSW and NCN, Poland; FCT, Portugal; MNE/IFA, Romania; MES of Russia and NRC KI, Russian Federation; JINR; MESTD, Serbia; MSSR, Slovakia; ARRS and MIZŠ, Slovenia; DST/NRF, South Africa; MINECO, Spain; SRC and Wallenberg Foundation, Sweden; SERI, SNSF and Cantons of Bern and Geneva, Switzerland; MOST, Taiwan; TAEK, Turkey; STFC, United Kingdom; DOE and NSF, United States of America. In addition, individual groups and

JHEP03(2018)009

members have received support from BCKDF, the Canada Council, CANARIE, CRC, Compute Canada, FQRNT, and the Ontario Innovation Trust, Canada; EPLANET, ERC, ERDF, FP7, Horizon 2020 and Marie Skłodowska-Curie Actions, European Union; Investissements d'Avenir Labex and Idex, ANR, Région Auvergne and Fondation Partager le Savoir, France; DFG and AvH Foundation, Germany; Herakleitos, Thales and Aristeia programmes co-financed by EU-ESF and the Greek NSRF; BSF, GIF and Minerva, Israel; BRF, Norway; CERCA Programme Generalitat de Catalunya, Generalitat Valenciana, Spain; the Royal Society and Leverhulme Trust, United Kingdom.

The crucial computing support from all WLCG partners is acknowledged gratefully, in particular from CERN, the ATLAS Tier-1 facilities at TRIUMF (Canada), NDGF (Denmark, Norway, Sweden), CC-IN2P3 (France), KIT/GridKA (Germany), INFN-CNAF (Italy), NL-T1 (Netherlands), PIC (Spain), ASGC (Taiwan), RAL (UK) and BNL (USA), the Tier-2 facilities worldwide and large non-WLCG resource providers. Major contributors of computing resources are listed in ref. [100].

JHEP03(2018)009

References

[1] ATLAS collaboration, *Observation of a new particle in the search for the Standard Model Higgs boson with the ATLAS detector at the LHC*, *Phys. Lett.* **B 716** (2012) 1 [arXiv:1207.7214] [INSPIRE].

[2] CMS collaboration, *Observation of a new boson at a mass of 125 GeV with the CMS experiment at the LHC*, *Phys. Lett.* **B 716** (2012) 30 [arXiv:1207.7235] [INSPIRE].

[3] ATLAS collaboration, *Measurements of the Higgs boson production and decay rates and coupling strengths using pp collision data at $\sqrt{s} = 7$ and 8 TeV in the ATLAS experiment*, *Eur. Phys. J.* **C 76** (2016) 6 [arXiv:1507.04548] [INSPIRE].

[4] ATLAS collaboration, *Study of the spin and parity of the Higgs boson in diboson decays with the ATLAS detector*, *Eur. Phys. J.* **C 75** (2015) 476 [arXiv:1506.05669] [INSPIRE].

[5] CMS collaboration, *Precise determination of the mass of the Higgs boson and tests of compatibility of its couplings with the standard model predictions using proton collisions at 7 and 8 TeV*, *Eur. Phys. J.* **C 75** (2015) 212 [arXiv:1412.8662] [INSPIRE].

[6] CMS collaboration, *Constraints on the spin-parity and anomalous HVV couplings of the Higgs boson in proton collisions at 7 and 8 TeV*, *Phys. Rev.* **D 92** (2015) 012004 [arXiv:1411.3441] [INSPIRE].

[7] H.E. Haber and G.L. Kane, *The Search for Supersymmetry: Probing Physics Beyond the Standard Model*, *Phys. Rept.* **117** (1985) 75 [INSPIRE].

[8] N. Arkani-Hamed, S. Dimopoulos and G.R. Dvali, *The Hierarchy problem and new dimensions at a millimeter*, *Phys. Lett.* **B 429** (1998) 263 [hep-ph/9803315] [INSPIRE].

[9] G.F. Giudice, *Naturally Speaking: The Naturalness Criterion and Physics at the LHC*, arXiv:0801.2562 [INSPIRE].

[10] G.C. Branco, P.M. Ferreira, L. Lavoura, M.N. Rebelo, M. Sher and J.P. Silva, *Theory and phenomenology of two-Higgs-doublet models*, *Phys. Rept.* **516** (2012) 1 [arXiv:1106.0034] [INSPIRE].

[11] A. Hill and J.J. van der Bij, *Strongly interacting singlet-doublet Higgs model*, *Phys. Rev.* **D 36** (1987) 11.

[12] G. Altarelli, B. Mele and M. Ruiz-Altaba, *Searching for New Heavy Vector Bosons in $p\bar{p}$ Colliders*, *Z. Phys.* **C 45** (1989) 109 [*Erratum ibid.* **C 47** (1990) 676] [INSPIRE].

[13] L. Randall and R. Sundrum, *A Large mass hierarchy from a small extra dimension*, *Phys. Rev. Lett.* **83** (1999) 3370 [hep-ph/9905221] [INSPIRE].

[14] H. Davoudiasl, J.L. Hewett and T.G. Rizzo, *Bulk gauge fields in the Randall-Sundrum model*, *Phys. Lett.* **B 473** (2000) 43 [hep-ph/9911262] [INSPIRE].

[15] ATLAS collaboration, *Search for an additional, heavy Higgs boson in the $H \to ZZ$ decay channel at $\sqrt{s} = 8$ TeV in pp collision data with the ATLAS detector*, *Eur. Phys. J.* **C 76** (2016) 45 [arXiv:1507.05930] [INSPIRE].

[16] ATLAS collaboration, *Combination of searches for WW, WZ and ZZ resonances in pp collisions at $\sqrt{s} = 8$ TeV with the ATLAS detector*, *Phys. Lett.* **B 755** (2016) 285 [arXiv:1512.05099] [INSPIRE].

[17] CMS collaboration, *Combination of searches for heavy resonances decaying to WW, WZ, ZZ, WH and ZH boson pairs in proton-proton collisions at $\sqrt{s} = 8$ and 13 TeV*, *Phys. Lett.* **B 774** (2017) 533 [arXiv:1705.09171] [INSPIRE].

[18] ATLAS collaboration, *Searches for heavy diboson resonances in pp collisions at $\sqrt{s} = 13$ TeV with the ATLAS detector*, *JHEP* **09** (2016) 173 [arXiv:1606.04833] [INSPIRE].

[19] ATLAS collaboration, *Search for diboson resonances with boson-tagged jets in pp collisions at $\sqrt{s} = 13$ TeV with the ATLAS detector*, *Phys. Lett.* **B 777** (2018) 91 [arXiv:1708.04445] [INSPIRE].

[20] ATLAS collaboration, *The ATLAS Experiment at the CERN Large Hadron Collider*, 2008 *JINST* **3** S08003 [INSPIRE].

[21] L. Evans and P. Bryant, *LHC Machine*, 2008 *JINST* **3** S08001 [INSPIRE].

[22] ATLAS collaboration, *ATLAS Insertable B-Layer Technical Design Report*, ATLAS-TDR-19 (2010).

[23] ATLAS collaboration, *ATLAS Insertable B-Layer Technical Design Report Addendum*, ATLAS-TDR-19-ADD-1 (2012).

[24] ATLAS collaboration, *Performance of the ATLAS Trigger System in 2015*, *Eur. Phys. J.* **C 77** (2017) 317 [arXiv:1611.09661] [INSPIRE].

[25] ATLAS collaboration, *Selection of jets produced in 13 TeV proton-proton collisions with the ATLAS detector*, ATLAS-CONF-2015-029 (2015).

[26] V. Barger, P. Langacker, M. McCaskey, M.J. Ramsey-Musolf and G. Shaughnessy, *LHC Phenomenology of an Extended Standard Model with a Real Scalar Singlet*, *Phys. Rev.* **D 77** (2008) 035005 [arXiv:0706.4311] [INSPIRE].

[27] J. de Blas, J.M. Lizana and M. Pérez-Victoria, *Combining searches of Z' and W' bosons*, *JHEP* **01** (2013) 166 [arXiv:1211.2229] [INSPIRE].

JHEP03(2018)009

[28] D. Pappadopulo, A. Thamm, R. Torre and A. Wulzer, *Heavy Vector Triplets: Bridging Theory and Data*, *JHEP* **09** (2014) 060 [arXiv:1402.4431] [INSPIRE].

[29] K. Agashe, H. Davoudiasl, G. Perez and A. Soni, *Warped Gravitons at the LHC and Beyond*, *Phys. Rev.* **D 76** (2007) 036006 [hep-ph/0701186] [INSPIRE].

[30] A.L. Fitzpatrick, J. Kaplan, L. Randall and L.-T. Wang, *Searching for the Kaluza-Klein Graviton in Bulk RS Models*, *JHEP* **09** (2007) 013 [hep-ph/0701150] [INSPIRE].

[31] P. Nason, *A New method for combining NLO QCD with shower Monte Carlo algorithms*, *JHEP* **11** (2004) 040 [hep-ph/0409146] [INSPIRE].

[32] S. Frixione, P. Nason and C. Oleari, *Matching NLO QCD computations with Parton Shower simulations: the POWHEG method*, *JHEP* **11** (2007) 070 [arXiv:0709.2092] [INSPIRE].

[33] S. Alioli, P. Nason, C. Oleari and E. Re, *A general framework for implementing NLO calculations in shower Monte Carlo programs: the POWHEG BOX*, *JHEP* **06** (2010) 043 [arXiv:1002.2581] [INSPIRE].

[34] S. Alioli, P. Nason, C. Oleari and E. Re, *NLO Higgs boson production via gluon fusion matched with shower in POWHEG*, *JHEP* **04** (2009) 002 [arXiv:0812.0578] [INSPIRE].

[35] H.-L. Lai et al., *New parton distributions for collider physics*, *Phys. Rev.* **D 82** (2010) 074024 [arXiv:1007.2241] [INSPIRE].

[36] J. Alwall et al., *The automated computation of tree-level and next-to-leading order differential cross sections and their matching to parton shower simulations*, *JHEP* **07** (2014) 079 [arXiv:1405.0301] [INSPIRE].

[37] R.D. Ball et al., *Parton distributions with LHC data*, *Nucl. Phys.* **B 867** (2013) 244 [arXiv:1207.1303] [INSPIRE].

[38] T. Sjöstrand, S. Mrenna and P.Z. Skands, *A Brief Introduction to PYTHIA 8.1*, *Comput. Phys. Commun.* **178** (2008) 852 [arXiv:0710.3820] [INSPIRE].

[39] ATLAS collaboration, *ATLAS Run 1 PYTHIA8 tunes*, ATL-PHYS-PUB-2014-021 (2014).

[40] ATLAS collaboration, *Measurement of the Z/γ^* boson transverse momentum distribution in pp collisions at $\sqrt{s} = 7$ TeV with the ATLAS detector*, *JHEP* **09** (2014) 145 [arXiv:1406.3660] [INSPIRE].

[41] T. Gleisberg et al., *Event generation with SHERPA 1.1*, *JHEP* **02** (2009) 007 [arXiv:0811.4622] [INSPIRE].

[42] T. Gleisberg and S. Hoeche, *Comix, a new matrix element generator*, *JHEP* **12** (2008) 039 [arXiv:0808.3674] [INSPIRE].

[43] F. Cascioli, P. Maierhofer and S. Pozzorini, *Scattering Amplitudes with Open Loops*, *Phys. Rev. Lett.* **108** (2012) 111601 [arXiv:1111.5206] [INSPIRE].

[44] S. Hoeche, F. Krauss, M. Schonherr and F. Siegert, *QCD matrix elements + parton showers: The NLO case*, *JHEP* **04** (2013) 027 [arXiv:1207.5030] [INSPIRE].

[45] S. Frixione, P. Nason and G. Ridolfi, *A Positive-weight next-to-leading-order Monte Carlo for heavy flavour hadroproduction*, *JHEP* **09** (2007) 126 [arXiv:0707.3088] [INSPIRE].

[46] S. Alioli, P. Nason, C. Oleari and E. Re, *NLO single-top production matched with shower in POWHEG: s- and t-channel contributions*, *JHEP* **09** (2009) 111 [*Erratum ibid.* **1002** (2010) 011] [arXiv:0907.4076] [INSPIRE].

JHEP03(2018)009

[47] R. Frederix, E. Re and P. Torrielli, *Single-top t-channel hadroproduction in the four-flavour scheme with POWHEG and aMC@NLO*, *JHEP* **09** (2012) 130 [arXiv:1207.5391] [INSPIRE].

[48] E. Re, *Single-top Wt-channel production matched with parton showers using the POWHEG method*, *Eur. Phys. J.* **C 71** (2011) 1547 [arXiv:1009.2450] [INSPIRE].

[49] T. Sjöstrand, S. Mrenna and P.Z. Skands, *PYTHIA 6.4 Physics and Manual*, *JHEP* **05** (2006) 026 [hep-ph/0603175] [INSPIRE].

[50] J. Pumplin, D.R. Stump, J. Huston, H.L. Lai, P.M. Nadolsky and W.K. Tung, *New generation of parton distributions with uncertainties from global QCD analysis*, *JHEP* **07** (2002) 012 [hep-ph/0201195] [INSPIRE].

[51] P.Z. Skands, *Tuning Monte Carlo Generators: The Perugia Tunes*, *Phys. Rev.* **D 82** (2010) 074018 [arXiv:1005.3457] [INSPIRE].

[52] D.J. Lange, *The EvtGen particle decay simulation package*, *Nucl. Instrum. Meth.* **A 462** (2001) 152 [INSPIRE].

[53] C. Anastasiou, L.J. Dixon, K. Melnikov and F. Petriello, *High precision QCD at hadron colliders: Electroweak gauge boson rapidity distributions at NNLO*, *Phys. Rev.* **D 69** (2004) 094008 [hep-ph/0312266] [INSPIRE].

[54] S. Hoche, F. Krauss, M. Schonherr and F. Siegert, *NLO matrix elements and truncated showers*, *JHEP* **08** (2011) 123 [arXiv:1009.1127] [INSPIRE].

[55] M. Czakon, P. Fiedler and A. Mitov, *Total Top-Quark Pair-Production Cross section at Hadron Colliders Through $O(\alpha_S^4)$*, *Phys. Rev. Lett.* **110** (2013) 252004 [arXiv:1303.6254] [INSPIRE].

[56] M. Czakon and A. Mitov, *Top++: A Program for the Calculation of the Top-Pair Cross-Section at Hadron Colliders*, *Comput. Phys. Commun.* **185** (2014) 2930 [arXiv:1112.5675] [INSPIRE].

[57] N. Kidonakis, *NNLL resummation for s-channel single top quark production*, *Phys. Rev.* **D 81** (2010) 054028 [arXiv:1001.5034] [INSPIRE].

[58] N. Kidonakis, *Two-loop soft anomalous dimensions for single top quark associated production with a W^- or H^-*, *Phys. Rev.* **D 82** (2010) 054018 [arXiv:1005.4451] [INSPIRE].

[59] ATLAS collaboration, *The ATLAS Simulation Infrastructure*, *Eur. Phys. J.* **C 70** (2010) 823 [arXiv:1005.4568] [INSPIRE].

[60] GEANT4 collaboration, S. Agostinelli et al., *GEANT4: A Simulation toolkit*, *Nucl. Instrum. Meth.* **A 506** (2003) 250 [INSPIRE].

[61] ATLAS collaboration, *Electron efficiency measurements with the ATLAS detector using the 2012 LHC proton-proton collision data*, ATLAS-CONF-2014-032 (2014).

[62] ATLAS collaboration, *Muon reconstruction performance of the ATLAS detector in proton–proton collision data at $\sqrt{s} = 13$ TeV*, *Eur. Phys. J.* **C 76** (2016) 292 [arXiv:1603.05598] [INSPIRE].

[63] M. Cacciari, G.P. Salam and G. Soyez, *The Anti-k_t jet clustering algorithm*, *JHEP* **04** (2008) 063 [arXiv:0802.1189] [INSPIRE].

[64] M. Cacciari, G.P. Salam and G. Soyez, *FastJet User Manual*, *Eur. Phys. J.* **C 72** (2012) 1896 [arXiv:1111.6097] [INSPIRE].

JHEP03(2018)009

[65] ATLAS Collaboration, *Jet energy scale measurements and their systematic uncertainties in proton-proton collisions at $\sqrt{s} = 13$ TeV with the ATLAS detector*, CERN-EP-2017-038 (2017).

[66] ATLAS collaboration, *Tagging and suppression of pileup jets with the ATLAS detector*, ATLAS-CONF-2014-018 (2014).

[67] ATLAS collaboration, *Performance of b-Jet Identification in the ATLAS Experiment*, 2016 *JINST* **11** P04008 [arXiv:1512.01094] [INSPIRE].

[68] ATLAS collaboration, *Optimisation of the ATLAS b-tagging performance for the 2016 LHC Run*, ATL-PHYS-PUB-2016-012 (2016).

[69] D. Krohn, J. Thaler and L.-T. Wang, *Jet Trimming*, *JHEP* **02** (2010) 084 [arXiv:0912.1342] [INSPIRE].

[70] S.D. Ellis and D.E. Soper, *Successive combination jet algorithm for hadron collisions*, *Phys. Rev.* **D 48** (1993) 3160 [hep-ph/9305266] [INSPIRE].

[71] ATLAS collaboration, *Performance of jet substructure techniques for large-R jets in proton-proton collisions at $\sqrt{s} = 7$ TeV using the ATLAS detector*, *JHEP* **09** (2013) 076 [arXiv:1306.4945] [INSPIRE].

[72] ATLAS collaboration, *Jet mass reconstruction with the ATLAS Detector in early Run 2 data*, ATLAS-CONF-2016-035 (2016).

[73] ATLAS collaboration, *Identification of boosted, hadronically decaying W bosons and comparisons with ATLAS data taken at $\sqrt{s} = 8$ TeV*, *Eur. Phys. J.* **C 76** (2016) 154 [arXiv:1510.05821] [INSPIRE].

[74] ATLAS collaboration, *Identification of boosted, hadronically-decaying W and Z bosons in $\sqrt{s} = 13$ TeV Monte Carlo Simulations for ATLAS*, ATL-PHYS-PUB-2015-033 (2015).

[75] A.J. Larkoski, I. Moult and D. Neill, *Power Counting to Better Jet Observables*, *JHEP* **12** (2014) 009 [arXiv:1409.6298] [INSPIRE].

[76] A.J. Larkoski, I. Moult and D. Neill, *Analytic Boosted Boson Discrimination*, *JHEP* **05** (2016) 117 [arXiv:1507.03018] [INSPIRE].

[77] ATLAS collaboration, *Performance of algorithms that reconstruct missing transverse momentum in $\sqrt{s} = 8$ TeV proton-proton collisions in the ATLAS detector*, *Eur. Phys. J.* **C 77** (2017) 241 [arXiv:1609.09324] [INSPIRE].

[78] ATLAS collaboration, *Performance of missing transverse momentum reconstruction for the ATLAS detector in the first proton-proton collisions at at $\sqrt{s} = 13$ TeV*, ATL-PHYS-PUB-2015-027 (2015).

[79] ATLAS collaboration, *Expected performance of missing transverse momentum reconstruction for the ATLAS detector at $\sqrt{s} = 13$ TeV*, ATL-PHYS-PUB-2015-023 (2015).

[80] Particle Data Group collaboration, K.A. Olive et al., *Review of Particle Physics*, *Chin. Phys.* **C 38** (2014) 090001 [INSPIRE].

[81] ATLAS collaboration, *Luminosity determination in pp collisions at $\sqrt{s} = 8$ TeV using the ATLAS detector at the LHC*, *Eur. Phys. J.* **C 76** (2016) 653 [arXiv:1608.03953] [INSPIRE].

[82] ATLAS collaboration, *Measurement of the Inelastic Proton-Proton Cross section at $\sqrt{s} = 13$ TeV with the ATLAS Detector at the LHC*, *Phys. Rev. Lett.* **117** (2016) 182002 [arXiv:1606.02625] [INSPIRE].

JHEP03(2018)009

[83] ATLAS collaboration, *Muon reconstruction performance in early $\sqrt{s} = 13$ TeV data*, ATL-PHYS-PUB-2015-037 (2015).

[84] ATLAS collaboration, *Electron identification measurements in ATLAS using $\sqrt{s} = 13$ TeV data with 50 ns bunch spacing*, ATL-PHYS-PUB-2015-041 (2015).

[85] ATLAS collaboration, *Jet Calibration and Systematic Uncertainties for Jets Reconstructed in the ATLAS Detector at $\sqrt{s} = 13$ TeV*, ATL-PHYS-PUB-2015-015 (2015).

[86] ATLAS collaboration, *Commissioning of the ATLAS b-tagging algorithms using $t\bar{t}$ events in early Run-2 data*, ATL-PHYS-PUB-2015-039 (2015).

[87] ATLAS collaboration, *Expected performance of the ATLAS b-tagging algorithms in Run-2*, ATL-PHYS-PUB-2015-022 (2015).

[88] G. Corcella et al., *HERWIG 6: An Event generator for hadron emission reactions with interfering gluons (including supersymmetric processes)*, *JHEP* **01** (2001) 010 [hep-ph/0011363] [INSPIRE].

[89] J.M. Campbell, R.K. Ellis and C. Williams, *Vector boson pair production at the LHC*, *JHEP* **07** (2011) 018 [arXiv:1105.0020] [INSPIRE].

[90] L.A. Harland-Lang, A.D. Martin, P. Motylinski and R.S. Thorne, *Parton distributions in the LHC era: MMHT 2014 PDFs*, *Eur. Phys. J.* **C 75** (2015) 204 [arXiv:1412.3989] [INSPIRE].

[91] NNPDF collaboration, R.D. Ball et al., *Parton distributions for the LHC Run II*, *JHEP* **04** (2015) 040 [arXiv:1410.8849] [INSPIRE].

[92] ATLAS collaboration, *Combined search for the Standard Model Higgs boson in pp collisions at $\sqrt{s} = 7$ TeV with the ATLAS detector*, *Phys. Rev.* **D 86** (2012) 032003 [arXiv:1207.0319] [INSPIRE].

[93] L. Moneta et al., *The RooStats Project*, PoS(ACAT2010)057 [arXiv:1009.1003] [INSPIRE].

[94] W. Verkerke and D.P. Kirkby, *The RooFit toolkit for data modeling*, *eConf* **C 0303241** (2003) MOLT007 [physics/0306116] [INSPIRE].

[95] M. Baak, S. Gadatsch, R. Harrington and W. Verkerke, *Interpolation between multi-dimensional histograms using a new non-linear moment morphing method*, *Nucl. Instrum. Meth.* **A 771** (2015) 39 [arXiv:1410.7388] [INSPIRE].

[96] ATLAS, CMS and The LHC Higgs Combination Group collaborations, *Procedure for the LHC Higgs boson search combination in Summer 2011*, ATL-PHYS-PUB-2011-011 (2011).

[97] A.L. Read, *Presentation of search results: the CL_s technique*, *J. Phys.* **G 28** (2002) 2693.

[98] G. Cowan, K. Cranmer, E. Gross and O. Vitells, *Asymptotic formulae for likelihood-based tests of new physics*, *Eur. Phys. J.* **C 71** (2011) 1554 [*Erratum ibid.* **C 73** (2013) 2501] [arXiv:1007.1727] [INSPIRE].

[99] E. Gross and O. Vitells, *Trial factors for the look elsewhere effect in high energy physics*, *Eur. Phys. J.* **C 70** (2010) 525 [arXiv:1005.1891] [INSPIRE].

[100] ATLAS collaboration, *ATLAS Computing Acknowledgements*, ATL-GEN-PUB-2016-002 (2016).

JHEP03(2018)009

The ATLAS collaboration

M. Aaboud[137d], G. Aad[88], B. Abbott[115], O. Abdinov[12,*], B. Abeloos[119], S.H. Abidi[161], O.S. AbouZeid[139], N.L. Abraham[151], H. Abramowicz[155], H. Abreu[154], R. Abreu[118], Y. Abulaiti[148a,148b], B.S. Acharya[167a,167b,a], S. Adachi[157], L. Adamczyk[41a], J. Adelman[110], M. Adersberger[102], T. Adye[133], A.A. Affolder[139], Y. Afik[154], T. Agatonovic-Jovin[14], C. Agheorghiesei[28c], J.A. Aguilar-Saavedra[128a,128f], S.P. Ahlen[24], F. Ahmadov[68,b], G. Aielli[135a,135b], S. Akatsuka[71], H. Akerstedt[148a,148b], T.P.A. Åkesson[84], E. Akilli[52], A.V. Akimov[98], G.L. Alberghi[22a,22b], J. Albert[172], P. Albicocco[50], M.J. Alconada Verzini[74], S.C. Alderweireldt[108], M. Aleksa[32], I.N. Aleksandrov[68], C. Alexa[28b], G. Alexander[155], T. Alexopoulos[10], M. Alhroob[115], B. Ali[130], M. Aliev[76a,76b], G. Alimonti[94a], J. Alison[33], S.P. Alkire[38], B.M.M. Allbrooke[151], B.W. Allen[118], P.P. Allport[19], A. Aloisio[106a,106b], A. Alonso[39], F. Alonso[74], C. Alpigiani[140], A.A. Alshehri[56], M.I. Alstaty[88], B. Alvarez Gonzalez[32], D. Álvarez Piqueras[170], M.G. Alviggi[106a,106b], B.T. Amadio[16], Y. Amaral Coutinho[26a], C. Amelung[25], D. Amidei[92], S.P. Amor Dos Santos[128a,128c], S. Amoroso[32], G. Amundsen[25], C. Anastopoulos[141], L.S. Ancu[52], N. Andari[19], T. Andeen[11], C.F. Anders[60b], J.K. Anders[77], K.J. Anderson[33], A. Andreazza[94a,94b], V. Andrei[60a], S. Angelidakis[37], I. Angelozzi[109], A. Angerami[38], A.V. Anisenkov[111,c], N. Anjos[13], A. Annovi[126a,126b], C. Antel[60a], M. Antonelli[50], A. Antonov[100,*], D.J. Antrim[166], F. Anulli[134a], M. Aoki[69], L. Aperio Bella[32], G. Arabidze[93], Y. Arai[69], J.P. Araque[128a], V. Araujo Ferraz[26a], A.T.H. Arce[48], R.E. Ardell[80], F.A. Arduh[74], J-F. Arguin[97], S. Argyropoulos[66], M. Arik[20a], A.J. Armbruster[32], L.J. Armitage[79], O. Arnaez[161], H. Arnold[51], M. Arratia[30], O. Arslan[23], A. Artamonov[99,*], G. Artoni[122], S. Artz[86], S. Asai[157], N. Asbah[45], A. Ashkenazi[155], L. Asquith[151], K. Assamagan[27], R. Astalos[146a], M. Atkinson[169], N.B. Atlay[143], K. Augsten[130], G. Avolio[32], B. Axen[16], M.K. Ayoub[35a], G. Azuelos[97,d], A.E. Baas[60a], M.J. Baca[19], H. Bachacou[138], K. Bachas[76a,76b], M. Backes[122], P. Bagnaia[134a,134b], M. Bahmani[42], H. Bahrasemani[144], J.T. Baines[133], M. Bajic[39], O.K. Baker[179], P.J. Bakker[109], E.M. Baldin[111,c], P. Balek[175], F. Balli[138], W.K. Balunas[124], E. Banas[42], A. Bandyopadhyay[23], Sw. Banerjee[176,e], A.A.E. Bannoura[178], L. Barak[155], E.L. Barberio[91], D. Barberis[53a,53b], M. Barbero[88], T. Barillari[103], M-S Barisits[32], J.T. Barkeloo[118], T. Barklow[145], N. Barlow[30], S.L. Barnes[36c], B.M. Barnett[133], R.M. Barnett[16], Z. Barnovska-Blenessy[36a], A. Baroncelli[136a], G. Barone[25], A.J. Barr[122], L. Barranco Navarro[170], F. Barreiro[85], J. Barreiro Guimarães da Costa[35a], R. Bartoldus[145], A.E. Barton[75], P. Bartos[146a], A. Basalaev[125], A. Bassalat[119,f], R.L. Bates[56], S.J. Batista[161], J.R. Batley[30], M. Battaglia[139], M. Bauce[134a,134b], F. Bauer[138], H.S. Bawa[145,g], J.B. Beacham[113], M.D. Beattie[75], T. Beau[83], P.H. Beauchemin[165], P. Bechtle[23], H.P. Beck[18,h], H.C. Beck[57], K. Becker[122], M. Becker[86], C. Becot[112], A.J. Beddall[20e], A. Beddall[20b], V.A. Bednyakov[68], M. Bedognetti[109], C.P. Bee[150], T.A. Beermann[32], M. Begalli[26a], M. Begel[27], J.K. Behr[45], A.S. Bell[81], G. Bella[155], L. Bellagamba[22a], A. Bellerive[31], M. Bellomo[154], K. Belotskiy[100], O. Beltramello[32], N.L. Belyaev[100], O. Benary[155,*], D. Benchekroun[137a], M. Bender[102], N. Benekos[10], Y. Benhammou[155], E. Benhar Noccioli[179], J. Benitez[66], D.P. Benjamin[48], M. Benoit[52], J.R. Bensinger[25], S. Bentvelsen[109], L. Beresford[122], M. Beretta[50], D. Berge[109], E. Bergeaas Kuutmann[168], N. Berger[5], J. Beringer[16], S. Berlendis[58], N.R. Bernard[89], G. Bernardi[83], C. Bernius[145], F.U. Bernlochner[23], T. Berry[80], P. Berta[86], C. Bertella[35a], G. Bertoli[148a,148b], I.A. Bertram[75], C. Bertsche[45], D. Bertsche[115], G.J. Besjes[39], O. Bessidskaia Bylund[148a,148b], M. Bessner[45], N. Besson[138], A. Bethani[87], S. Bethke[103], A. Betti[23], A.J. Bevan[79], J. Beyer[103], R.M. Bianchi[127], O. Biebel[102], D. Biedermann[17], R. Bielski[87], K. Bierwagen[86], N.V. Biesuz[126a,126b], M. Biglietti[136a], T.R.V. Billoud[97], H. Bilokon[50], M. Bindi[57], A. Bingul[20b], C. Bini[134a,134b], S. Biondi[22a,22b], T. Bisanz[57],

JHEP03(2018)009

C. Bittrich[47], D.M. Bjergaard[48], J.E. Black[145], K.M. Black[24], R.E. Blair[6], T. Blazek[146a], I. Bloch[45], C. Blocker[25], A. Blue[56], U. Blumenschein[79], S. Blunier[34a], G.J. Bobbink[109], V.S. Bobrovnikov[111,c], S.S. Bocchetta[84], A. Bocci[48], C. Bock[102], M. Boehler[51], D. Boerner[178], D. Bogavac[102], A.G. Bogdanchikov[111], C. Bohm[148a], V. Boisvert[80], P. Bokan[168,i], T. Bold[41a], A.S. Boldyrev[101], A.E. Bolz[60b], M. Bomben[83], M. Bona[79], M. Boonekamp[138], A. Borisov[132], G. Borissov[75], J. Bortfeldt[32], D. Bortoletto[122], V. Bortolotto[62a], D. Boscherini[22a], M. Bosman[13], J.D. Bossio Sola[29], J. Boudreau[127], J. Bouffard[2], E.V. Bouhova-Thacker[75], D. Boumediene[37], C. Bourdarios[119], S.K. Boutle[56], A. Boveia[113], J. Boyd[32], I.R. Boyko[68], A.J. Bozson[80], J. Bracinik[19], A. Brandt[8], G. Brandt[57], O. Brandt[60a], F. Braren[45], U. Bratzler[158], B. Brau[89], J.E. Brau[118], W.D. Breaden Madden[56], K. Brendlinger[45], A.J. Brennan[91], L. Brenner[109], R. Brenner[168], S. Bressler[175], D.L. Briglin[19], T.M. Bristow[49], D. Britton[56], D. Britzger[45], F.M. Brochu[30], I. Brock[23], R. Brock[93], G. Brooijmans[38], T. Brooks[80], W.K. Brooks[34b], J. Brosamer[16], E. Brost[110], J.H Broughton[19], P.A. Bruckman de Renstrom[42], D. Bruncko[146b], A. Bruni[22a], G. Bruni[22a], L.S. Bruni[109], S. Bruno[135a,135b], BH Brunt[30], M. Bruschi[22a], N. Bruscino[127], P. Bryant[33], L. Bryngemark[45], T. Buanes[15], Q. Buat[144], P. Buchholz[143], A.G. Buckley[56], I.A. Budagov[68], F. Buehrer[51], M.K. Bugge[121], O. Bulekov[100], D. Bullock[8], T.J. Burch[110], S. Burdin[77], C.D. Burgard[51], A.M. Burger[5], B. Burghgrave[110], K. Burka[42], S. Burke[133], I. Burmeister[46], J.T.P. Burr[122], E. Busato[37], D. Büscher[51], V. Büscher[86], P. Bussey[56], J.M. Butler[24], C.M. Buttar[56], J.M. Butterworth[81], P. Butti[32], W. Buttinger[27], A. Buzatu[153], A.R. Buzykaev[111,c], S. Cabrera Urbán[170], D. Caforio[130], H. Cai[169], V.M. Cairo[40a,40b], O. Cakir[4a], N. Calace[52], P. Calafiura[16], A. Calandri[88], G. Calderini[83], P. Calfayan[64], G. Callea[40a,40b], L.P. Caloba[26a], S. Calvente Lopez[85], D. Calvet[37], S. Calvet[37], T.P. Calvet[88], R. Camacho Toro[33], S. Camarda[32], P. Camarri[135a,135b], D. Cameron[121], R. Caminal Armadans[169], C. Camincher[58], S. Campana[32], M. Campanelli[81], A. Camplani[94a,94b], A. Campoverde[143], V. Canale[106a,106b], M. Cano Bret[36c], J. Cantero[116], T. Cao[155], M.D.M. Capeans Garrido[32], I. Caprini[28b], M. Caprini[28b], M. Capua[40a,40b], R.M. Carbone[38], R. Cardarelli[135a], F. Cardillo[51], I. Carli[131], T. Carli[32], G. Carlino[106a], B.T. Carlson[127], L. Carminati[94a,94b], R.M.D. Carney[148a,148b], S. Caron[108], E. Carquin[34b], S. Carrá[94a,94b], G.D. Carrillo-Montoya[32], D. Casadei[19], M.P. Casado[13,j], M. Casolino[13], D.W. Casper[166], R. Castelijn[109], V. Castillo Gimenez[170], N.F. Castro[128a,k], A. Catinaccio[32], J.R. Catmore[121], A. Cattai[32], J. Caudron[23], V. Cavaliere[169], E. Cavallaro[13], D. Cavalli[94a], M. Cavalli-Sforza[13], V. Cavasinni[126a,126b], E. Celebi[20d], F. Ceradini[136a,136b], L. Cerda Alberich[170], A.S. Cerqueira[26b], A. Cerri[151], L. Cerrito[135a,135b], F. Cerutti[16], A. Cervelli[22a,22b], S.A. Cetin[20d], A. Chafaq[137a], D. Chakraborty[110], S.K. Chan[59], W.S. Chan[109], Y.L. Chan[62a], P. Chang[169], J.D. Chapman[30], D.G. Charlton[19], C.C. Chau[31], C.A. Chavez Barajas[151], S. Che[113], S. Cheatham[167a,167c], A. Chegwidden[93], S. Chekanov[6], S.V. Chekulaev[163a], G.A. Chelkov[68,l], M.A. Chelstowska[32], C. Chen[36a], C. Chen[67], H. Chen[27], J. Chen[36a], S. Chen[35b], S. Chen[157], X. Chen[35c,m], Y. Chen[70], H.C. Cheng[92], H.J. Cheng[35a], A. Cheplakov[68], E. Cheremushkina[132], R. Cherkaoui El Moursli[137e], E. Cheu[7], K. Cheung[63], L. Chevalier[138], V. Chiarella[50], G. Chiarelli[126a,126b], G. Chiodini[76a], A.S. Chisholm[32], A. Chitan[28b], Y.H. Chiu[172], M.V. Chizhov[68], K. Choi[64], A.R. Chomont[37], S. Chouridou[156], Y.S. Chow[62a], V. Christodoulou[81], M.C. Chu[62a], J. Chudoba[129], A.J. Chuinard[90], J.J. Chwastowski[42], L. Chytka[117], A.K. Ciftci[4a], D. Cinca[46], V. Cindro[78], I.A. Cioara[23], A. Ciocio[16], F. Cirotto[106a,106b], Z.H. Citron[175], M. Citterio[94a], M. Ciubancan[28b], A. Clark[52], B.L. Clark[59], M.R. Clark[38], P.J. Clark[49], R.N. Clarke[16], C. Clement[148a,148b], Y. Coadou[88], M. Cobal[167a,167c], A. Coccaro[52], J. Cochran[67], L. Colasurdo[108], B. Cole[38], A.P. Colijn[109], J. Collot[58], T. Colombo[166], P. Conde Muiño[128a,128b], E. Coniavitis[51], S.H. Connell[147b], I.A. Connelly[87], S. Constantinescu[28b], G. Conti[32], F. Conventi[106a,n], M. Cooke[16], A.M. Cooper-Sarkar[122],

JHEP03(2018)009

F. Cormier[171], K.J.R. Cormier[161], M. Corradi[134a,134b], F. Corriveau[90,o], A. Cortes-Gonzalez[32], G. Costa[94a], M.J. Costa[170], D. Costanzo[141], G. Cottin[30], G. Cowan[80], B.E. Cox[87], K. Cranmer[112], S.J. Crawley[56], R.A. Creager[124], G. Cree[31], S. Crépé-Renaudin[58], F. Crescioli[83], W.A. Cribbs[148a,148b], M. Cristinziani[23], V. Croft[112], G. Crosetti[40a,40b], A. Cueto[85], T. Cuhadar Donszelmann[141], A.R. Cukierman[145], J. Cummings[179], M. Curatolo[50], J. Cúth[86], S. Czekierda[42], P. Czodrowski[32], G. D'amen[22a,22b], S. D'Auria[56], L. D'eramo[83], M. D'Onofrio[77], M.J. Da Cunha Sargedas De Sousa[128a,128b], C. Da Via[87], W. Dabrowski[41a], T. Dado[146a], T. Dai[92], O. Dale[15], F. Dallaire[97], C. Dallapiccola[89], M. Dam[39], J.R. Dandoy[124], M.F. Daneri[29], N.P. Dang[176], A.C. Daniells[19], N.S. Dann[87], M. Danninger[171], M. Dano Hoffmann[138], V. Dao[150], G. Darbo[53a], S. Darmora[8], J. Dassoulas[3], A. Dattagupta[118], T. Daubney[45], W. Davey[23], C. David[45], T. Davidek[131], D.R. Davis[48], P. Davison[81], E. Dawe[91], I. Dawson[141], K. De[8], R. de Asmundis[106a], A. De Benedetti[115], S. De Castro[22a,22b], S. De Cecco[83], N. De Groot[108], P. de Jong[109], H. De la Torre[93], F. De Lorenzi[67], A. De Maria[57], D. De Pedis[134a], A. De Salvo[134a], U. De Sanctis[135a,135b], A. De Santo[151], K. De Vasconcelos Corga[88], J.B. De Vivie De Regie[119], R. Debbe[27], C. Debenedetti[139], D.V. Dedovich[68], N. Dehghanian[3], I. Deigaard[109], M. Del Gaudio[40a,40b], J. Del Peso[85], D. Delgove[119], F. Deliot[138], C.M. Delitzsch[7], A. Dell'Acqua[32], L. Dell'Asta[24], M. Dell'Orso[126a,126b], M. Della Pietra[106a,106b], D. della Volpe[52], M. Delmastro[5], C. Delporte[119], P.A. Delsart[58], D.A. DeMarco[161], S. Demers[179], M. Demichev[68], A. Demilly[83], S.P. Denisov[132], D. Denysiuk[138], D. Derendarz[42], J.E. Derkaoui[137d], F. Derue[83], P. Dervan[77], K. Desch[23], C. Deterre[45], K. Dette[161], M.R. Devesa[29], P.O. Deviveiros[32], A. Dewhurst[133], S. Dhaliwal[25], F.A. Di Bello[52], A. Di Ciaccio[135a,135b], L. Di Ciaccio[5], W.K. Di Clemente[124], C. Di Donato[106a,106b], A. Di Girolamo[32], B. Di Girolamo[32], B. Di Micco[136a,136b], R. Di Nardo[32], K.F. Di Petrillo[59], A. Di Simone[51], R. Di Sipio[161], D. Di Valentino[31], C. Diaconu[88], M. Diamond[161], F.A. Dias[39], M.A. Diaz[34a], E.B. Diehl[92], J. Dietrich[17], S. Díez Cornell[45], A. Dimitrievska[14], J. Dingfelder[23], P. Dita[28b], S. Dita[28b], F. Dittus[32], F. Djama[88], T. Djobava[54b], J.I. Djuvsland[60a], M.A.B. do Vale[26c], D. Dobos[32], M. Dobre[28b], D. Dodsworth[25], C. Doglioni[84], J. Dolejsi[131], Z. Dolezal[131], M. Donadelli[26d], S. Donati[126a,126b], P. Dondero[123a,123b], J. Donini[37], J. Dopke[133], A. Doria[106a], M.T. Dova[74], A.T. Doyle[56], E. Drechsler[57], M. Dris[10], Y. Du[36b], J. Duarte-Campderros[155], F. Dubinin[98], A. Dubreuil[52], E. Duchovni[175], G. Duckeck[102], A. Ducourthial[83], O.A. Ducu[97,p], D. Duda[109], A. Dudarev[32], A.Chr. Dudder[86], E.M. Duffield[16], L. Duflot[119], M. Dührssen[32], C. Dulsen[178], M. Dumancic[175], A.E. Dumitriu[28b], A.K. Duncan[56], M. Dunford[60a], A. Duperrin[88], H. Duran Yildiz[4a], M. Düren[55], A. Durglishvili[54b], D. Duschinger[47], B. Dutta[45], D. Duvnjak[1], M. Dyndal[45], B.S. Dziedzic[42], C. Eckardt[45], K.M. Ecker[103], R.C. Edgar[92], T. Eifert[32], G. Eigen[15], K. Einsweiler[16], T. Ekelof[168], M. El Kacimi[137c], R. El Kosseifi[88], V. Ellajosyula[88], M. Ellert[168], S. Elles[5], F. Ellinghaus[178], A.A. Elliot[172], N. Ellis[32], J. Elmsheuser[27], M. Elsing[32], D. Emeliyanov[133], Y. Enari[157], O.C. Endner[86], J.S. Ennis[173], M.B. Epland[48], J. Erdmann[46], A. Ereditato[18], M. Ernst[27], S. Errede[169], M. Escalier[119], C. Escobar[170], B. Esposito[50], O. Estrada Pastor[170], A.I. Etienvre[138], E. Etzion[155], H. Evans[64], A. Ezhilov[125], M. Ezzi[137e], F. Fabbri[22a,22b], L. Fabbri[22a,22b], V. Fabiani[108], G. Facini[81], R.M. Fakhrutdinov[132], S. Falciano[134a], R.J. Falla[81], J. Faltova[32], Y. Fang[35a], M. Fanti[94a,94b], A. Farbin[8], A. Farilla[136a], C. Farina[127], E.M. Farina[123a,123b], T. Farooque[93], S. Farrell[16], S.M. Farrington[173], P. Farthouat[32], F. Fassi[137e], P. Fassnacht[32], D. Fassouliotis[9], M. Faucci Giannelli[49], A. Favareto[53a,53b], W.J. Fawcett[122], L. Fayard[119], O.L. Fedin[125,q], W. Fedorko[171], S. Feigl[121], L. Feligioni[88], C. Feng[36b], E.J. Feng[32], M.J. Fenton[56], A.B. Fenyuk[132], L. Feremenga[8], P. Fernandez Martinez[170], S. Fernandez Perez[13], J. Ferrando[45], A. Ferrari[168], P. Ferrari[109], R. Ferrari[123a], D.E. Ferreira de Lima[60b], A. Ferrer[170], D. Ferrere[52], C. Ferretti[92], F. Fiedler[86], A. Filipčič[78], M. Filipuzzi[45], F. Filthaut[108], M. Fincke-Keeler[172], K.D. Finelli[152],

JHEP03(2018)009

M.C.N. Fiolhais[128a,128c,r], L. Fiorini[170], A. Fischer[2], C. Fischer[13], J. Fischer[178], W.C. Fisher[93], N. Flaschel[45], I. Fleck[143], P. Fleischmann[92], R.R.M. Fletcher[124], T. Flick[178], B.M. Flierl[102], L.R. Flores Castillo[62a], M.J. Flowerdew[103], G.T. Forcolin[87], A. Formica[138], F.A. Förster[13], A. Forti[87], A.G. Foster[19], D. Fournier[119], H. Fox[75], S. Fracchia[141], P. Francavilla[83], M. Franchini[22a,22b], S. Franchino[60a], D. Francis[32], L. Franconi[121], M. Franklin[59], M. Frate[166], M. Fraternali[123a,123b], D. Freeborn[81], S.M. Fressard-Batraneanu[32], B. Freund[97], D. Froidevaux[32], J.A. Frost[122], C. Fukunaga[158], T. Fusayasu[104], J. Fuster[170], O. Gabizon[154], A. Gabrielli[22a,22b], A. Gabrielli[16], G.P. Gach[41a], S. Gadatsch[32], S. Gadomski[80], G. Gagliardi[53a,53b], L.G. Gagnon[97], C. Galea[108], B. Galhardo[128a,128c], E.J. Gallas[122], B.J. Gallop[133], P. Gallus[130], G. Galster[39], K.K. Gan[113], S. Ganguly[37], Y. Gao[77], Y.S. Gao[145,g], F.M. Garay Walls[34a], C. García[170], J.E. García Navarro[170], J.A. García Pascual[35a], M. Garcia-Sciveres[16], R.W. Gardner[33], N. Garelli[145], V. Garonne[121], A. Gascon Bravo[45], K. Gasnikova[45], C. Gatti[50], A. Gaudiello[53a,53b], G. Gaudio[123a], I.L. Gavrilenko[98], C. Gay[171], G. Gaycken[23], E.N. Gazis[10], C.N.P. Gee[133], J. Geisen[57], M. Geisen[86], M.P. Geisler[60a], K. Gellerstedt[148a,148b], C. Gemme[53a], M.H. Genest[58], C. Geng[92], S. Gentile[134a,134b], C. Gentsos[156], S. George[80], D. Gerbaudo[13], G. Geßner[46], S. Ghasemi[143], M. Ghneimat[23], B. Giacobbe[22a], S. Giagu[134a,134b], N. Giangiacomi[22a,22b], P. Giannetti[126a,126b], A. Giannini[106a,106b], S.M. Gibson[80], M. Gignac[171], M. Gilchriese[16], D. Gillberg[31], G. Gilles[178], D.M. Gingrich[3,d], M.P. Giordani[167a,167c], F.M. Giorgi[22a], P.F. Giraud[138], P. Giromini[59], G. Giugliarelli[167a,167c], D. Giugni[94a], F. Giuli[122], C. Giuliani[103], M. Giulini[60b], B.K. Gjelsten[121], S. Gkaitatzis[156], I. Gkialas[9,s], E.L. Gkougkousis[13], P. Gkountoumis[10], L.K. Gladilin[101], C. Glasman[85], J. Glatzer[13], P.C.F. Glaysher[45], A. Glazov[45], M. Goblirsch-Kolb[25], J. Godlewski[42], S. Goldfarb[91], T. Golling[52], D. Golubkov[132], A. Gomes[128a,128b,128d], R. Gonçalo[128a], R. Goncalves Gama[26a], J. Goncalves Pinto Firmino Da Costa[138], G. Gonella[51], L. Gonella[19], A. Gongadze[68], S. González de la Hoz[170], S. Gonzalez-Sevilla[52], L. Goossens[32], P.A. Gorbounov[99], H.A. Gordon[27], I. Gorelov[107], B. Gorini[32], E. Gorini[76a,76b], A. Gorišek[78], A.T. Goshaw[48], C. Gössling[46], M.I. Gostkin[68], C.A. Gottardo[23], C.R. Goudet[119], D. Goujdami[137c], A.G. Goussiou[140], N. Govender[147b,t], E. Gozani[154], I. Grabowska-Bold[41a], P.O.J. Gradin[168], J. Gramling[166], E. Gramstad[121], S. Grancagnolo[17], V. Gratchev[125], P.M. Gravila[28f], C. Gray[56], H.M. Gray[16], Z.D. Greenwood[82,u], C. Grefe[23], K. Gregersen[81], I.M. Gregor[45], P. Grenier[145], K. Grevtsov[5], J. Griffiths[8], A.A. Grillo[139], K. Grimm[75], S. Grinstein[13,v], Ph. Gris[37], J.-F. Grivaz[119], S. Groh[86], E. Gross[175], J. Grosse-Knetter[57], G.C. Grossi[82], Z.J. Grout[81], A. Grummer[107], L. Guan[92], W. Guan[176], J. Guenther[32], F. Guescini[163a], D. Guest[166], O. Gueta[155], B. Gui[113], E. Guido[53a,53b], T. Guillemin[5], S. Guindon[32], U. Gul[56], C. Gumpert[32], J. Guo[36c], W. Guo[92], Y. Guo[36a,w], R. Gupta[43], S. Gupta[122], S. Gurbuz[20a], G. Gustavino[115], B.J. Gutelman[154], P. Gutierrez[115], N.G. Gutierrez Ortiz[81], C. Gutschow[81], C. Guyot[138], M.P. Guzik[41a], C. Gwenlan[122], C.B. Gwilliam[77], A. Haas[112], C. Haber[16], H.K. Hadavand[8], N. Haddad[137e], A. Hadef[88], S. Hageböck[23], M. Hagihara[164], H. Hakobyan[180,*], M. Haleem[45], J. Haley[116], G. Halladjian[93], G.D. Hallewell[88], K. Hamacher[178], P. Hamal[117], K. Hamano[172], A. Hamilton[147a], G.N. Hamity[141], P.G. Hamnett[45], L. Han[36a], S. Han[35a], K. Hanagaki[69,x], K. Hanawa[157], M. Hance[139], B. Haney[124], P. Hanke[60a], J.B. Hansen[39], J.D. Hansen[39], M.C. Hansen[23], P.H. Hansen[39], K. Hara[164], A.S. Hard[176], T. Harenberg[178], F. Hariri[119], S. Harkusha[95], P.F. Harrison[173], N.M. Hartmann[102], Y. Hasegawa[142], A. Hasib[49], S. Hassani[138], S. Haug[18], R. Hauser[93], L. Hauswald[47], L.B. Havener[38], M. Havranek[130], C.M. Hawkes[19], R.J. Hawkings[32], D. Hayakawa[159], D. Hayden[93], C.P. Hays[122], J.M. Hays[79], H.S. Hayward[77], S.J. Haywood[133], S.J. Head[19], T. Heck[86], V. Hedberg[84], L. Heelan[8], S. Heer[23], K.K. Heidegger[51], S. Heim[45], T. Heim[16], B. Heinemann[45,y], J.J. Heinrich[102], L. Heinrich[112], C. Heinz[55], J. Hejbal[129], L. Helary[32], A. Held[171], S. Hellman[148a,148b], C. Helsens[32], R.C.W. Henderson[75],

JHEP03(2018)009

Y. Heng[176], S. Henkelmann[171], A.M. Henriques Correia[32], S. Henrot-Versille[119], G.H. Herbert[17], H. Herde[25], V. Herget[177], Y. Hernández Jiménez[147c], H. Herr[86], G. Herten[51], R. Hertenberger[102], L. Hervas[32], T.C. Herwig[124], G.G. Hesketh[81], N.P. Hessey[163a], J.W. Hetherly[43], S. Higashino[69], E. Higón-Rodriguez[170], K. Hildebrand[33], E. Hill[172], J.C. Hill[30], K.H. Hiller[45], S.J. Hillier[19], M. Hils[47], I. Hinchliffe[16], M. Hirose[51], D. Hirschbuehl[178], B. Hiti[78], O. Hladik[129], X. Hoad[49], J. Hobbs[150], N. Hod[163a], M.C. Hodgkinson[141], P. Hodgson[141], A. Hoecker[32], M.R. Hoeferkamp[107], F. Hoenig[102], D. Hohn[23], T.R. Holmes[33], M. Homann[46], S. Honda[164], T. Honda[69], T.M. Hong[127], B.H. Hooberman[169], W.H. Hopkins[118], Y. Horii[105], A.J. Horton[144], J-Y. Hostachy[58], A. Hostiuc[140], S. Hou[153], A. Hoummada[137a], J. Howarth[87], J. Hoya[74], M. Hrabovsky[117], J. Hrdinka[32], I. Hristova[17], J. Hrivnac[119], T. Hryn'ova[5], A. Hrynevich[96], P.J. Hsu[63], S.-C. Hsu[140], Q. Hu[36a], S. Hu[36c], Y. Huang[35a], Z. Hubacek[130], F. Hubaut[88], F. Huegging[23], T.B. Huffman[122], E.W. Hughes[38], M. Huhtinen[32], R.F.H. Hunter[31], P. Huo[150], N. Huseynov[68,b], J. Huston[93], J. Huth[59], R. Hyneman[92], G. Iacobucci[52], G. Iakovidis[27], I. Ibragimov[143], L. Iconomidou-Fayard[119], Z. Idrissi[137e], P. Iengo[32], O. Igonkina[109,z], T. Iizawa[174], Y. Ikegami[69], M. Ikeno[69], Y. Ilchenko[11,aa], D. Iliadis[156], N. Ilic[145], F. Iltzsche[47], G. Introzzi[123a,123b], P. Ioannou[9,*], M. Iodice[136a], K. Iordanidou[38], V. Ippolito[59], M.F. Isacson[168], N. Ishijima[120], M. Ishino[157], M. Ishitsuka[159], C. Issever[122], S. Istin[20a], F. Ito[164], J.M. Iturbe Ponce[62a], R. Iuppa[162a,162b], H. Iwasaki[69], J.M. Izen[44], V. Izzo[106a], S. Jabbar[3], P. Jackson[1], R.M. Jacobs[23], V. Jain[2], K.B. Jakobi[86], K. Jakobs[51], S. Jakobsen[65], T. Jakoubek[129], D.O. Jamin[116], D.K. Jana[82], R. Jansky[52], J. Janssen[23], M. Janus[57], P.A. Janus[41a], G. Jarlskog[84], N. Javadov[68,b], T. Javůrek[51], M. Javurkova[51], F. Jeanneau[138], L. Jeanty[16], J. Jejelava[54a,ab], A. Jelinskas[173], P. Jenni[51,ac], C. Jeske[173], S. Jézéquel[5], H. Ji[176], J. Jia[150], H. Jiang[67], Y. Jiang[36a], Z. Jiang[145], S. Jiggins[81], J. Jimenez Pena[170], S. Jin[35a], A. Jinaru[28b], O. Jinnouchi[159], H. Jivan[147c], P. Johansson[141], K.A. Johns[7], C.A. Johnson[64], W.J. Johnson[140], K. Jon-And[148a,148b], R.W.L. Jones[75], S.D. Jones[151], S. Jones[7], T.J. Jones[77], J. Jongmanns[60a], P.M. Jorge[128a,128b], J. Jovicevic[163a], X. Ju[176], A. Juste Rozas[13,v], M.K. Köhler[175], A. Kaczmarska[42], M. Kado[119], H. Kagan[113], M. Kagan[145], S.J. Kahn[88], T. Kaji[174], E. Kajomovitz[154], C.W. Kalderon[84], A. Kaluza[86], S. Kama[43], A. Kamenshchikov[132], N. Kanaya[157], L. Kanjir[78], V.A. Kantserov[100], J. Kanzaki[69], B. Kaplan[112], L.S. Kaplan[176], D. Kar[147c], K. Karakostas[10], N. Karastathis[10], M.J. Kareem[163b], E. Karentzos[10], S.N. Karpov[68], Z.M. Karpova[68], K. Karthik[112], V. Kartvelishvili[75], A.N. Karyukhin[132], K. Kasahara[164], L. Kashif[176], R.D. Kass[113], A. Kastanas[149], Y. Kataoka[157], C. Kato[157], A. Katre[52], J. Katzy[45], K. Kawade[70], K. Kawagoe[73], T. Kawamoto[157], G. Kawamura[57], E.F. Kay[77], V.F. Kazanin[111,c], R. Keeler[172], R. Kehoe[43], J.S. Keller[31], E. Kellermann[84], J.J. Kempster[80], J Kendrick[19], H. Keoshkerian[161], O. Kepka[129], B.P. Kerševan[78], S. Kersten[178], R.A. Keyes[90], M. Khader[169], F. Khalil-zada[12], A. Khanov[116], A.G. Kharlamov[111,c], T. Kharlamova[111,c], A. Khodinov[160], T.J. Khoo[52], V. Khovanskiy[99,*], E. Khramov[68], J. Khubua[54b,ad], S. Kido[70], C.R. Kilby[80], H.Y. Kim[8], S.H. Kim[164], Y.K. Kim[33], N. Kimura[156], O.M. Kind[17], B.T. King[77], D. Kirchmeier[47], J. Kirk[133], A.E. Kiryunin[103], T. Kishimoto[157], D. Kisielewska[41a], V. Kitali[45], O. Kivernyk[5], E. Kladiva[146b], T. Klapdor-Kleingrothaus[51], M.H. Klein[92], M. Klein[77], U. Klein[77], K. Kleinknecht[86], P. Klimek[110], A. Klimentov[27], R. Klingenberg[46,*], T. Klingl[23], T. Klioutchnikova[32], E.-E. Kluge[60a], P. Kluit[109], S. Kluth[103], E. Kneringer[65], E.B.F.G. Knoops[88], A. Knue[103], A. Kobayashi[157], D. Kobayashi[73], T. Kobayashi[157], M. Kobel[47], M. Kocian[145], P. Kodys[131], T. Koffas[31], E. Koffeman[109], N.M. Köhler[103], T. Koi[145], M. Kolb[60b], I. Koletsou[5], A.A. Komar[98,*], T. Kondo[69], N. Kondrashova[36c], K. Köneke[51], A.C. König[108], T. Kono[69,ae], R. Konoplich[112,af], N. Konstantinidis[81], R. Kopeliansky[64], S. Koperny[41a], A.K. Kopp[51], K. Korcyl[42], K. Kordas[156], A. Korn[81], A.A. Korol[111,c], I. Korolkov[13], E.V. Korolkova[141], O. Kortner[103], S. Kortner[103], T. Kosek[131], V.V. Kostyukhin[23], A. Kotwal[48],

JHEP03(2018)009

A. Koulouris[10], A. Kourkoumeli-Charalampidi[123a,123b], C. Kourkoumelis[9], E. Kourlitis[141], V. Kouskoura[27], A.B. Kowalewska[42], R. Kowalewski[172], T.Z. Kowalski[41a], C. Kozakai[157], W. Kozanecki[138], A.S. Kozhin[132], V.A. Kramarenko[101], G. Kramberger[78], D. Krasnopevtsev[100], M.W. Krasny[83], A. Krasznahorkay[32], D. Krauss[103], J.A. Kremer[41a], J. Kretzschmar[77], K. Kreutzfeldt[55], P. Krieger[161], K. Krizka[16], K. Kroeninger[46], H. Kroha[103], J. Kroll[129], J. Kroll[124], J. Kroseberg[23], J. Krstic[14], U. Kruchonak[68], H. Krüger[23], N. Krumnack[67], M.C. Kruse[48], T. Kubota[91], H. Kucuk[81], S. Kuday[4b], J.T. Kuechler[178], S. Kuehn[32], A. Kugel[60a], F. Kuger[177], T. Kuhl[45], V. Kukhtin[68], R. Kukla[88], Y. Kulchitsky[95], S. Kuleshov[34b], Y.P. Kulinich[169], M. Kuna[134a,134b], T. Kunigo[71], A. Kupco[129], T. Kupfer[46], O. Kuprash[155], H. Kurashige[70], L.L. Kurchaninov[163a], Y.A. Kurochkin[95], M.G. Kurth[35a], E.S. Kuwertz[172], M. Kuze[159], J. Kvita[117], T. Kwan[172], D. Kyriazopoulos[141], A. La Rosa[103], J.L. La Rosa Navarro[26d], L. La Rotonda[40a,40b], F. La Ruffa[40a,40b], C. Lacasta[170], F. Lacava[134a,134b], J. Lacey[45], D.P.J. Lack[87], H. Lacker[17], D. Lacour[83], E. Ladygin[68], R. Lafaye[5], B. Laforge[83], T. Lagouri[179], S. Lai[57], S. Lammers[64], W. Lampl[7], E. Lançon[27], U. Landgraf[51], M.P.J. Landon[79], M.C. Lanfermann[52], V.S. Lang[45], J.C. Lange[13], R.J. Langenberg[32], A.J. Lankford[166], F. Lanni[27], K. Lantzsch[23], A. Lanza[123a], A. Lapertosa[53a,53b], S. Laplace[83], J.F. Laporte[138], T. Lari[94a], F. Lasagni Manghi[22a,22b], M. Lassnig[32], T.S. Lau[62a], P. Laurelli[50], W. Lavrijsen[16], A.T. Law[139], P. Laycock[77], T. Lazovich[59], M. Lazzaroni[94a,94b], B. Le[91], O. Le Dortz[83], E. Le Guirriec[88], E.P. Le Quilleuc[138], M. LeBlanc[172], T. LeCompte[6], F. Ledroit-Guillon[58], C.A. Lee[27], G.R. Lee[34a], S.C. Lee[153], L. Lee[59], B. Lefebvre[90], G. Lefebvre[83], M. Lefebvre[172], F. Legger[102], C. Leggett[16], G. Lehmann Miotto[32], X. Lei[7], W.A. Leight[45], M.A.L. Leite[26d], R. Leitner[131], D. Lellouch[175], B. Lemmer[57], K.J.C. Leney[81], T. Lenz[23], B. Lenzi[32], R. Leone[7], S. Leone[126a,126b], C. Leonidopoulos[49], G. Lerner[151], C. Leroy[97], R. Les[161], A.A.J. Lesage[138], C.G. Lester[30], M. Levchenko[125], J. Levêque[5], D. Levin[92], L.J. Levinson[175], M. Levy[19], D. Lewis[79], B. Li[36a,w], C.-Q. Li[36a], H. Li[150], L. Li[36c], Q. Li[35a], Q. Li[36a], S. Li[48], X. Li[36c], Y. Li[143], Z. Liang[35a], B. Liberti[135a], A. Liblong[161], K. Lie[62c], J. Liebal[23], W. Liebig[15], A. Limosani[152], K. Lin[93], S.C. Lin[182], T.H. Lin[86], R.A. Linck[64], B.E. Lindquist[150], A.E. Lionti[52], E. Lipeles[124], A. Lipniacka[15], M. Lisovyi[60b], T.M. Liss[169,ag], A. Lister[171], A.M. Litke[139], B. Liu[67], H. Liu[92], H. Liu[27], J.K.K. Liu[122], J. Liu[36b], J.B. Liu[36a], K. Liu[88], L. Liu[169], M. Liu[36a], Y.L. Liu[36a], Y. Liu[36a], M. Livan[123a,123b], A. Lleres[58], J. Llorente Merino[35a], S.L. Lloyd[79], C.Y. Lo[62b], F. Lo Sterzo[43], E.M. Lobodzinska[45], P. Loch[7], F.K. Loebinger[87], A. Loesle[51], K.M. Loew[25], T. Lohse[17], K. Lohwasser[141], M. Lokajicek[129], B.A. Long[24], J.D. Long[169], R.E. Long[75], L. Longo[76a,76b], K.A. Looper[113], J.A. Lopez[34b], I. Lopez Paz[13], A. Lopez Solis[83], J. Lorenz[102], N. Lorenzo Martinez[5], M. Losada[21], P.J. Lösel[102], X. Lou[35a], A. Lounis[119], J. Love[6], P.A. Love[75], H. Lu[62a], N. Lu[92], Y.J. Lu[63], H.J. Lubatti[140], C. Luci[134a,134b], A. Lucotte[58], C. Luedtke[51], F. Luehring[64], W. Lukas[65], L. Luminari[134a], O. Lundberg[148a,148b], B. Lund-Jensen[149], M.S. Lutz[89], P.M. Luzi[83], D. Lynn[27], R. Lysak[129], E. Lytken[84], F. Lyu[35a], V. Lyubushkin[68], H. Ma[27], L.L. Ma[36b], Y. Ma[36b], G. Maccarrone[50], A. Macchiolo[103], C.M. Macdonald[141], B. Maček[78], J. Machado Miguens[124,128b], D. Madaffari[170], R. Madar[37], W.F. Mader[47], A. Madsen[45], N. Madysa[47], J. Maeda[70], S. Maeland[15], T. Maeno[27], A.S. Maevskiy[101], V. Magerl[51], C. Maiani[119], C. Maidantchik[26a], T. Maier[102], A. Maio[128a,128b,128d], O. Majersky[146a], S. Majewski[118], Y. Makida[69], N. Makovec[119], B. Malaescu[83], Pa. Malecki[42], V.P. Maleev[125], F. Malek[58], U. Mallik[66], D. Malon[6], C. Malone[30], S. Maltezos[10], S. Malyukov[32], J. Mamuzic[170], G. Mancini[50], I. Mandić[78], J. Maneira[128a,128b], L. Manhaes de Andrade Filho[26b], J. Manjarres Ramos[47], K.H. Mankinen[84], A. Mann[102], A. Manousos[32], B. Mansoulie[138], J.D. Mansour[35a], R. Mantifel[90], M. Mantoani[57], S. Manzoni[94a,94b], L. Mapelli[32], G. Marceca[29], L. March[52], L. Marchese[122], G. Marchiori[83],

JHEP03(2018)009

M. Marcisovsky[129], C.A. Marin Tobon[32], M. Marjanovic[37], D.E. Marley[92], F. Marroquim[26a], S.P. Marsden[87], Z. Marshall[16], M.U.F Martensson[168], S. Marti-Garcia[170], C.B. Martin[113], T.A. Martin[173], V.J. Martin[49], B. Martin dit Latour[15], M. Martinez[13,v], V.I. Martinez Outschoorn[169], S. Martin-Haugh[133], V.S. Martoiu[28b], A.C. Martyniuk[81], A. Marzin[32], L. Masetti[86], T. Mashimo[157], R. Mashinistov[98], J. Masik[87], A.L. Maslennikov[111,c], L.H. Mason[91], L. Massa[135a,135b], P. Mastrandrea[5], A. Mastroberardino[40a,40b], T. Masubuchi[157], P. Mättig[178], J. Maurer[28b], S.J. Maxfield[77], D.A. Maximov[111,c], R. Mazini[153], I. Maznas[156], S.M. Mazza[94a,94b], N.C. Mc Fadden[107], G. Mc Goldrick[161], S.P. Mc Kee[92], A. McCarn[92], R.L. McCarthy[150], T.G. McCarthy[103], L.I. McClymont[81], E.F. McDonald[91], J.A. Mcfayden[32], G. Mchedlidze[57], S.J. McMahon[133], P.C. McNamara[91], C.J. McNicol[173], R.A. McPherson[172,o], S. Meehan[140], T.J. Megy[51], S. Mehlhase[102], A. Mehta[77], T. Meideck[58], K. Meier[60a], B. Meirose[44], D. Melini[170,ah], B.R. Mellado Garcia[147c], J.D. Mellenthin[57], M. Melo[146a], F. Meloni[18], A. Melzer[23], S.B. Menary[87], L. Meng[77], X.T. Meng[92], A. Mengarelli[22a,22b], S. Menke[103], E. Meoni[40a,40b], S. Mergelmeyer[17], C. Merlassino[18], P. Mermod[52], L. Merola[106a,106b], C. Meroni[94a], F.S. Merritt[33], A. Messina[134a,134b], J. Metcalfe[6], A.S. Mete[166], C. Meyer[124], J-P. Meyer[138], J. Meyer[109], H. Meyer Zu Theenhausen[60a], F. Miano[151], R.P. Middleton[133], S. Miglioranzi[53a,53b], L. Mijović[49], G. Mikenberg[175], M. Mikestikova[129], M. Mikuž[78], M. Milesi[91], A. Milic[161], D.A. Millar[79], D.W. Miller[33], C. Mills[49], A. Milov[175], D.A. Milstead[148a,148b], A.A. Minaenko[132], Y. Minami[157], I.A. Minashvili[54b], A.I. Mincer[112], B. Mindur[41a], M. Mineev[68], Y. Minegishi[157], Y. Ming[176], L.M. Mir[13], A. Mirto[76a,76b], K.P. Mistry[124], T. Mitani[174], J. Mitrevski[102], V.A. Mitsou[170], A. Miucci[18], P.S. Miyagawa[141], A. Mizukami[69], J.U. Mjörnmark[84], T. Mkrtchyan[180], M. Mlynarikova[131], T. Moa[148a,148b], K. Mochizuki[97], P. Mogg[51], S. Mohapatra[38], S. Molander[148a,148b], R. Moles-Valls[23], M.C. Mondragon[93], K. Mönig[45], J. Monk[39], E. Monnier[88], A. Montalbano[150], J. Montejo Berlingen[32], F. Monticelli[74], S. Monzani[94a,94b], R.W. Moore[3], N. Morange[119], D. Moreno[21], M. Moreno Llácer[32], P. Morettini[53a], S. Morgenstern[32], D. Mori[144], T. Mori[157], M. Morii[59], M. Morinaga[174], V. Morisbak[121], A.K. Morley[32], G. Mornacchi[32], J.D. Morris[79], L. Morvaj[150], P. Moschovakos[10], M. Mosidze[54b], H.J. Moss[141], J. Moss[145,ai], K. Motohashi[159], R. Mount[145], E. Mountricha[27], E.J.W. Moyse[89], S. Muanza[88], F. Mueller[103], J. Mueller[127], R.S.P. Mueller[102], D. Muenstermann[75], P. Mullen[56], G.A. Mullier[18], F.J. Munoz Sanchez[87], W.J. Murray[173,133], H. Musheghyan[32], M. Muškinja[78], A.G. Myagkov[132,aj], M. Myska[130], B.P. Nachman[16], O. Nackenhorst[52], K. Nagai[122], R. Nagai[69,ae], K. Nagano[69], Y. Nagasaka[61], K. Nagata[164], M. Nagel[51], E. Nagy[88], A.M. Nairz[32], Y. Nakahama[105], K. Nakamura[69], T. Nakamura[157], I. Nakano[114], R.F. Naranjo Garcia[45], R. Narayan[11], D.I. Narrias Villar[60a], I. Naryshkin[125], T. Naumann[45], G. Navarro[21], R. Nayyar[7], H.A. Neal[92], P.Yu. Nechaeva[98], T.J. Neep[138], A. Negri[123a,123b], M. Negrini[22a], S. Nektarijevic[108], C. Nellist[57], A. Nelson[166], M.E. Nelson[122], S. Nemecek[129], P. Nemethy[112], M. Nessi[32,ak], M.S. Neubauer[169], M. Neumann[178], P.R. Newman[19], T.Y. Ng[62c], T. Nguyen Manh[97], R.B. Nickerson[122], R. Nicolaidou[138], J. Nielsen[139], N. Nikiforou[11], V. Nikolaenko[132,aj], I. Nikolic-Audit[83], K. Nikolopoulos[19], J.K. Nilsen[121], P. Nilsson[27], Y. Ninomiya[157], A. Nisati[134a], N. Nishu[36c], R. Nisius[103], I. Nitsche[46], T. Nitta[174], T. Nobe[157], Y. Noguchi[71], M. Nomachi[120], I. Nomidis[31], M.A. Nomura[27], T. Nooney[79], M. Nordberg[32], N. Norjoharuddeen[122], O. Novgorodova[47], M. Nozaki[69], L. Nozka[117], K. Ntekas[166], E. Nurse[81], F. Nuti[91], K. O'connor[25], D.C. O'Neil[144], A.A. O'Rourke[45], V. O'Shea[56], F.G. Oakham[31,d], H. Oberlack[103], T. Obermann[23], J. Ocariz[83], A. Ochi[70], I. Ochoa[38], J.P. Ochoa-Ricoux[34a], S. Oda[73], S. Odaka[69], A. Oh[87], S.H. Oh[48], C.C. Ohm[149], H. Ohman[168], H. Oide[53a,53b], H. Okawa[164], Y. Okumura[157], T. Okuyama[69], A. Olariu[28b], L.F. Oleiro Seabra[128a], S.A. Olivares Pino[34a], D. Oliveira Damazio[27], A. Olszewski[42], J. Olszowska[42], A. Onofre[128a,128e], K. Onogi[105], P.U.E. Onyisi[11,aa],

JHEP03(2018)009

H. Oppen[121], M.J. Oreglia[33], Y. Oren[155], D. Orestano[136a,136b], N. Orlando[62b], R.S. Orr[161], B. Osculati[53a,53b,*], R. Ospanov[36a], G. Otero y Garzon[29], H. Otono[73], M. Ouchrif[137d], F. Ould-Saada[121], A. Ouraou[138], K.P. Oussoren[109], Q. Ouyang[35a], M. Owen[56], R.E. Owen[19], V.E. Ozcan[20a], N. Ozturk[8], K. Pachal[144], A. Pacheco Pages[13], L. Pacheco Rodriguez[138], C. Padilla Aranda[13], S. Pagan Griso[16], M. Paganini[179], F. Paige[27], G. Palacino[64], S. Palazzo[40a,40b], S. Palestini[32], M. Palka[41b], D. Pallin[37], E.St. Panagiotopoulou[10], I. Panagoulias[10], C.E. Pandini[52], J.G. Panduro Vazquez[80], P. Pani[32], S. Panitkin[27], D. Pantea[28b], L. Paolozzi[52], Th.D. Papadopoulou[10], K. Papageorgiou[9,s], A. Paramonov[6], D. Paredes Hernandez[179], A.J. Parker[75], M.A. Parker[30], K.A. Parker[45], F. Parodi[53a,53b], J.A. Parsons[38], U. Parzefall[51], V.R. Pascuzzi[161], J.M. Pasner[139], E. Pasqualucci[134a], S. Passaggio[53a], Fr. Pastore[80], S. Pataraia[86], J.R. Pater[87], T. Pauly[32], B. Pearson[103], S. Pedraza Lopez[170], R. Pedro[128a,128b], S.V. Peleganchuk[111,c], O. Penc[129], C. Peng[35a], H. Peng[36a], J. Penwell[64], B.S. Peralva[26b], M.M. Perego[138], D.V. Perepelitsa[27], F. Peri[17], L. Perini[94a,94b], H. Pernegger[32], S. Perrella[106a,106b], R. Peschke[45], V.D. Peshekhonov[68,*], K. Peters[45], R.F.Y. Peters[87], B.A. Petersen[32], T.C. Petersen[39], E. Petit[58], A. Petridis[1], C. Petridou[156], P. Petroff[119], E. Petrolo[134a], M. Petrov[122], F. Petrucci[136a,136b], N.E. Pettersson[89], A. Peyaud[138], R. Pezoa[34b], F.H. Phillips[93], P.W. Phillips[133], G. Piacquadio[150], E. Pianori[173], A. Picazio[89], E. Piccaro[79], M.A. Pickering[122], R. Piegaia[29], J.E. Pilcher[33], A.D. Pilkington[87], M. Pinamonti[135a,135b], J.L. Pinfold[3], H. Pirumov[45], M. Pitt[175], L. Plazak[146a], M.-A. Pleier[27], V. Pleskot[86], E. Plotnikova[68], D. Pluth[67], P. Podberezko[111], R. Poettgen[84], R. Poggi[123a,123b], L. Poggioli[119], I. Pogrebnyak[93], D. Pohl[23], I. Pokharel[57], G. Polesello[123a], A. Poley[45], A. Policicchio[40a,40b], R. Polifka[32], A. Polini[22a], C.S. Pollard[56], V. Polychronakos[27], K. Pommès[32], D. Ponomarenko[100], L. Pontecorvo[134a], G.A. Popeneciu[28d], D.M. Portillo Quintero[83], S. Pospisil[130], K. Potamianos[45], I.N. Potrap[68], C.J. Potter[30], H. Potti[11], T. Poulsen[84], J. Poveda[32], M.E. Pozo Astigarraga[32], P. Pralavorio[88], A. Pranko[16], S. Prell[67], D. Price[87], M. Primavera[76a], S. Prince[90], N. Proklova[100], K. Prokofiev[62c], F. Prokoshin[34b], S. Protopopescu[27], J. Proudfoot[6], M. Przybycien[41a], A. Puri[169], P. Puzo[119], J. Qian[92], G. Qin[56], Y. Qin[87], A. Quadt[57], M. Queitsch-Maitland[45], D. Quilty[56], S. Raddum[121], V. Radeka[27], V. Radescu[122], S.K. Radhakrishnan[150], P. Radloff[118], P. Rados[91], F. Ragusa[94a,94b], G. Rahal[181], J.A. Raine[87], S. Rajagopalan[27], C. Rangel-Smith[168], T. Rashid[119], S. Raspopov[5], M.G. Ratti[94a,94b], D.M. Rauch[45], F. Rauscher[102], S. Rave[86], I. Ravinovich[175], J.H. Rawling[87], M. Raymond[32], A.L. Read[121], N.P. Readioff[58], M. Reale[76a,76b], D.M. Rebuzzi[123a,123b], A. Redelbach[177], G. Redlinger[27], R. Reece[139], R.G. Reed[147c], K. Reeves[44], L. Rehnisch[17], J. Reichert[124], A. Reiss[86], C. Rembser[32], H. Ren[35a], M. Rescigno[134a], S. Resconi[94a], E.D. Resseguie[124], S. Rettie[171], E. Reynolds[19], O.L. Rezanova[111,c], P. Reznicek[131], R. Rezvani[97], R. Richter[103], S. Richter[81], E. Richter-Was[41b], O. Ricken[23], M. Ridel[83], P. Rieck[103], C.J. Riegel[178], J. Rieger[57], O. Rifki[115], M. Rijssenbeek[150], A. Rimoldi[123a,123b], M. Rimoldi[18], L. Rinaldi[22a], G. Ripellino[149], B. Ristić[32], E. Ritsch[32], I. Riu[13], F. Rizatdinova[116], E. Rizvi[79], C. Rizzi[13], R.T. Roberts[87], S.H. Robertson[90,o], A. Robichaud-Veronneau[90], D. Robinson[30], J.E.M. Robinson[45], A. Robson[56], E. Rocco[86], C. Roda[126a,126b], Y. Rodina[88,al], S. Rodriguez Bosca[170], A. Rodriguez Perez[13], D. Rodriguez Rodriguez[170], S. Roe[32], C.S. Rogan[59], O. Røhne[121], J. Roloff[59], A. Romaniouk[100], M. Romano[22a,22b], S.M. Romano Saez[37], E. Romero Adam[170], N. Rompotis[77], M. Ronzani[51], L. Roos[83], S. Rosati[134a], K. Rosbach[51], P. Rose[139], N.-A. Rosien[57], E. Rossi[106a,106b], L.P. Rossi[53a], J.H.N. Rosten[30], R. Rosten[140], M. Rotaru[28b], J. Rothberg[140], D. Rousseau[119], A. Rozanov[88], Y. Rozen[154], X. Ruan[147c], F. Rubbo[145], F. Rühr[51], A. Ruiz-Martinez[31], Z. Rurikova[51], N.A. Rusakovich[68], H.L. Russell[90], J.P. Rutherfoord[7], N. Ruthmann[32], Y.F. Ryabov[125], M. Rybar[169], G. Rybkin[119], S. Ryu[6], A. Ryzhov[132], G.F. Rzehorz[57],

JHEP03(2018)009

A.F. Saavedra[152], G. Sabato[109], S. Sacerdoti[29], H.F-W. Sadrozinski[139], R. Sadykov[68], F. Safai Tehrani[134a], P. Saha[110], M. Sahinsoy[60a], M. Saimpert[45], M. Saito[157], T. Saito[157], H. Sakamoto[157], Y. Sakurai[174], G. Salamanna[136a,136b], J.E. Salazar Loyola[34b], D. Salek[109], P.H. Sales De Bruin[168], D. Salihagic[103], A. Salnikov[145], J. Salt[170], D. Salvatore[40a,40b], F. Salvatore[151], A. Salvucci[62a,62b,62c], A. Salzburger[32], D. Sammel[51], D. Sampsonidis[156], D. Sampsonidou[156], J. Sánchez[170], V. Sanchez Martinez[170], A. Sanchez Pineda[167a,167c], H. Sandaker[121], R.L. Sandbach[79], C.O. Sander[45], M. Sandhoff[178], C. Sandoval[21], D.P.C. Sankey[133], M. Sannino[53a,53b], Y. Sano[105], A. Sansoni[50], C. Santoni[37], H. Santos[128a], I. Santoyo Castillo[151], A. Sapronov[68], J.G. Saraiva[128a,128d], B. Sarrazin[23], O. Sasaki[69], K. Sato[164], E. Sauvan[5], G. Savage[80], P. Savard[161,d], N. Savic[103], C. Sawyer[133], L. Sawyer[82,u], J. Saxon[33], C. Sbarra[22a], A. Sbrizzi[22a,22b], T. Scanlon[81], D.A. Scannicchio[166], J. Schaarschmidt[140], P. Schacht[103], B.M. Schachtner[102], D. Schaefer[33], L. Schaefer[124], R. Schaefer[45], J. Schaeffer[86], S. Schaepe[23], S. Schaetzel[60b], U. Schäfer[86], A.C. Schaffer[119], D. Schaile[102], R.D. Schamberger[150], V.A. Schegelsky[125], D. Scheirich[131], M. Schernau[166], C. Schiavi[53a,53b], S. Schier[139], L.K. Schildgen[23], C. Schillo[51], M. Schioppa[40a,40b], S. Schlenker[32], K.R. Schmidt-Sommerfeld[103], K. Schmieden[32], C. Schmitt[86], S. Schmitt[45], S. Schmitz[86], U. Schnoor[51], L. Schoeffel[138], A. Schoening[60b], B.D. Schoenrock[93], E. Schopf[23], M. Schott[86], J.F.P. Schouwenberg[108], J. Schovancova[32], S. Schramm[52], N. Schuh[86], A. Schulte[86], M.J. Schultens[23], H.-C. Schultz-Coulon[60a], H. Schulz[17], M. Schumacher[51], B.A. Schumm[139], Ph. Schune[138], A. Schwartzman[145], T.A. Schwarz[92], H. Schweiger[87], Ph. Schwemling[138], R. Schwienhorst[93], J. Schwindling[138], A. Sciandra[23], G. Sciolla[25], M. Scornajenghi[40a,40b], F. Scuri[126a,126b], F. Scutti[91], J. Searcy[92], P. Seema[23], S.C. Seidel[107], A. Seiden[139], J.M. Seixas[26a], G. Sekhniaidze[106a], K. Sekhon[92], S.J. Sekula[43], N. Semprini-Cesari[22a,22b], S. Senkin[37], C. Serfon[121], L. Serin[119], L. Serkin[167a,167b], M. Sessa[136a,136b], R. Seuster[172], H. Severini[115], T. Sfiligoj[78], F. Sforza[165], A. Sfyrla[52], E. Shabalina[57], N.W. Shaikh[148a,148b], L.Y. Shan[35a], R. Shang[169], J.T. Shank[24], M. Shapiro[16], P.B. Shatalov[99], K. Shaw[167a,167b], S.M. Shaw[87], A. Shcherbakova[148a,148b], C.Y. Shehu[151], Y. Shen[115], N. Sherafati[31], P. Sherwood[81], L. Shi[153,am], S. Shimizu[70], C.O. Shimmin[179], M. Shimojima[104], I.P.J. Shipsey[122], S. Shirabe[73], M. Shiyakova[68,an], J. Shlomi[175], A. Shmeleva[98], D. Shoaleh Saadi[97], M.J. Shochet[33], S. Shojaii[94a,94b], D.R. Shope[115], S. Shrestha[113], E. Shulga[100], M.A. Shupe[7], P. Sicho[129], A.M. Sickles[169], P.E. Sidebo[149], E. Sideras Haddad[147c], O. Sidiropoulou[177], A. Sidoti[22a,22b], F. Siegert[47], Dj. Sijacki[14], J. Silva[128a,128d], S.B. Silverstein[148a], V. Simak[130], L. Simic[68], S. Simion[119], E. Simioni[86], B. Simmons[81], M. Simon[86], P. Sinervo[161], N.B. Sinev[118], M. Sioli[22a,22b], G. Siragusa[177], I. Siral[92], S.Yu. Sivoklokov[101], J. Sjölin[148a,148b], M.B. Skinner[75], P. Skubic[115], M. Slater[19], T. Slavicek[130], M. Slawinska[42], K. Sliwa[165], R. Slovak[131], V. Smakhtin[175], B.H. Smart[5], J. Smiesko[146a], N. Smirnov[100], S.Yu. Smirnov[100], Y. Smirnov[100], L.N. Smirnova[101,ao], O. Smirnova[84], J.W. Smith[57], M.N.K. Smith[38], R.W. Smith[38], M. Smizanska[75], K. Smolek[130], A.A. Snesarev[98], I.M. Snyder[118], S. Snyder[27], R. Sobie[172,o], F. Socher[47], A. Soffer[155], A. Søgaard[49], D.A. Soh[153], G. Sokhrannyi[78], C.A. Solans Sanchez[32], M. Solar[130], E.Yu. Soldatov[100], U. Soldevila[170], A.A. Solodkov[132], A. Soloshenko[68], O.V. Solovyanov[132], V. Solovyev[125], P. Sommer[51], H. Son[165], A. Sopczak[130], D. Sosa[60b], C.L. Sotiropoulou[126a,126b], S. Sottocornola[123a,123b], R. Soualah[167a,167c], A.M. Soukharev[111,c], D. South[45], B.C. Sowden[80], S. Spagnolo[76a,76b], M. Spalla[126a,126b], M. Spangenberg[173], F. Spanò[80], D. Sperlich[17], F. Spettel[103], T.M. Spieker[60a], R. Spighi[22a], G. Spigo[32], L.A. Spiller[91], M. Spousta[131], R.D. St. Denis[56,*], A. Stabile[94a], R. Stamen[60a], S. Stamm[17], E. Stanecka[42], R.W. Stanek[6], C. Stanescu[136a], M.M. Stanitzki[45], B.S. Stapf[109], S. Stapnes[121], E.A. Starchenko[132], G.H. Stark[33], J. Stark[58], S.H Stark[39], P. Staroba[129], P. Starovoitov[60a], S. Stärz[32], R. Staszewski[42], M. Stegler[45], P. Steinberg[27], B. Stelzer[144], H.J. Stelzer[32],

JHEP03(2018)009

O. Stelzer-Chilton[163a], H. Stenzel[55], G.A. Stewart[56], M.C. Stockton[118], M. Stoebe[90], G. Stoicea[28b], P. Stolte[57], S. Stonjek[103], A.R. Stradling[8], A. Straessner[47], M.E. Stramaglia[18], J. Strandberg[149], S. Strandberg[148a,148b], M. Strauss[115], P. Strizenec[146b], R. Ströhmer[177], D.M. Strom[118], R. Stroynowski[43], A. Strubig[49], S.A. Stucci[27], B. Stugu[15], N.A. Styles[45], D. Su[145], J. Su[127], S. Suchek[60a], Y. Sugaya[120], M. Suk[130], V.V. Sulin[98], DMS Sultan[162a,162b], S. Sultansoy[4c], T. Sumida[71], S. Sun[59], X. Sun[3], K. Suruliz[151], C.J.E. Suster[152], M.R. Sutton[151], S. Suzuki[69], M. Svatos[129], M. Swiatlowski[33], S.P. Swift[2], I. Sykora[146a], T. Sykora[131], D. Ta[51], K. Tackmann[45], J. Taenzer[155], A. Taffard[166], R. Tafirout[163a], E. Tahirovic[79], N. Taiblum[155], H. Takai[27], R. Takashima[72], E.H. Takasugi[103], K. Takeda[70], T. Takeshita[142], Y. Takubo[69], M. Talby[88], A.A. Talyshev[111,c], J. Tanaka[157], M. Tanaka[159], R. Tanaka[119], S. Tanaka[69], R. Tanioka[70], B.B. Tannenwald[113], S. Tapia Araya[34b], S. Tapprogge[86], S. Tarem[154], G.F. Tartarelli[94a], P. Tas[131], M. Tasevsky[129], T. Tashiro[71], E. Tassi[40a,40b], A. Tavares Delgado[128a,128b], Y. Tayalati[137e], A.C. Taylor[107], A.J. Taylor[49], G.N. Taylor[91], P.T.E. Taylor[91], W. Taylor[163b], P. Teixeira-Dias[80], D. Temple[144], H. Ten Kate[32], P.K. Teng[153], J.J. Teoh[120], F. Tepel[178], S. Terada[69], K. Terashi[157], J. Terron[85], S. Terzo[13], M. Testa[50], R.J. Teuscher[161,o], S.J. Thais[179], T. Theveneaux-Pelzer[88], F. Thiele[39], J.P. Thomas[19], J. Thomas-Wilsker[80], P.D. Thompson[19], A.S. Thompson[56], L.A. Thomsen[179], E. Thomson[124], Y. Tian[38], M.J. Tibbetts[16], R.E. Ticse Torres[88], V.O. Tikhomirov[98,ap], Yu.A. Tikhonov[111,c], S. Timoshenko[100], P. Tipton[179], S. Tisserant[88], K. Todome[159], S. Todorova-Nova[5], S. Todt[47], J. Tojo[73], S. Tokár[146a], K. Tokushuku[69], E. Tolley[59], L. Tomlinson[87], M. Tomoto[105], L. Tompkins[145,aq], K. Toms[107], B. Tong[59], P. Tornambe[51], E. Torrence[118], H. Torres[47], E. Torró Pastor[140], J. Toth[88,ar], F. Touchard[88], D.R. Tovey[141], C.J. Treado[112], T. Trefzger[177], F. Tresoldi[151], A. Tricoli[27], I.M. Trigger[163a], S. Trincaz-Duvoid[83], M.F. Tripiana[13], W. Trischuk[161], B. Trocmé[58], A. Trofymov[45], C. Troncon[94a], M. Trottier-McDonald[16], M. Trovatelli[172], L. Truong[147b], M. Trzebinski[42], A. Trzupek[42], K.W. Tsang[62a], J.C-L. Tseng[122], P.V. Tsiareshka[95], G. Tsipolitis[10], N. Tsirintanis[9], S. Tsiskaridze[13], V. Tsiskaridze[51], E.G. Tskhadadze[54a], I.I. Tsukerman[99], V. Tsulaia[16], S. Tsuno[69], D. Tsybychev[150], Y. Tu[62b], A. Tudorache[28b], V. Tudorache[28b], T.T. Tulbure[28a], A.N. Tuna[59], S. Turchikhin[68], D. Turgeman[175], I. Turk Cakir[4b,as], R. Turra[94a], P.M. Tuts[38], G. Ucchielli[22a,22b], I. Ueda[69], M. Ughetto[148a,148b], F. Ukegawa[164], G. Unal[32], A. Undrus[27], G. Unel[166], F.C. Ungaro[91], Y. Unno[69], K. Uno[157], C. Unverdorben[102], J. Urban[146b], P. Urquijo[91], P. Urrejola[86], G. Usai[8], J. Usui[69], L. Vacavant[88], V. Vacek[130], B. Vachon[90], K.O.H. Vadla[121], A. Vaidya[81], C. Valderanis[102], E. Valdes Santurio[148a,148b], M. Valente[52], S. Valentinetti[22a,22b], A. Valero[170], L. Valéry[13], S. Valkar[131], A. Vallier[5], J.A. Valls Ferrer[170], W. Van Den Wollenberg[109], H. van der Graaf[109], P. van Gemmeren[6], J. Van Nieuwkoop[144], I. van Vulpen[109], M.C. van Woerden[109], M. Vanadia[135a,135b], W. Vandelli[32], A. Vaniachine[160], P. Vankov[109], G. Vardanyan[180], R. Vari[134a], E.W. Varnes[7], C. Varni[53a,53b], T. Varol[43], D. Varouchas[119], A. Vartapetian[8], K.E. Varvell[152], J.G. Vasquez[179], G.A. Vasquez[34b], F. Vazeille[37], D. Vazquez Furelos[13], T. Vazquez Schroeder[90], J. Veatch[57], V. Veeraraghavan[7], L.M. Veloce[161], F. Veloso[128a,128c], S. Veneziano[134a], A. Ventura[76a,76b], M. Venturi[172], N. Venturi[32], A. Venturini[25], V. Vercesi[123a], M. Verducci[136a,136b], W. Verkerke[109], A.T. Vermeulen[109], J.C. Vermeulen[109], M.C. Vetterli[144,d], N. Viaux Maira[34b], O. Viazlo[84], I. Vichou[169,*], T. Vickey[141], O.E. Vickey Boeriu[141], G.H.A. Viehhauser[122], S. Viel[16], L. Vigani[122], M. Villa[22a,22b], M. Villaplana Perez[94a,94b], E. Vilucchi[50], M.G. Vincter[31], V.B. Vinogradov[68], A. Vishwakarma[45], C. Vittori[22a,22b], I. Vivarelli[151], S. Vlachos[10], M. Vogel[178], P. Vokac[130], G. Volpi[13], H. von der Schmitt[103], E. von Toerne[23], V. Vorobel[131], K. Vorobev[100], M. Vos[170], R. Voss[32], J.H. Vossebeld[77], N. Vranjes[14], M. Vranjes Milosavljevic[14], V. Vrba[130], M. Vreeswijk[109], R. Vuillermet[32], I. Vukotic[33], P. Wagner[23], W. Wagner[178], J. Wagner-Kuhr[102],

JHEP03(2018)009

H. Wahlberg[74], S. Wahrmund[47], J. Walder[75], R. Walker[102], W. Walkowiak[143], V. Wallangen[148a,148b], C. Wang[35b], C. Wang[36b,at], F. Wang[176], H. Wang[16], H. Wang[3], J. Wang[45], J. Wang[152], Q. Wang[115], R.-J. Wang[83], R. Wang[6], S.M. Wang[153], T. Wang[38], W. Wang[153,au], W. Wang[36a,av], Z. Wang[36c], C. Wanotayaroj[45], A. Warburton[90], C.P. Ward[30], D.R. Wardrope[81], A. Washbrook[49], P.M. Watkins[19], A.T. Watson[19], M.F. Watson[19], G. Watts[140], S. Watts[87], B.M. Waugh[81], A.F. Webb[11], S. Webb[86], M.S. Weber[18], S.M. Weber[60a], S.W. Weber[177], S.A. Weber[31], J.S. Webster[6], A.R. Weidberg[122], B. Weinert[64], J. Weingarten[57], M. Weirich[86], C. Weiser[51], H. Weits[109], P.S. Wells[32], T. Wenaus[27], T. Wengler[32], S. Wenig[32], N. Wermes[23], M.D. Werner[67], P. Werner[32], M. Wessels[60a], T.D. Weston[18], K. Whalen[118], N.L. Whallon[140], A.M. Wharton[75], A.S. White[92], A. White[8], M.J. White[1], R. White[34b], D. Whiteson[166], B.W. Whitmore[75], F.J. Wickens[133], W. Wiedenmann[176], M. Wielers[133], C. Wiglesworth[39], L.A.M. Wiik-Fuchs[51], A. Wildauer[103], F. Wilk[87], H.G. Wilkens[32], H.H. Williams[124], S. Williams[109], C. Willis[93], S. Willocq[89], J.A. Wilson[19], I. Wingerter-Seez[5], E. Winkels[151], F. Winklmeier[118], O.J. Winston[151], B.T. Winter[23], M. Wittgen[145], M. Wobisch[82,u], T.M.H. Wolf[109], R. Wolff[88], M.W. Wolter[42], H. Wolters[128a,128c], V.W.S. Wong[171], N.L. Woods[139], S.D. Worm[19], B.K. Wosiek[42], J. Wotschack[32], K.W. Wozniak[42], M. Wu[33], S.L. Wu[176], X. Wu[52], Y. Wu[92], T.R. Wyatt[87], B.M. Wynne[49], S. Xella[39], Z. Xi[92], L. Xia[35c], D. Xu[35a], L. Xu[27], T. Xu[138], B. Yabsley[152], S. Yacoob[147a], D. Yamaguchi[159], Y. Yamaguchi[159], A. Yamamoto[69], S. Yamamoto[157], T. Yamanaka[157], F. Yamane[70], M. Yamatani[157], Y. Yamazaki[70], Z. Yan[24], H. Yang[36c], H. Yang[16], Y. Yang[153], Z. Yang[15], W-M. Yao[16], Y.C. Yap[45], Y. Yasu[69], E. Yatsenko[5], K.H. Yau Wong[23], J. Ye[43], S. Ye[27], I. Yeletskikh[68], E. Yigitbasi[24], E. Yildirim[86], K. Yorita[174], K. Yoshihara[124], C. Young[145], C.J.S. Young[32], J. Yu[8], J. Yu[67], S.P.Y. Yuen[23], I. Yusuff[30,aw], B. Zabinski[42], G. Zacharis[10], R. Zaidan[13], A.M. Zaitsev[132,aj], N. Zakharchuk[45], J. Zalieckas[15], A. Zaman[150], S. Zambito[59], D. Zanzi[91], C. Zeitnitz[178], G. Zemaityte[122], A. Zemla[41a], J.C. Zeng[169], Q. Zeng[145], O. Zenin[132], T. Ženiš[146a], D. Zerwas[119], D. Zhang[36b], D. Zhang[92], F. Zhang[176], G. Zhang[36a,av], H. Zhang[119], J. Zhang[6], L. Zhang[51], L. Zhang[36a], M. Zhang[169], P. Zhang[35b], R. Zhang[23], R. Zhang[36a,at], X. Zhang[36b], Y. Zhang[35a], Z. Zhang[119], X. Zhao[43], Y. Zhao[36b,ax], Z. Zhao[36a], A. Zhemchugov[68], B. Zhou[92], C. Zhou[176], L. Zhou[43], M. Zhou[35a], M. Zhou[150], N. Zhou[36c], C.G. Zhu[36b], H. Zhu[35a], J. Zhu[92], Y. Zhu[36a], X. Zhuang[35a], K. Zhukov[98], A. Zibell[177], D. Zieminska[64], N.I. Zimine[68], C. Zimmermann[86], S. Zimmermann[51], Z. Zinonos[103], M. Zinser[86], M. Ziolkowski[143], L. Živković[14], G. Zobernig[176], A. Zoccoli[22a,22b], R. Zou[33], M. zur Nedden[17], L. Zwalinski[32].

[1] *Department of Physics, University of Adelaide, Adelaide, Australia*
[2] *Physics Department, SUNY Albany, Albany NY, U.S.A.*
[3] *Department of Physics, University of Alberta, Edmonton AB, Canada*
[4] [(a)] *Department of Physics, Ankara University, Ankara;* [(b)] *Istanbul Aydin University, Istanbul;* [(c)] *Division of Physics, TOBB University of Economics and Technology, Ankara, Turkey*
[5] *LAPP, CNRS/IN2P3 and Université Savoie Mont Blanc, Annecy-le-Vieux, France*
[6] *High Energy Physics Division, Argonne National Laboratory, Argonne IL, U.S.A.*
[7] *Department of Physics, University of Arizona, Tucson AZ, U.S.A.*
[8] *Department of Physics, The University of Texas at Arlington, Arlington TX, U.S.A.*
[9] *Physics Department, National and Kapodistrian University of Athens, Athens, Greece*
[10] *Physics Department, National Technical University of Athens, Zografou, Greece*
[11] *Department of Physics, The University of Texas at Austin, Austin TX, U.S.A.*
[12] *Institute of Physics, Azerbaijan Academy of Sciences, Baku, Azerbaijan*
[13] *Institut de Física d'Altes Energies (IFAE), The Barcelona Institute of Science and Technology, Barcelona, Spain*
[14] *Institute of Physics, University of Belgrade, Belgrade, Serbia*
[15] *Department for Physics and Technology, University of Bergen, Bergen, Norway*

JHEP03(2018)009

[16] Physics Division, Lawrence Berkeley National Laboratory and University of California, Berkeley CA, U.S.A.
[17] Department of Physics, Humboldt University, Berlin, Germany
[18] Albert Einstein Center for Fundamental Physics and Laboratory for High Energy Physics, University of Bern, Bern, Switzerland
[19] School of Physics and Astronomy, University of Birmingham, Birmingham, U.K.
[20] [a] Department of Physics, Bogazici University, Istanbul; [b] Department of Physics Engineering, Gaziantep University, Gaziantep; [d] Istanbul Bilgi University, Faculty of Engineering and Natural Sciences, Istanbul; [e] Bahcesehir University, Faculty of Engineering and Natural Sciences, Istanbul, Turkey
[21] Centro de Investigaciones, Universidad Antonio Narino, Bogota, Colombia
[22] [a] INFN Sezione di Bologna; [b] Dipartimento di Fisica e Astronomia, Università di Bologna, Bologna, Italy
[23] Physikalisches Institut, University of Bonn, Bonn, Germany
[24] Department of Physics, Boston University, Boston MA, U.S.A.
[25] Department of Physics, Brandeis University, Waltham MA, U.S.A.
[26] [a] Universidade Federal do Rio De Janeiro COPPE/EE/IF, Rio de Janeiro; [b] Electrical Circuits Department, Federal University of Juiz de Fora (UFJF), Juiz de Fora; [c] Federal University of Sao Joao del Rei (UFSJ), Sao Joao del Rei; [d] Instituto de Fisica, Universidade de Sao Paulo, Sao Paulo, Brazil
[27] Physics Department, Brookhaven National Laboratory, Upton NY, U.S.A.
[28] [a] Transilvania University of Brasov, Brasov; [b] Horia Hulubei National Institute of Physics and Nuclear Engineering, Bucharest; [c] Department of Physics, Alexandru Ioan Cuza University of Iasi, Iasi; [d] National Institute for Research and Development of Isotopic and Molecular Technologies, Physics Department, Cluj Napoca; [e] University Politehnica Bucharest, Bucharest; [f] West University in Timisoara, Timisoara, Romania
[29] Departamento de Física, Universidad de Buenos Aires, Buenos Aires, Argentina
[30] Cavendish Laboratory, University of Cambridge, Cambridge, U.K.
[31] Department of Physics, Carleton University, Ottawa ON, Canada
[32] CERN, Geneva, Switzerland
[33] Enrico Fermi Institute, University of Chicago, Chicago IL, U.S.A.
[34] [a] Departamento de Física, Pontificia Universidad Católica de Chile, Santiago; [b] Departamento de Física, Universidad Técnica Federico Santa María, Valparaíso, Chile
[35] [a] Institute of High Energy Physics, Chinese Academy of Sciences, Beijing; [b] Department of Physics, Nanjing University, Jiangsu; [c] Physics Department, Tsinghua University, Beijing 100084, China
[36] [a] Department of Modern Physics and State Key Laboratory of Particle Detection and Electronics, University of Science and Technology of China, Anhui; [b] School of Physics, Shandong University, Shandong; [c] Department of Physics and Astronomy, Key Laboratory for Particle Physics, Astrophysics and Cosmology, Ministry of Education; Shanghai Key Laboratory for Particle Physics and Cosmology, Shanghai Jiao Tong University, Shanghai(also at PKU-CHEP), China
[37] Université Clermont Auvergne, CNRS/IN2P3, LPC, Clermont-Ferrand, France
[38] Nevis Laboratory, Columbia University, Irvington NY, U.S.A.
[39] Niels Bohr Institute, University of Copenhagen, Kobenhavn, Denmark
[40] [a] INFN Gruppo Collegato di Cosenza, Laboratori Nazionali di Frascati; [b] Dipartimento di Fisica, Università della Calabria, Rende, Italy
[41] [a] AGH University of Science and Technology, Faculty of Physics and Applied Computer Science, Krakow; [b] Marian Smoluchowski Institute of Physics, Jagiellonian University, Krakow, Poland
[42] Institute of Nuclear Physics Polish Academy of Sciences, Krakow, Poland
[43] Physics Department, Southern Methodist University, Dallas TX, U.S.A.
[44] Physics Department, University of Texas at Dallas, Richardson TX, U.S.A.
[45] DESY, Hamburg and Zeuthen, Germany

JHEP03(2018)009

[46] Lehrstuhl für Experimentelle Physik IV, Technische Universität Dortmund, Dortmund, Germany
[47] Institut für Kern- und Teilchenphysik, Technische Universität Dresden, Dresden, Germany
[48] Department of Physics, Duke University, Durham NC, U.S.A.
[49] SUPA - School of Physics and Astronomy, University of Edinburgh, Edinburgh, U.K.
[50] INFN e Laboratori Nazionali di Frascati, Frascati, Italy
[51] Fakultät für Mathematik und Physik, Albert-Ludwigs-Universität, Freiburg, Germany
[52] Departement de Physique Nucleaire et Corpusculaire, Université de Genève, Geneva, Switzerland
[53] [(a)] INFN Sezione di Genova; [(b)] Dipartimento di Fisica, Università di Genova, Genova, Italy
[54] [(a)] E. Andronikashvili Institute of Physics, Iv. Javakhishvili Tbilisi State University, Tbilisi; [(b)] High Energy Physics Institute, Tbilisi State University, Tbilisi, Georgia
[55] II Physikalisches Institut, Justus-Liebig-Universität Giessen, Giessen, Germany
[56] SUPA - School of Physics and Astronomy, University of Glasgow, Glasgow, U.K.
[57] II Physikalisches Institut, Georg-August-Universität, Göttingen, Germany
[58] Laboratoire de Physique Subatomique et de Cosmologie, Université Grenoble-Alpes, CNRS/IN2P3, Grenoble, France
[59] Laboratory for Particle Physics and Cosmology, Harvard University, Cambridge MA, U.S.A.
[60] [(a)] Kirchhoff-Institut für Physik, Ruprecht-Karls-Universität Heidelberg, Heidelberg; [(b)] Physikalisches Institut, Ruprecht-Karls-Universität Heidelberg, Heidelberg, Germany
[61] Faculty of Applied Information Science, Hiroshima Institute of Technology, Hiroshima, Japan
[62] [(a)] Department of Physics, The Chinese University of Hong Kong, Shatin, N.T., Hong Kong; [(b)] Department of Physics, The University of Hong Kong, Hong Kong; [(c)] Department of Physics and Institute for Advanced Study, The Hong Kong University of Science and Technology, Clear Water Bay, Kowloon, Hong Kong, China
[63] Department of Physics, National Tsing Hua University, Taiwan, Taiwan
[64] Department of Physics, Indiana University, Bloomington IN, U.S.A.
[65] Institut für Astro- und Teilchenphysik, Leopold-Franzens-Universität, Innsbruck, Austria
[66] University of Iowa, Iowa City IA, U.S.A.
[67] Department of Physics and Astronomy, Iowa State University, Ames IA, U.S.A.
[68] Joint Institute for Nuclear Research, JINR Dubna, Dubna, Russia
[69] KEK, High Energy Accelerator Research Organization, Tsukuba, Japan
[70] Graduate School of Science, Kobe University, Kobe, Japan
[71] Faculty of Science, Kyoto University, Kyoto, Japan
[72] Kyoto University of Education, Kyoto, Japan
[73] Research Center for Advanced Particle Physics and Department of Physics, Kyushu University, Fukuoka, Japan
[74] Instituto de Física La Plata, Universidad Nacional de La Plata and CONICET, La Plata, Argentina
[75] Physics Department, Lancaster University, Lancaster, U.K.
[76] [(a)] INFN Sezione di Lecce; [(b)] Dipartimento di Matematica e Fisica, Università del Salento, Lecce, Italy
[77] Oliver Lodge Laboratory, University of Liverpool, Liverpool, U.K.
[78] Department of Experimental Particle Physics, Jožef Stefan Institute and Department of Physics, University of Ljubljana, Ljubljana, Slovenia
[79] School of Physics and Astronomy, Queen Mary University of London, London, U.K.
[80] Department of Physics, Royal Holloway University of London, Surrey, U.K.
[81] Department of Physics and Astronomy, University College London, London, U.K.
[82] Louisiana Tech University, Ruston LA, U.S.A.
[83] Laboratoire de Physique Nucléaire et de Hautes Energies, UPMC and Université Paris-Diderot and CNRS/IN2P3, Paris, France
[84] Fysiska institutionen, Lunds universitet, Lund, Sweden
[85] Departamento de Fisica Teorica C-15, Universidad Autonoma de Madrid, Madrid, Spain
[86] Institut für Physik, Universität Mainz, Mainz, Germany
[87] School of Physics and Astronomy, University of Manchester, Manchester, U.K.

JHEP03(2018)009

[88] CPPM, Aix-Marseille Université and CNRS/IN2P3, Marseille, France
[89] Department of Physics, University of Massachusetts, Amherst MA, U.S.A.
[90] Department of Physics, McGill University, Montreal QC, Canada
[91] School of Physics, University of Melbourne, Victoria, Australia
[92] Department of Physics, The University of Michigan, Ann Arbor MI, U.S.A.
[93] Department of Physics and Astronomy, Michigan State University, East Lansing MI, U.S.A.
[94] [(a)] INFN Sezione di Milano; [(b)] Dipartimento di Fisica, Università di Milano, Milano, Italy
[95] B.I. Stepanov Institute of Physics, National Academy of Sciences of Belarus, Minsk, Republic of Belarus
[96] Research Institute for Nuclear Problems of Byelorussian State University, Minsk, Republic of Belarus
[97] Group of Particle Physics, University of Montreal, Montreal QC, Canada
[98] P.N. Lebedev Physical Institute of the Russian Academy of Sciences, Moscow, Russia
[99] Institute for Theoretical and Experimental Physics (ITEP), Moscow, Russia
[100] National Research Nuclear University MEPhI, Moscow, Russia
[101] D.V. Skobeltsyn Institute of Nuclear Physics, M.V. Lomonosov Moscow State University, Moscow, Russia
[102] Fakultät für Physik, Ludwig-Maximilians-Universität München, München, Germany
[103] Max-Planck-Institut für Physik (Werner-Heisenberg-Institut), München, Germany
[104] Nagasaki Institute of Applied Science, Nagasaki, Japan
[105] Graduate School of Science and Kobayashi-Maskawa Institute, Nagoya University, Nagoya, Japan
[106] [(a)] INFN Sezione di Napoli; [(b)] Dipartimento di Fisica, Università di Napoli, Napoli, Italy
[107] Department of Physics and Astronomy, University of New Mexico, Albuquerque NM, U.S.A.
[108] Institute for Mathematics, Astrophysics and Particle Physics, Radboud University Nijmegen/Nikhef, Nijmegen, Netherlands
[109] Nikhef National Institute for Subatomic Physics and University of Amsterdam, Amsterdam, Netherlands
[110] Department of Physics, Northern Illinois University, DeKalb IL, U.S.A.
[111] Budker Institute of Nuclear Physics, SB RAS, Novosibirsk, Russia
[112] Department of Physics, New York University, New York NY, U.S.A.
[113] Ohio State University, Columbus OH, U.S.A.
[114] Faculty of Science, Okayama University, Okayama, Japan
[115] Homer L. Dodge Department of Physics and Astronomy, University of Oklahoma, Norman OK, U.S.A.
[116] Department of Physics, Oklahoma State University, Stillwater OK, U.S.A.
[117] Palacký University, RCPTM, Olomouc, Czech Republic
[118] Center for High Energy Physics, University of Oregon, Eugene OR, U.S.A.
[119] LAL, Univ. Paris-Sud, CNRS/IN2P3, Université Paris-Saclay, Orsay, France
[120] Graduate School of Science, Osaka University, Osaka, Japan
[121] Department of Physics, University of Oslo, Oslo, Norway
[122] Department of Physics, Oxford University, Oxford, U.K.
[123] [(a)] INFN Sezione di Pavia; [(b)] Dipartimento di Fisica, Università di Pavia, Pavia, Italy
[124] Department of Physics, University of Pennsylvania, Philadelphia PA, U.S.A.
[125] National Research Centre "Kurchatov Institute" B.P.Konstantinov Petersburg Nuclear Physics Institute, St. Petersburg, Russia
[126] [(a)] INFN Sezione di Pisa; [(b)] Dipartimento di Fisica E. Fermi, Università di Pisa, Pisa, Italy
[127] Department of Physics and Astronomy, University of Pittsburgh, Pittsburgh PA, U.S.A.
[128] [(a)] Laboratório de Instrumentação e Física Experimental de Partículas - LIP, Lisboa; [(b)] Faculdade de Ciências, Universidade de Lisboa, Lisboa; [(c)] Department of Physics, University of Coimbra, Coimbra; [(d)] Centro de Física Nuclear da Universidade de Lisboa, Lisboa; [(e)] Departamento de Fisica, Universidade do Minho, Braga; [(f)] Departamento de Fisica Teorica y del Cosmos, Universidad de Granada, Granada; [(g)] Dep Fisica and CEFITEC of Faculdade de Ciencias e Tecnologia, Universidade Nova de Lisboa, Caparica, Portugal

JHEP03(2018)009

[129] *Institute of Physics, Academy of Sciences of the Czech Republic, Praha, Czech Republic*
[130] *Czech Technical University in Prague, Praha, Czech Republic*
[131] *Charles University, Faculty of Mathematics and Physics, Prague, Czech Republic*
[132] *State Research Center Institute for High Energy Physics (Protvino), NRC KI, Russia*
[133] *Particle Physics Department, Rutherford Appleton Laboratory, Didcot, U.K.*
[134] [(a)] *INFN Sezione di Roma;* [(b)] *Dipartimento di Fisica, Sapienza Università di Roma, Roma, Italy*
[135] [(a)] *INFN Sezione di Roma Tor Vergata;* [(b)] *Dipartimento di Fisica, Università di Roma Tor Vergata, Roma, Italy*
[136] [(a)] *INFN Sezione di Roma Tre;* [(b)] *Dipartimento di Matematica e Fisica, Università Roma Tre, Roma, Italy*
[137] [(a)] *Faculté des Sciences Ain Chock, Réseau Universitaire de Physique des Hautes Energies - Université Hassan II, Casablanca;* [(b)] *Centre National de l'Energie des Sciences Techniques Nucleaires, Rabat;* [(c)] *Faculté des Sciences Semlalia, Université Cadi Ayyad, LPHEA-Marrakech;* [(d)] *Faculté des Sciences, Université Mohamed Premier and LPTPM, Oujda;* [(e)] *Faculté des sciences, Université Mohammed V, Rabat, Morocco*
[138] *DSM/IRFU (Institut de Recherches sur les Lois Fondamentales de l'Univers), CEA Saclay (Commissariat à l'Energie Atomique et aux Energies Alternatives), Gif-sur-Yvette, France*
[139] *Santa Cruz Institute for Particle Physics, University of California Santa Cruz, Santa Cruz CA, U.S.A.*
[140] *Department of Physics, University of Washington, Seattle WA, U.S.A.*
[141] *Department of Physics and Astronomy, University of Sheffield, Sheffield, U.K.*
[142] *Department of Physics, Shinshu University, Nagano, Japan*
[143] *Department Physik, Universität Siegen, Siegen, Germany*
[144] *Department of Physics, Simon Fraser University, Burnaby BC, Canada*
[145] *SLAC National Accelerator Laboratory, Stanford CA, U.S.A.*
[146] [(a)] *Faculty of Mathematics, Physics & Informatics, Comenius University, Bratislava;* [(b)] *Department of Subnuclear Physics, Institute of Experimental Physics of the Slovak Academy of Sciences, Kosice, Slovak Republic*
[147] [(a)] *Department of Physics, University of Cape Town, Cape Town;* [(b)] *Department of Physics, University of Johannesburg, Johannesburg;* [(c)] *School of Physics, University of the Witwatersrand, Johannesburg, South Africa*
[148] [(a)] *Department of Physics, Stockholm University;* [(b)] *The Oskar Klein Centre, Stockholm, Sweden*
[149] *Physics Department, Royal Institute of Technology, Stockholm, Sweden*
[150] *Departments of Physics & Astronomy and Chemistry, Stony Brook University, Stony Brook NY, U.S.A.*
[151] *Department of Physics and Astronomy, University of Sussex, Brighton, U.K.*
[152] *School of Physics, University of Sydney, Sydney, Australia*
[153] *Institute of Physics, Academia Sinica, Taipei, Taiwan*
[154] *Department of Physics, Technion: Israel Institute of Technology, Haifa, Israel*
[155] *Raymond and Beverly Sackler School of Physics and Astronomy, Tel Aviv University, Tel Aviv, Israel*
[156] *Department of Physics, Aristotle University of Thessaloniki, Thessaloniki, Greece*
[157] *International Center for Elementary Particle Physics and Department of Physics, The University of Tokyo, Tokyo, Japan*
[158] *Graduate School of Science and Technology, Tokyo Metropolitan University, Tokyo, Japan*
[159] *Department of Physics, Tokyo Institute of Technology, Tokyo, Japan*
[160] *Tomsk State University, Tomsk, Russia*
[161] *Department of Physics, University of Toronto, Toronto ON, Canada*
[162] [(a)] *INFN-TIFPA;* [(b)] *University of Trento, Trento, Italy*
[163] [(a)] *TRIUMF, Vancouver BC;* [(b)] *Department of Physics and Astronomy, York University, Toronto ON, Canada*
[164] *Faculty of Pure and Applied Sciences, and Center for Integrated Research in Fundamental Science and Engineering, University of Tsukuba, Tsukuba, Japan*

JHEP03(2018)009

[165] Department of Physics and Astronomy, Tufts University, Medford MA, U.S.A.
[166] Department of Physics and Astronomy, University of California Irvine, Irvine CA, U.S.A.
[167] [(a)] INFN Gruppo Collegato di Udine, Sezione di Trieste, Udine; [(b)] ICTP, Trieste; [(c)] Dipartimento di Chimica, Fisica e Ambiente, Università di Udine, Udine, Italy
[168] Department of Physics and Astronomy, University of Uppsala, Uppsala, Sweden
[169] Department of Physics, University of Illinois, Urbana IL, U.S.A.
[170] Instituto de Fisica Corpuscular (IFIC), Centro Mixto Universidad de Valencia - CSIC, Spain
[171] Department of Physics, University of British Columbia, Vancouver BC, Canada
[172] Department of Physics and Astronomy, University of Victoria, Victoria BC, Canada
[173] Department of Physics, University of Warwick, Coventry, U.K.
[174] Waseda University, Tokyo, Japan
[175] Department of Particle Physics, The Weizmann Institute of Science, Rehovot, Israel
[176] Department of Physics, University of Wisconsin, Madison WI, U.S.A.
[177] Fakultät für Physik und Astronomie, Julius-Maximilians-Universität, Würzburg, Germany
[178] Fakultät für Mathematik und Naturwissenschaften, Fachgruppe Physik, Bergische Universität Wuppertal, Wuppertal, Germany
[179] Department of Physics, Yale University, New Haven CT, U.S.A.
[180] Yerevan Physics Institute, Yerevan, Armenia
[181] Centre de Calcul de l'Institut National de Physique Nucléaire et de Physique des Particules (IN2P3), Villeurbanne, France
[182] Academia Sinica Grid Computing, Institute of Physics, Academia Sinica, Taipei, Taiwan

[a] Also at Department of Physics, King's College London, London, U.K.
[b] Also at Institute of Physics, Azerbaijan Academy of Sciences, Baku, Azerbaijan
[c] Also at Novosibirsk State University, Novosibirsk, Russia
[d] Also at TRIUMF, Vancouver BC, Canada
[e] Also at Department of Physics & Astronomy, University of Louisville, Louisville, KY, U.S.A.
[f] Also at Physics Department, An-Najah National University, Nablus, Palestine
[g] Also at Department of Physics, California State University, Fresno CA, U.S.A.
[h] Also at Department of Physics, University of Fribourg, Fribourg, Switzerland
[i] Also at II Physikalisches Institut, Georg-August-Universität, Göttingen, Germany
[j] Also at Departament de Fisica de la Universitat Autonoma de Barcelona, Barcelona, Spain
[k] Also at Departamento de Fisica e Astronomia, Faculdade de Ciencias, Universidade do Porto, Portugal
[l] Also at Tomsk State University, Tomsk, and Moscow Institute of Physics and Technology State University, Dolgoprudny, Russia
[m] Also at The Collaborative Innovation Center of Quantum Matter (CICQM), Beijing, China
[n] Also at Universita di Napoli Parthenope, Napoli, Italy
[o] Also at Institute of Particle Physics (IPP), Canada
[p] Also at Horia Hulubei National Institute of Physics and Nuclear Engineering, Bucharest, Romania
[q] Also at Department of Physics, St. Petersburg State Polytechnical University, St. Petersburg, Russia
[r] Also at Borough of Manhattan Community College, City University of New York, New York City, U.S.A.
[s] Also at Department of Financial and Management Engineering, University of the Aegean, Chios, Greece
[t] Also at Centre for High Performance Computing, CSIR Campus, Rosebank, Cape Town, South Africa
[u] Also at Louisiana Tech University, Ruston LA, U.S.A.
[v] Also at Institucio Catalana de Recerca i Estudis Avancats, ICREA, Barcelona, Spain
[w] Also at Department of Physics, The University of Michigan, Ann Arbor MI, U.S.A.
[x] Also at Graduate School of Science, Osaka University, Osaka, Japan

JHEP03(2018)009

[y] Also at Fakultät für Mathematik und Physik, Albert-Ludwigs-Universität, Freiburg, Germany
[z] Also at Institute for Mathematics, Astrophysics and Particle Physics, Radboud University Nijmegen/Nikhef, Nijmegen, Netherlands
[aa] Also at Department of Physics, The University of Texas at Austin, Austin TX, U.S.A.
[ab] Also at Institute of Theoretical Physics, Ilia State University, Tbilisi, Georgia
[ac] Also at CERN, Geneva, Switzerland
[ad] Also at Georgian Technical University (GTU),Tbilisi, Georgia
[ae] Also at Ochadai Academic Production, Ochanomizu University, Tokyo, Japan
[af] Also at Manhattan College, New York NY, U.S.A.
[ag] Also at The City College of New York, New York NY, U.S.A.
[ah] Also at Departamento de Fisica Teorica y del Cosmos, Universidad de Granada, Granada, Portugal
[ai] Also at Department of Physics, California State University, Sacramento CA, U.S.A.
[aj] Also at Moscow Institute of Physics and Technology State University, Dolgoprudny, Russia
[ak] Also at Departement de Physique Nucleaire et Corpusculaire, Université de Genève, Geneva, Switzerland
[al] Also at Institut de Física d'Altes Energies (IFAE), The Barcelona Institute of Science and Technology, Barcelona, Spain
[am] Also at School of Physics, Sun Yat-sen University, Guangzhou, China
[an] Also at Institute for Nuclear Research and Nuclear Energy (INRNE) of the Bulgarian Academy of Sciences, Sofia, Bulgaria
[ao] Also at Faculty of Physics, M.V.Lomonosov Moscow State University, Moscow, Russia
[ap] Also at National Research Nuclear University MEPhI, Moscow, Russia
[aq] Also at Department of Physics, Stanford University, Stanford CA, U.S.A.
[ar] Also at Institute for Particle and Nuclear Physics, Wigner Research Centre for Physics, Budapest, Hungary
[as] Also at Giresun University, Faculty of Engineering, Turkey
[at] Also at CPPM, Aix-Marseille Université and CNRS/IN2P3, Marseille, France
[au] Also at Department of Physics, Nanjing University, Jiangsu, China
[av] Also at Institute of Physics, Academia Sinica, Taipei, Taiwan
[aw] Also at University of Malaya, Department of Physics, Kuala Lumpur, Malaysia
[ax] Also at LAL, Univ. Paris-Sud, CNRS/IN2P3, Université Paris-Saclay, Orsay, France
[*] Deceased

JHEP03(2018)009